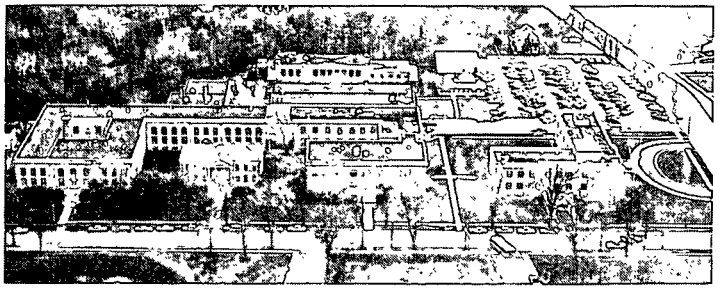

THE INSTITUTE OF PAPER CHEMISTRY, APPLETON, WISCONSIN

HIGH-INTENSITY DRYING PROCESSES

REPORT ONE

BY

DR. CLYDE H. SPRAGUE

PROJECT 3470

DOE CONTRACT NO. DE-FG02-85CE40738

August 1985

NOTICE & DISCLAIMER

The Institute of Paper Chemistry (IPC) has provided a high standard of professional service and has exerted its best efforts within the time and funds available for this project. The information and conclusions are advisory and are intended only for the internal use by any company who may receive this report. Each company must decide for itself the best approach to solving any problems it may have and how, or whether, this reported information should be considered in its approach.

IPC does not recommend particular products, procedures, materials, or services. These are included only in the interest of completeness within a laboratory context and budgetary constraint. Actual products, procedures, materials, and services used may differ and are peculiar to the operations of each company.

In no event shall IPC or its employees and agents have any obligation or liability for damages, including, but not limited to, consequential damages, arising out of or in connection with any company's use of, or inability to use, the reported information. IPC provides no warranty or guaranty of results.

The work reported herein was performed, in large part, before the inception of Contract No. DE-FG02-85CE40738. It is being distributed under this contract at this time to serve as background for subsequent reports on high-intensity drying.

TABLE OF CONTENTS

THE INSTITUTE OF PAPER CHEMISTRY

Appleton, Wisconsin

HIGH INTENSITY DRYING PROCESSES

SUMMARY

Since 1980, a sustained dues-funded research program, supported by extensive student work, has been directed toward the investigation and evaluation of some advanced paper drying processes having very significant potential benefits to the pulp and paper industry. The three drying processes or regimes which have been studied are elevated temperature/pressure drying, thermal/vacuum drying, and impulse drying. These processes are related by the fact that they all involve intensive heat input, resulting in the development of vapor pressures inside the sheet that exceed the ambient pressure. The conditions required for intensive heating, together with the vapor pressure that results, provide the basis for the following significant potential benefits of high-intensity drying: very high drying rate, reduced quantity and/or quality of drying energy, and favorable impact on paper properties.

This report focuses on the two major aspects of the completed research in the high-intensity drying area: exploratory studies of the performance of these processes and development of a process description based on detailed experimental and mathematical analyses. The report concludes with a long-range plan for future work directed toward extending the current understanding to include the comprehensive data base required for the effective and efficient commercial application of high-intensity drying processes, primarily impulse drying.

INTRODUCTION

OVERVIEW AND OBJECTIVES

The Institute of Paper Chemistry is involved in the study of advanced water removal processes that offer the potential to significantly change the drying of paper. New drying concepts have been identified and explored. In bench-scale experiments, significantly higher drying rates have been achieved with these "high-intensity" drying processes compared to conventional drying methods. For example, drying rates of 5 to more than 1000 times those typical of cylinder drying have been observed. Since the size and cost of a dryer system tends to be inversely related to the drying rate, a substantial decrease in the cost of a drying system is possible using these advanced concepts. The operating speed of a paper machine is often dryer-limited. Space limitations or other factors may preclude increasing the size of the dryer to increase speed. However, using these advanced concepts, the dryer system could be sized for a higher capacity while still being physically smaller than a conventional system.

The energy implications of using advanced drying concepts are very significant. Smaller dryer systems can be made more energy efficient; less energy is lost to heating air and radiation losses to the ambient are reduced. The opportunities for energy recovery in these advanced systems are also enhanced. Furthermore, data on one of the new drying concepts - "impulse drying" - indicate that more than 30% of the water can be removed in the liquid phase, thus greatly reducing the energy required for evaporation.

About one-third of the total energy used in an integrated mill (and even more in an unintegrated mill) is used to dry paper. If these new drying concepts are commercialized, a conservative estimate is that at least 10% of the

energy currently used by the industry can be saved; this amounts to about 0.2 quads of energy per year. If impulse drying becomes prevalent, the savings may appreciably exceed this level.

Another major benefit expected from high-intensity drying methods (especially impulse drying), resulting from their positive effects on paper properties, is product improvement and perhaps the development of new products. These techniques should also permit given product specifications to be achieved with a reduced quantity or quality of raw material. This represents a large potential for energy and cost savings, also.

The majority of the work to date in this project has been of two types: (1) exploratory work aimed at gaining information on the performance characteristics (mainly water removal and to a lesser extent energy use and paper properties) of various high-intensity drying processes, and (2) work aimed at developing an improved understanding or description of these processes. This work has resulted in demonstration of the technical feasibility and the significant potential benefits of the high-intensity drying processes, and in elucidation of their key technical features. Communication of the important results of the completed exploratory and fundamental research is the main objective of this report.

BACKGROUND

Energy Use in the Pulp and Paper Industry

The pulp and paper industry is the fifth largest manufacturing industry in the U.S. It uses more than 10% of the total energy used by U.S. manufacturers, ranking fourth after chemicals, steel, and petroleum[1]. In 1979, the pulp and paper industry ranked first in residual oil use (32.1% vs. 19.0% for

the second industry - chemicals and allied products), seventh in natural gas, third in coal, and third in purchased electricity.[2]

In 1981, the total energy consumption of the industry was 2.15×10^{15} Btu. Purchased energy was 1.06×10^{15} Btu, with natural gas accounting for 18.6% of the total energy, residual oil at 12.2%, coal at 11.2%, and purchased energy at 6.5%.[2]

Currently, about 50% of the total energy is self-generated, primarily from spent cooking liquor (37.6% of the total), hogged fuel (6.7%), and bark (5.0%). Significant progress has been made in reducing the fraction of purchased energy. From 1972 to 1981, the percentage of self-generated energy increased from 40.7 to 50.2%.[2]

Hersh[1] reported typical energy flows in a modern integrated pulp and paper mill; these flows are illustrated in Fig. I.1. His analysis is based on the kraft pulping process, which accounts for about 70% of the paper and paperboard manufactured in the U.S., and an average energy consumption of 30×10^6 Btu/ton. The energy required to produce paper products (e.g., Btu of energy per ton of product) depends on the particular product; e.g., printing and writing papers require $37\text{-}47 \times 10^6$ Btu/ton and linerboard requires about 31×10^6 Btu/ton.[1]

The highest energy consumption is associated with the papermaking process, about 36% of the total consumption.[1] Energy is used to drive the equipment, pump white water around the machine, and dry the paper. In papermaking, the drying process is the major consumer of energy. A dryer system employing steam heated cylinders uses $6.5\text{-}12.5 \times 10^6$ Btu/ton, and a Yankee dryer for tissue grades uses $5.5\text{-}7.0 \times 10^6$ Btu/ton.[3] Thus, the dryer section of a paper machine constitutes nearly one-third of the total energy requirement of an integrated mill and an even larger fraction of the energy requirements of a nonintegrated mill.

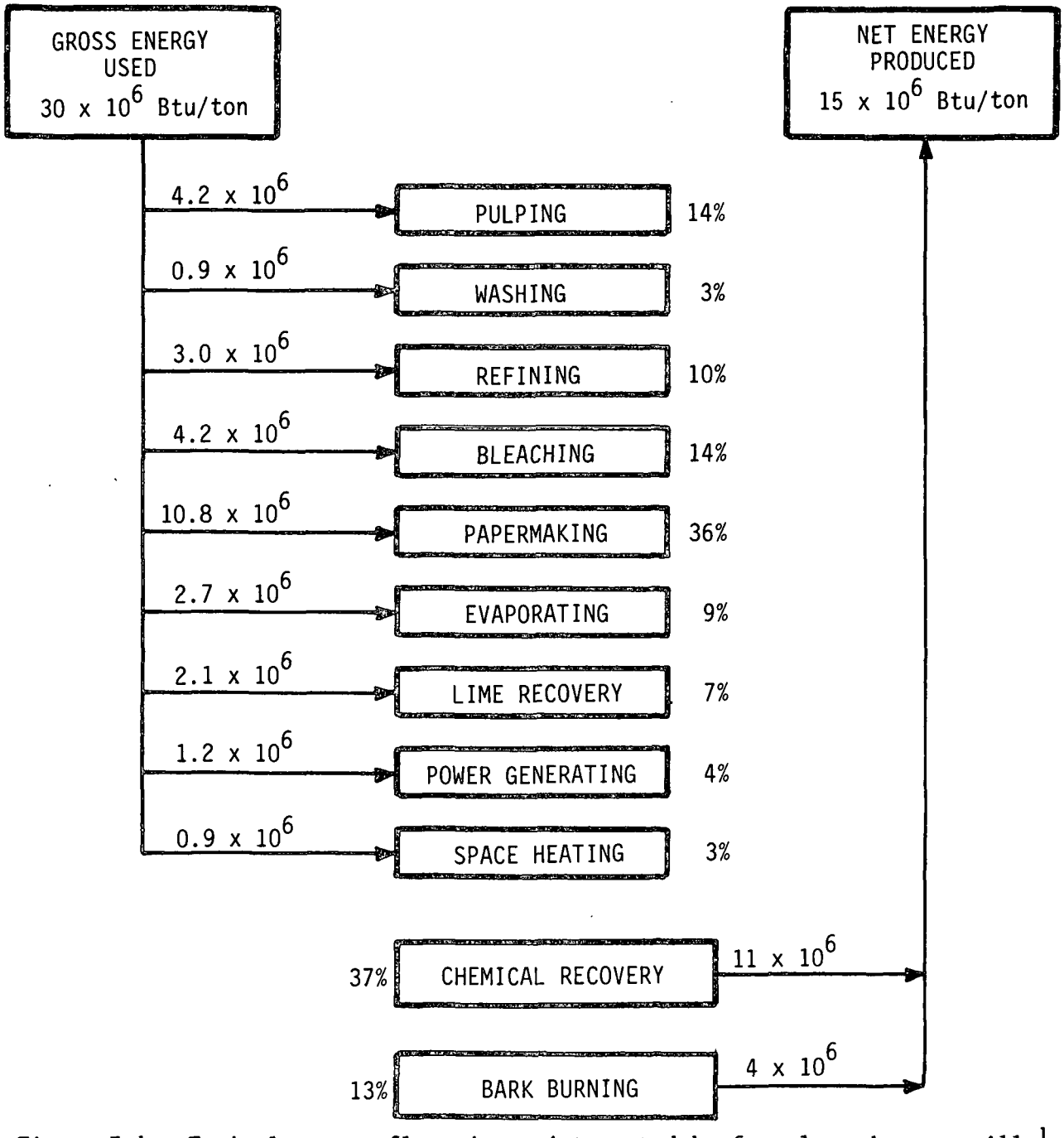

Figure I-1. Typical energy flows in an integrated kraft pulp and paper mill.[1]

Water Removal Processes in Drying

The Cost of Water Removal

McConnell[4] analyzed the economics of the papermaking process. He concluded that operating costs are dominated by the cost of energy for operating the dryers.

As illustrated in Fig. I.2, in a typical paper machine, nearly 99% of the water is mechanically removed at the wet end, about 1% of the water is removed at the presses, and less than 0.5% of the water is removed in the dryers. However, because of the use of energy for evaporation, the cost of removing the water in the dryer section dominates the cost of water removal, as illustrated in Fig. I.3. Also, drying costs have increased dramatically since 1973. The cost of steam for drying may be as high as 75% of the operating cost of a paper machine.[4] Thus, reducing dryer energy use is an important goal.

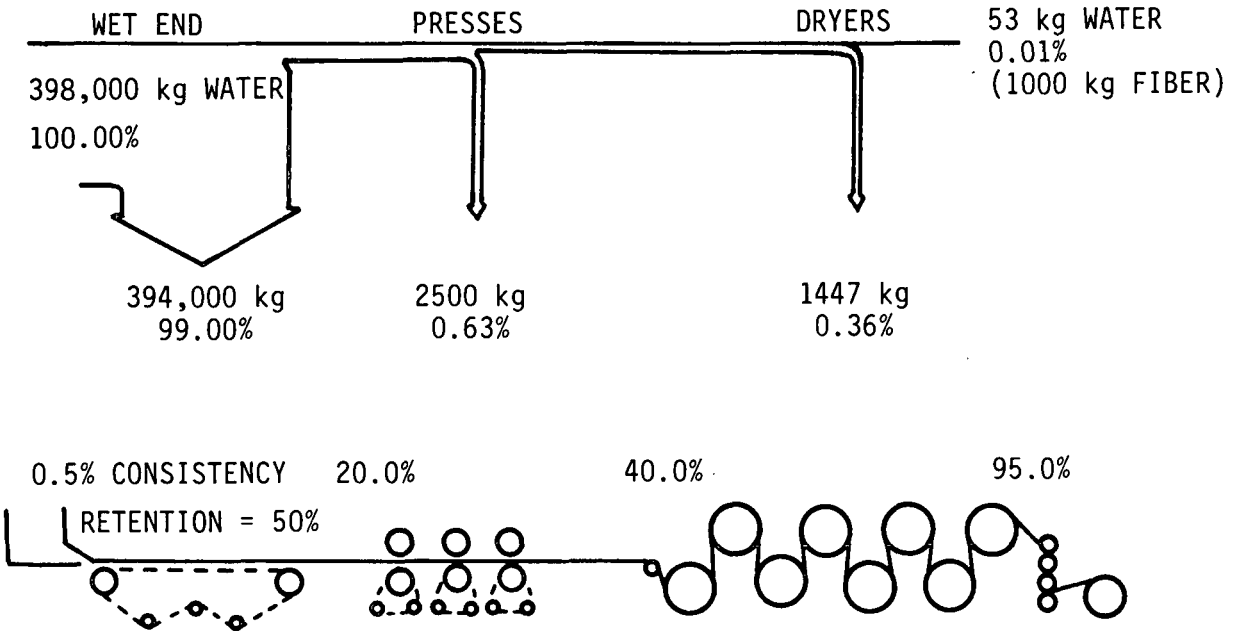

Figure I.2. Water removal in the paper machine.[4]

Three methods can be used to reduce the amount of energy necessary for drying: (1) increase the dryer energy efficiency, (2) remove more water before the dryer section, and (3) increase the amount of water left in the paper after drying. It is estimated that drying energy is reduced by 4% for every additional percentage point increase in the dryness out of the presses. The reel moisture target can often be raised by improving the cross direction moisture uniformity. Paper is often overdried to improve the moisture profile and eliminate wet streaks.

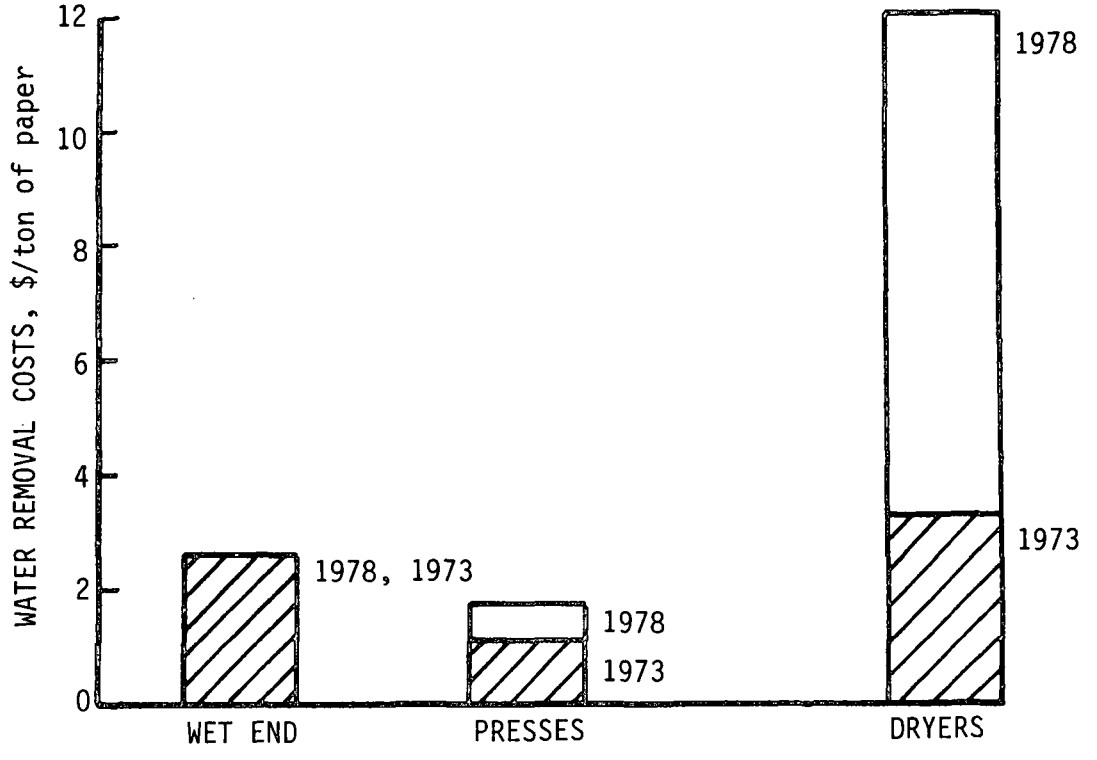

Figure I.3. Relative water removal costs for the wet end, presses, and dryers expressed in terms of the cost for water removal at the wet end.

Types of Dryers

The possibilities for increasing energy efficiency are dependent on the dryer type. Several different types of dryers are used to dry paper and pulp. The most common dryers are drum, air impingement, Yankee, infrared, through, flash, vacuum, dielectric, and microwave dryers.

Through a survey of the U.S. paper industry, McConnell[4] developed an estimate of the distribution of dryers in the industry. The results of his survey are presented in Table I.1. He assumed that the water removed is proportional to the amount of product produced. Thus, about 7% of the water is removed in pulp drying, 6% in tissue drying, 34% in paper drying, 51% in paperboard drying, and 2% in coatings drying.

For each product, the distribution of dryer types used is presented in Table I.1. For example, in pulp drying, about 70% of the pulp is dried by impingement (floater) dryers, 15% in flash dryers, and 15% in vacuum dryers. The table also illustrates the percentage of water removed for each type of dryer. This was determined by multiplying the percent of the dryer distribution by the fraction of water removed in each product. Thus, about 82% of the industry's drying is done using conventional drum dryers. Less than 8% of the drying is done using impingement dryers. About 4% of the drying is done using Yankee dryers. Less than 3% of the drying is done using infrared dryers. Through, flash, and vacuum dryers each account for about 1% of the drying. Finally, almost no drying is done on dielectric and microwave dryers.

Table I.1. Dryer distribution in the U.S. paper industry.[4]

	Paper Industry Drying Application					Totals, %
	Pulp	Tissue	Paper	Board	Coating[a]	
	Water Removed, %					
	7	6	34	51	2	100
	Dryer Distribution, %					
Drum section dryer		15	95	95	35	82.35
Impingement dryer	70		2	2	50	7.60
Yankee dryer		70				4.20
Infrared dryer			3	3	15	2.85
Through dryer		15				0.90
Flash dryer	15					1.05
Vacuum dryer	15					1.05
Dielectric dryer[b]						
Microwave dryer[b]						
Totals	100	100	100	100	100	100.00

[a]This includes both on- and off-machine coating operations.
[b]A small number of dielectric and microwave dryers are currently in use.

The conventional (multicylinder) drum dryer is dominant in the industry. The impingement dryer, which is used mainly for pulp drying, is the next most common dryer type. Yankee dryers follow in importance and dominate tissue drying. Furthermore, drum dryers and Yankee dryers use steam to evaporate water from the wet web. About 86% of the water removal by drying in the industry is performed using steam as a thermal energy source in drum and Yankee dryers.[4]

Steam Economy

Since steam is the major source of thermal energy for drying, it is important to consider the efficiency of steam utilization for drying in the U.S. paper industry. This efficiency is expressed in terms of a "steam economy," which is defined as the pounds of steam used divided by the pounds of water evaporated from the sheet. The minimum theoretical steam requirement to heat 1 lb of water from 90 to 212°F and evaporate it at atmospheric pressure is about 1.09 lb of steam/lb of water. In practice, a figure of 1.25-1.30 is presently considered excellent, while values above 1.5 are far more common for older dryer systems,[5] which are still prevalent in the industry.

The extra heat is consumed in the following ways:

1. Desorption heat, which is the additional heat needed to remove water that is physically or chemically bound to the fibers. Usually, this heat requirement is not a significant factor until the paper reaches 10% moisture.
2. In heating the air used to carry away the liberated water vapor.
3. In heating the paper sheet.
4. Heat losses, mainly through convection and radiation.

In order to estimate the total magnitude of drying inefficiencies, consider the following assumptions:

- 30% of the total energy is used for drying
- 85% of drying uses steam having an average steam economy of 1.50
- 1981 basis -- 2.15×10^{15} Btu consumed by industry

Using these estimates, the theoretical inefficiency resulting just from the use of steam in 1981 was about 1.764×10^{14} Btu, 28 million barrels of oil (residual) equivalent. This is about 8.2% of the energy consumed by the industry.

This simple example illustrates the significant potential for reducing energy use and operating costs in paper drying. Improved dryer systems can have a significant impact on the industry.

Size of Dryer Systems

The physical size of dryers significantly impacts the capital cost of the paper machine. A parameter that can be used to characterize the performance and size of dryers is the "drying rate," which is defined as the pounds of water removed per hour divided by the heat transfer surface area of the dryers. The size (and cost) of a dryer is inversely related to its drying rate.

For a wide variety of paper and board grades dried on drum (i.e., multicylinder) dryers, the drying rate is typically 2-5 $lb/(hr\text{-}ft^2)$. The drying rate increases approximately linearly with steam temperature.[6]

Impingement, Yankee, and through dryers have drying rates significantly higher than drum dryers. Steam-heated cylinder-impingement air dryer combination systems have drying rates of about 15 $lb/(hr\text{-}ft^2)$. Yankee dryers using high-velocity impingement air have drying rates of 20-40 $lb/(hr\text{-}ft^2)$; they are used primarily on tissue, toweling, or machine-glazed papers. Air through dryers, which are used for drying permeable sheets, have drying rates of about 18-20 $lb/(hr\text{-}ft^2)$.[6]

Because of the low drying rates of drum dryers, many cylinders are needed to remove the water from the different paper grades. These systems are large and capital-intensive. Physically, they dominate the paper machine. For example, drying of linerboard at conventional production rates requires a dryer section with on the order of one acre of heat transfer area! In contrast, Yankee and through dryers usually use one large diameter (e.g., 15 ft) cylinder to accomplish most of the drying. They occupy a fraction of the space of a drum dryer system.

Paper machines using drum dryers are often production limited by the dryer section; room does not exist or it is not practical to add more cylinders to increase speed. High-intensity, smaller drying systems are needed to replace drum dryers. They would require less capital and would permit higher production rates.

The Institute of Paper Chemistry has identified some advanced water removal concepts that have very high drying rates as well as energy and properties-related potential benefits. These concepts will be introduced next.

HIGH-INTENSITY DRYING PROCESSES

In simplest terms, conventional drying processes have two aspects - heat input and water vapor removal. Because most of the heat entering the sheet eventually causes evaporation, the vapor removal (drying) rate and the heat input rate will tend to achieve a natural balance in any given dryer. This implies that if either or both of these basic steps are either intrinsically impeded or effected by small "driving forces," the overall drying process will be relatively slow and, perhaps, inefficient.

In particular, the conventional multicylinder dryer section described in the preceding section suffers from significant impediments in both the heat input and the vapor removal steps.[7,8] Specifically, it is difficult to transfer

heat from the steam condensing inside the cylinder, through the dryer shell, across the interface between the cylinder and paper, and into the interior of the paper, where the moisture resides. A further barrier is associated with driving the evaporated water out of the paper; this involves relatively slow diffusion processes both within the paper and in the humid air boundary layer adjacent to the paper. Furthermore, the temperature difference and vapor partial pressure difference driving forces typically available during paper drying for heat and mass transfer, respectively, are not particularly large, thus placing limits on the achievable drying rates.

Water removal concepts directed toward the reduction or elimination of some of the barriers to rapid, efficient drying, and toward reduction of energy use and paper properties benefits, are the subject of research at The Institute of Paper Chemistry. The concepts being investigated form a family, in that they are all based on the principle of high-intensity drying. As will be discussed in this report, these concepts have the potential to dramatically alter the water removal process!

Basic Concept of High-Intensity Drying

High-intensity drying refers to hot-surface drying at sufficiently intensive heat input conditions so that the heated surface of the web attains a temperature in excess of the ambient boiling point. This leads to the fundamental difference between high-intensity drying and conventional drying processes. Namely, a vapor pressure in excess of the ambient pressure develops at the interface between the hot surface and the paper web. Important effects of this phenomenon include: (a) a bulk flow of hot vapor into (and through) the sheet, effected by the vapor pressure gradient, results in a rapid internal heatup (to temperatures at or above the ambient boiling point), (b) the vapor removal process involves a much larger driving force than prevails in conventional drying and is

unimpeded by external mass transfer resistances, so the drying rate may considerably exceed those typical of conventional drying, and (c) under certain conditions, the vapor pressure gradient may induce a significant liquid-phase water removal.

The differences in web thermal behavior between the conventional and high-intensity drying processes are indicated by the temperature responses in Fig. I.4 and I.5, respectively. While the web temperature (measured near the open surface) never reaches the boiling point during the "conventional" drying process and continuously decreases after the initial heatup, the corresponding temperature remains at the boiling through nearly all of the high-intensity process. This latter behavior suggests that the internal temperatures must also be at or above the boiling point.

The web temperature near the outer surface can never exceed the atmospheric boiling point as long as moisture is present, because of contact with the ambient pressure in that location. If, at particular operating conditions, the temperature does not reach this level after a reasonable period of contact between the sheet and hot surface, however, it must be concluded that high-intensity drying conditions do not prevail. The onset of high-intensity drying conditions can thus be defined experimentally in terms of the approach of the typical web temperature (e.g., measured about midway through the drying period) to the boiling point. A correlation between typical web temperature and average drying rate (directly related to the intensity of heat input), based on data from bench-scale drying experiments, is given in Fig. I.6. For a given applied mechanical pressure, the points with higher drying rate represent increased hot surface temperature conditions. These results illustrate that in the "low-intensity" region, drying rate is a gradually increasing function of web temperature. The sharp change in slope near the atmospheric boiling point (212°F) demonstrates

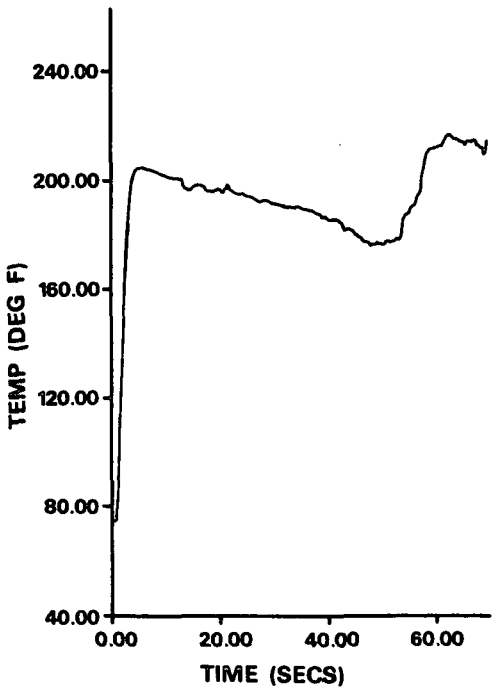

Figure I.4. Web temperature during simulated conventional drying (measured near outer surface) for 262°F heater temperature and 1.3 psi mechanical pressure. Southern softwood kraft handsheets, 570 mL CSF, 42 lb/1000 ft^2, 60% initial moisture content. Rapid temperature rise late in process denotes completion of drying.

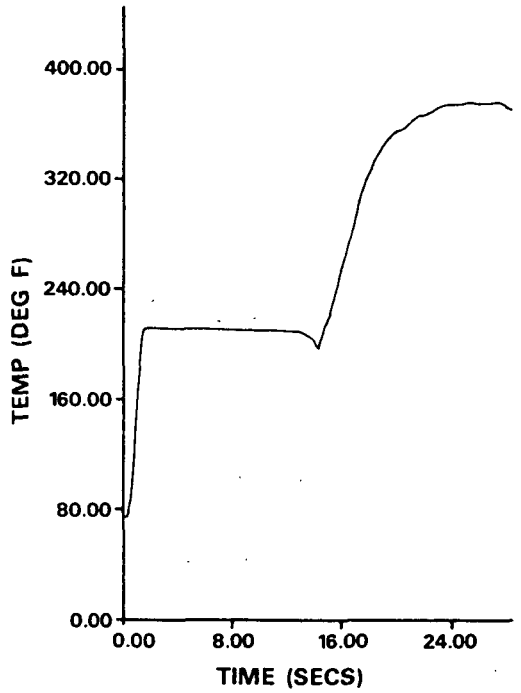

Figure I.5. Web temperature during high-intensity drying (measured near outer surface) for 448°F heated temperature and 3.3 psi mechanical pressure. Southern softwood kraft handsheets, 570 mL CSF, 42 lb/1000 ft^2, 60% initial moisture content. Rapid temperature rise late in process denotes completion of drying.

the drastic change in the basic mechanism of drying. From the data in Fig. I.6, it can be concluded that the rate of vapor removal in high-intensity drying can be very large, and is limited only by the rate at which heat can be supplied to the paper, not by mass transfer effects. Thus, increased productivity and/or smaller drying equipment can be expected to result from application of high-intensity drying principles.

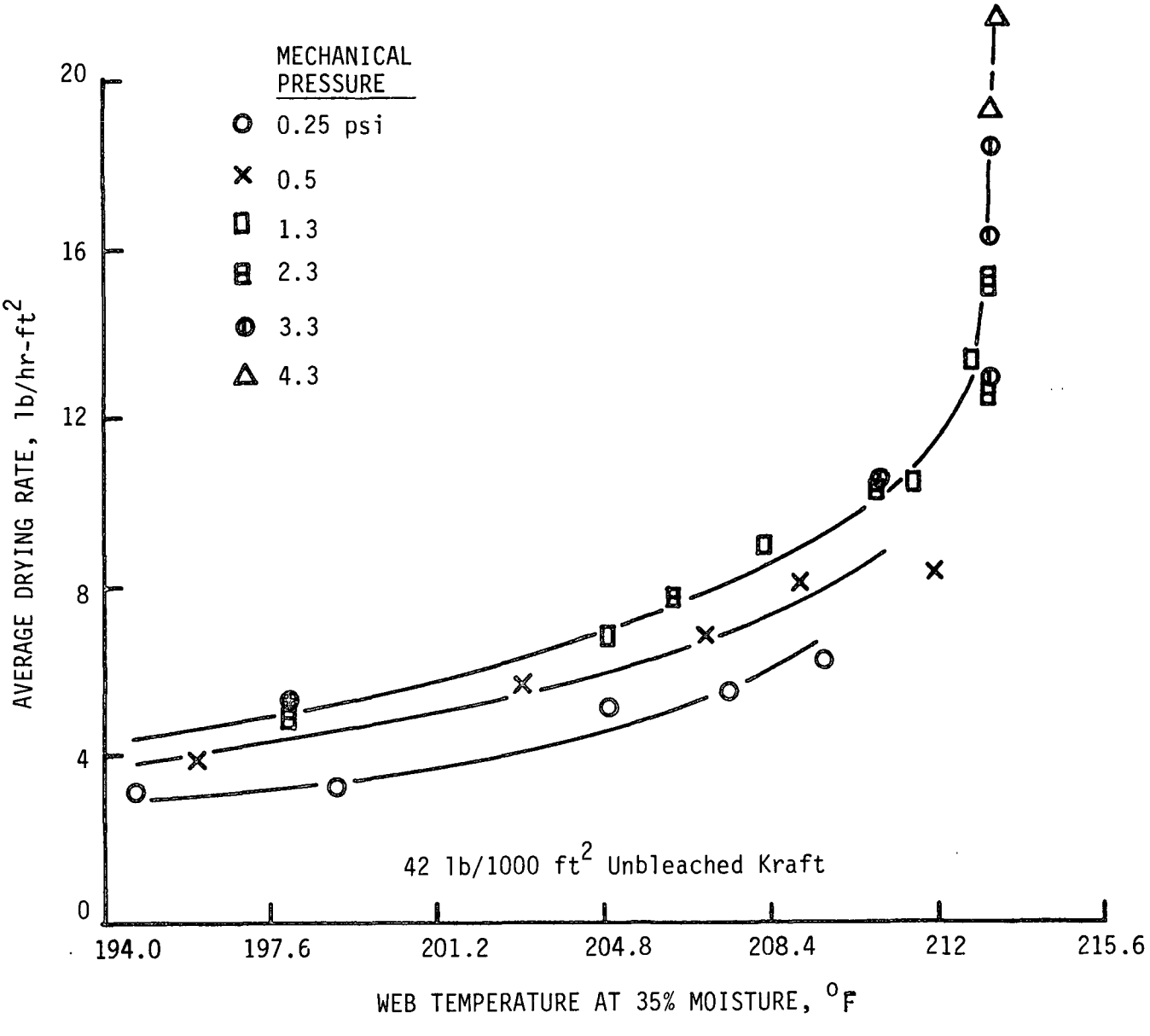

Figure I.6. Correlation of average drying rate with a typical paper web temperature: southern softwood kraft handsheets simulating a linerboard grade (42 lb/1000 ft^2).

It should be noted that high-intensity drying can be expected to lead to more energy-efficient dryers, too. The lack of dependence of drying rate on vapor partial pressure in the air surrounding the paper implies a reduced air heating and circulation requirement and more effective energy recovery from the humid exhaust (due to reduced air contamination). The reduced dryer system size expected to result from increased drying rates and reduced air requirements should also help to increase the thermal efficiency as a result of reduced heat losses. Certain specific processes to be discussed in this report have additional energy related benefits.

The key to high-intensity drying is to improve heat transfer to the wet web. This goal should be achievable through a combination of increased dryer surface temperature and considerably improved hot surface/web contact. Significantly increased temperature could be achieved by heating the dryer surface externally, e.g., with a high-temperature burner, rather than internally with comparatively low temperature condensing steam (as is conventionally done). Smaller temperature increases could be achieved by using higher temperature steam as the dryer heat source.

Improved contact could be achieved by a very high pressure loading (press roll or "extended nip") in the initial zone of contact between the web and dryer, and/or by considerably higher than conventional web restraining pressures (increased felt or wire tension) around the dryer periphery.

A noteworthy alternative way of achieving high-intensity drying is to reduce the boiling point temperature by reducing the ambient pressure in which the paper is dried. This, in turn, reduces the surface temperature required to produce rapid drying; the desirability of operating with improved contact would still remain.

Because high-intensity drying generally requires increased temperature and mechanical pressure, another potential benefit of its implementation could be a favorable impact on paper property development. If so, further economic benefits, related to raw material and energy costs for pulp production, would be expected.

Next, some variations on the high-intensity principle will be discussed. These variations have been investigated during the project and are considered throughout this report. They are presented in order of increasing potential impact on the water removal process, although the "dryer of the future" might ultimately be based on a combination of these ideas.

Specific Regimes and Concepts

Elevated Temperature and Mechanical Pressure

The threshold of the high-intensity drying regime defined in Fig. I.6 involves surface temperatures and mechancial pressures only modestly above those employed in conventional dryers via the use of steam condensation and felt tension. Therefore, motivated initially by the idea that high-intensity drying beneftis should be achievable in practice by increases in steam temperature and felt tension, the "elevated temperature/pressure" regime was selected for exploration in this project. However, it was felt that limits due to known practical difficulties in utilizing very high steam temperatures or fabric tensions should not be imposed on the research. Therefore, this regime actually was allowed to extend up to rather high surface temperatures and mechanical pressure levels more than two orders of magnitude greater than those associated with conventional drying.

Thermal/Vacuum Drying

Lehtinen[9] recently reported results from a preliminary experimental investigation of a new, thermally-driven, vacuum drying process for permeable

mats. Because this process has the potential for achieving both reduced equipment size and reduced energy use for drying, and since it qualifies as a high-intensity drying process, it was selected for study in this project. A brief description of the process (henceforth called "thermal/vacuum drying") follows. The moist mat to be dried (see Fig. I.7) is placed between a heater and a layer of a permeable filler material which is in contact with a cooled wall. The temperature difference imposed across the moist mat causes the heat transfer needed to sustain rapid evaporation. Condensation occurs at the cooled wall, creating a partial vacuum with respect to the vapor pressure within the moist mat. This induces vapor flow out of the mat. The filler material serves to retain the moisture and to minimize liquid rewetting of the mat.

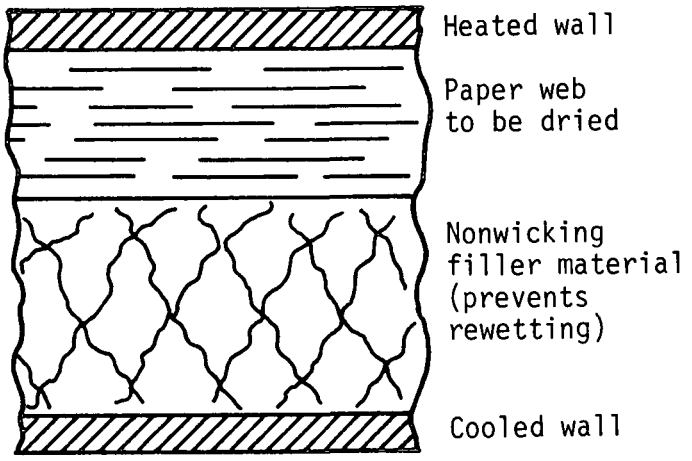

Figure I.7. Configuration for the thermal/vacuum drying process.

Because of the absence of atmospheric pressure air in the web during thermal/vacuum drying, a bulk vapor flow (i.e., high-intensity drying) condition can be achieved at low web temperatures, an advantage compared to the atmospheric high-intensity drying method discussed in the preceding section. In addition to the potentially very high rate of vapor removal with this process, the initial web heating process should be rapid, since the "evaporation/condensation cycle"

is unimpeded by diffusion effects. Furthermore, the external atmospheric pressure pushing on the paper in the vacuum zone (assuming a deformable heated or cooled wall) represents a much higher than conventional mechanical pressure loading. This yields a reduction in the thermal resistance between the heated surface and the paper web.

The fact that relatively high drying rates can be achieved at low temperature levels with the thermal/vacuum principle means that "waste heat" sources (e.g., hot condensate from other processes in the mill or lower pressure steam) could be utilized to supply the drying energy. Finally, since air-free water vapor is removed from the paper, more effective energy recovery will be possible as the vapor condenses on the cooled surface and transfers its heat to a cooler fluid, such as boiler feedwater. Thus, the thermal/vacuum concept also lends itself to cascaded configurations having still better energy utilization effectiveness.[10]

Impulse Drying

The results in Fig. I.6 confirm that increasing surface temperature and mechanical pressure give improved water removal characteristics. The logical extension of these ideas would suggest the usefulness of a high temperature press roll as the basis for a dryer system. A press nip is typically operated at average pressures more than 100 times those employed in conventional dryers (i.e., several hundred psi rather than ~ 1 psi). The high pressure, high heat flux water removal process occurring over a short time (much less than one second) in a hot press nip has led to the descriptive term, "impulse drying," for this concept. As will be shown later, the rate of water removal occurring during impulse drying can be remarkably higher than in conventional drying of paper webs. The apparent reason for this desirable behavior is that liquid-phase

removal of water, as well as evaporation, occurs as the steam generated at the hot surface passes through the sheet.

A comparison between impulse drying and conventional wet pressing may further help to clarify this new concept. In room temperature pressing, the dewatering limit is set by the compressibility of the paper web. At the point of maximum compression, the web is saturated, but no driving force or gradient exists for actually moving the interstitial water out of the sheet. Impulse drying introduces a new dimension to pressing by generating a steam pressure gradient, which may push interstitial water out of the sheet. Thus, appreciable liquid-phase dewatering is expected in impulse drying, and the dewatering limit is no longer related only to the compressibility of the web. However, an additional benefit of the heated nip may result because paper becomes more compressible at elevated temperatures which, in turn, leads to an enhanced wet pressing effect.

The possibility of extremely high water removal rates and a probable reduced drying energy requirement (stemming from the likelihood of liquid phase dewatering) are very exciting, making impulse drying an important concept for study in this project. Perhaps equally important benefits related to property development should also be anticipated, due to the intensive pressure and temperature conditions imposed on the web during water removal.

EXPLORATORY STUDIES OF HIGH-INTENSITY DRYING PERFORMANCE

INTRODUCTION

During the course of this project, the three regimes of high-intensity drying - elevated temperature/pressure, thermal/vacuum and impulse drying - have been extensively explored in two ways. First, numerous bench-scale experiments (i.e., involving the use of handsheets) have been performed to provide the performance-related data needed to quantify the potential benefits of these drying processes. This work is discussed in the present section. Second, experimental and analytical investigations oriented toward development of an understanding and description of high-intensity drying have been conducted. That work is covered in the following section.

The performance studies are presented in order of increasing departure from conventional drying practice: elevated temperature/pressure, thermal/vacuum, impulse drying. Based on the results to be presented, this tends to be the order of increasing potential benefit (in terms of increased water removal rate, reduced quality or quantity of drying energy, and impact on paper properties). The presentation order also tends to reflect the historical sequence of project emphasis, although the study of the three regimes has not been entirely serial in nature.

DRYING AT ELEVATED TEMPERATURE AND MECHANICAL PRESSURE

Experimental Systems

The majority of the drying experiments at elevated temperature/pressure were performed in an apparatus designed to provide a wide range of surface temperature, and mechanical pressures up to appoximately 10-20 times the levels

produced by felt tension in today's dryers (e.g., 0.25 psi). This original apparatus is shown schematically in Fig. II.1. Heat to evaporate the water from the wet web is supplied by a large copper block, preheated to the desired temperature using an electric heater bonded to the top surface of the block.

Fine-wire thermocouples are imbedded in the copper block to measure the drying surface temperature and several internal temperatures as a function of drying time. A fine-wire thermocrouple is also inserted through the screen and into the web to measure a typical web temperature during the drying process.

A control panel contains a controller for the heater temperature and a timer to set the duration of the drying process to within 0.1 s accuracy. The desired pressure is obtained by the use of weights and counterweights.

A test begins after the copper block reaches thermal equilibrium at the desired temperature. A handsheet is then placed on the screen, and the start button is pressed.

The motor begins to run, with the clutch and brake disconnected. The arm containing the web is driven upward by the pneumatic cylinder until the rack engages the pinion. The clutch is then connected and the motor drives the arm upward, causing the web to make contact with, and lift the block and weights. The arm moves away from the rod of the pneumatic cylinder by means of a slot in the arm which the connecting pin traverses.

As the copper block assembly is lifted, a limit switch is tripped, the brake is engaged, and the clutch is disconnected. At the end of the preset drying time, the brake is disconnected, and the arm drops downward to its original position.

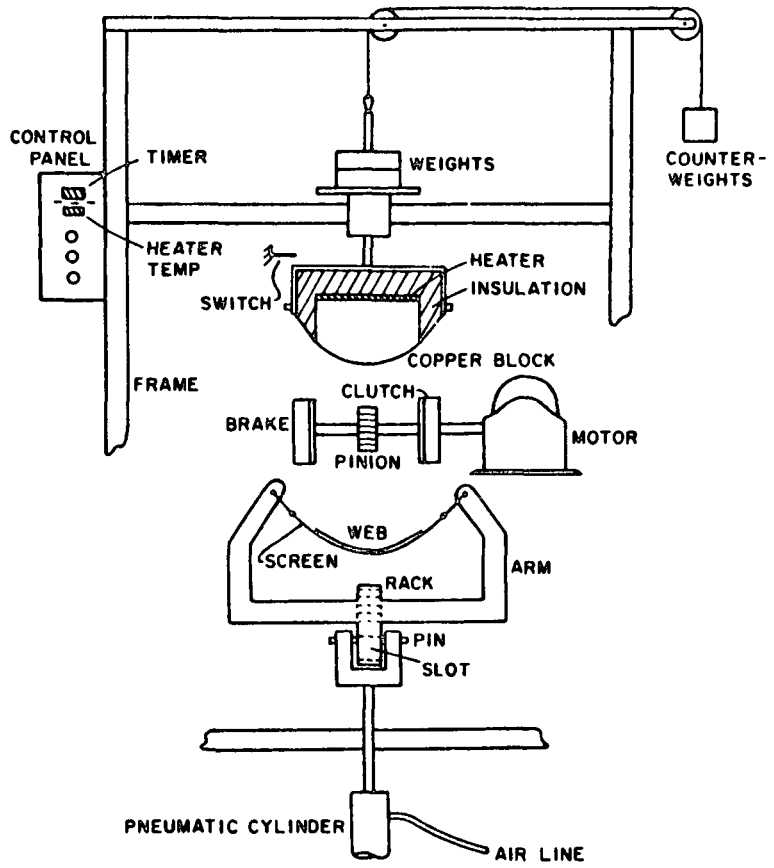

Figure II.1. Schematic diagram of original apparatus for investigation of elevated temperature/pressure drying.

With this apparatus, the surface temperature of the block can be varied from room temperature to about 600°F. Using the weights and counterweights, the pressure can be varied from 0.25 to 4.3 psi. At the maximum drying rates encountered during the experimental program, the decrease in the block surface temperature was less than about 4°C (7°F), due to the mass and large thermal diffusivity of the copper block.

In order to extend the range of mechanical pressure that can be applied to the sheet, the system shown schematically in Fig. II.2 was employed. Depending on pressure level desired, the applied load is produced by weights added to the upper copper block or by use of air cylinders connected between the upper block and a load frame (not shown). Force limitations dictate that pressures above

about 70 psi have to be achieved by using reduced handsheet diameters. As in the original system, a timer is used to control the duration of contact between the sheet and hot surface to within 0.1 s; air cylinders are used to quickly separate the sheet and hot surface at the end of a test run. The handsheet to be dried is attached to the support screens on the upper block by fine crossthreads, just prior to a run.

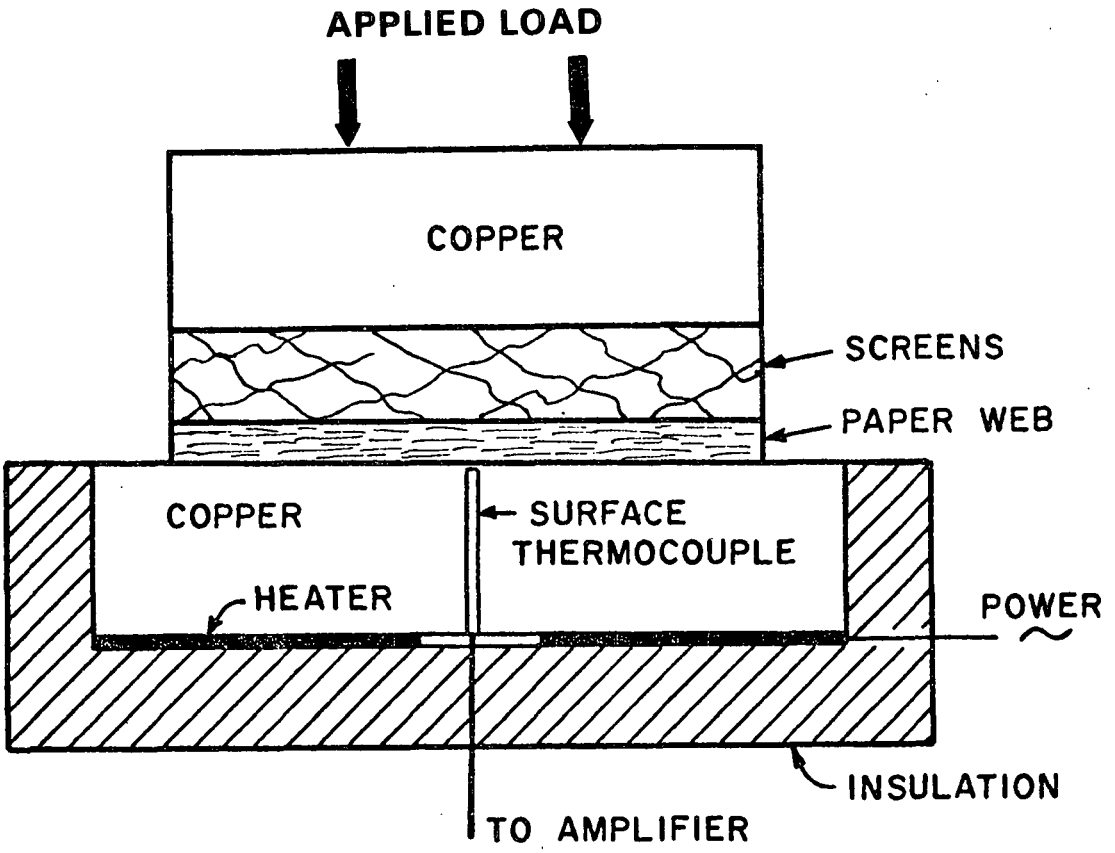

Figure II.2. Schematic diagram of apparatus used in higher mechanical pressure experiments (above 5 psi). For smaller diameter handsheets, an equal diameter felt is inserted between the web and the support screens, in order to provide a controlled mechanical pressure.

Water Removal

The vast majority of drying runs in the elevated temperature/pressure regime utilized handsheets prepared from never-dried, unbleached southern

softwood kraft pulps. In most cases the sheets had a basis weight of 42 lb/1000 ft^2 (205 g/m^2) and a pulp freeness of 560-570 mL CSF. These sheets were intended to simulate linerboard, because it is a very important, high-production grade. Limited testing of sheets from an unbleached northern softwood kraft pulp, and of other basis weight and freeness conditions, was performed. In all cases, the nominal initial moisture content (wet basis) was 60%.

The southern softwood kraft handsheets were produced using a slightly modified version of TAPPI Standard T-205. The TAPPI standard requires the use of a smooth pressure plate in contact with the wet web in the handsheet press, but these handsheets were pressed with the pressure plate removed, in order to give essentially the same surface finish on both sides. For those limited tests involving northern softwood kraft pulp, the handsheets were produced using the TAPPI standard procedure. These sheets had a smoother surface on the "wire side," which was the side in contact with the pressure plate. In all drying runs, the wire side was in contact with the hot surface.

The average drying rate ($lb/hr-ft^2$) was selected as the primary indicator of water removal performance. For the purpose of the studies described in this report, average drying rate denotes the equivalent constant drying rate that would produce a moisture change from the initial moisture content to a final moisture content of 6% in the measured drying time to this same final condition. The drying time is determined from the results of a series of drying runs at fixed pressure and temperature, but different contact time durations. For each run, the initial, final, and oven-dry sheet weights are measured. From these data, one can plot relative moisture removed (RMR)* as a function of drying time. The drying time can then be found by inspection, noting that 6%

*RMR = mass of moisture lost/initial mass of moisture in sheet.

final moisture content corresponds to RMR = 0.957 (provided the initial moisture content is 60%). A typical set of drying curves is presented in Fig. II.3.

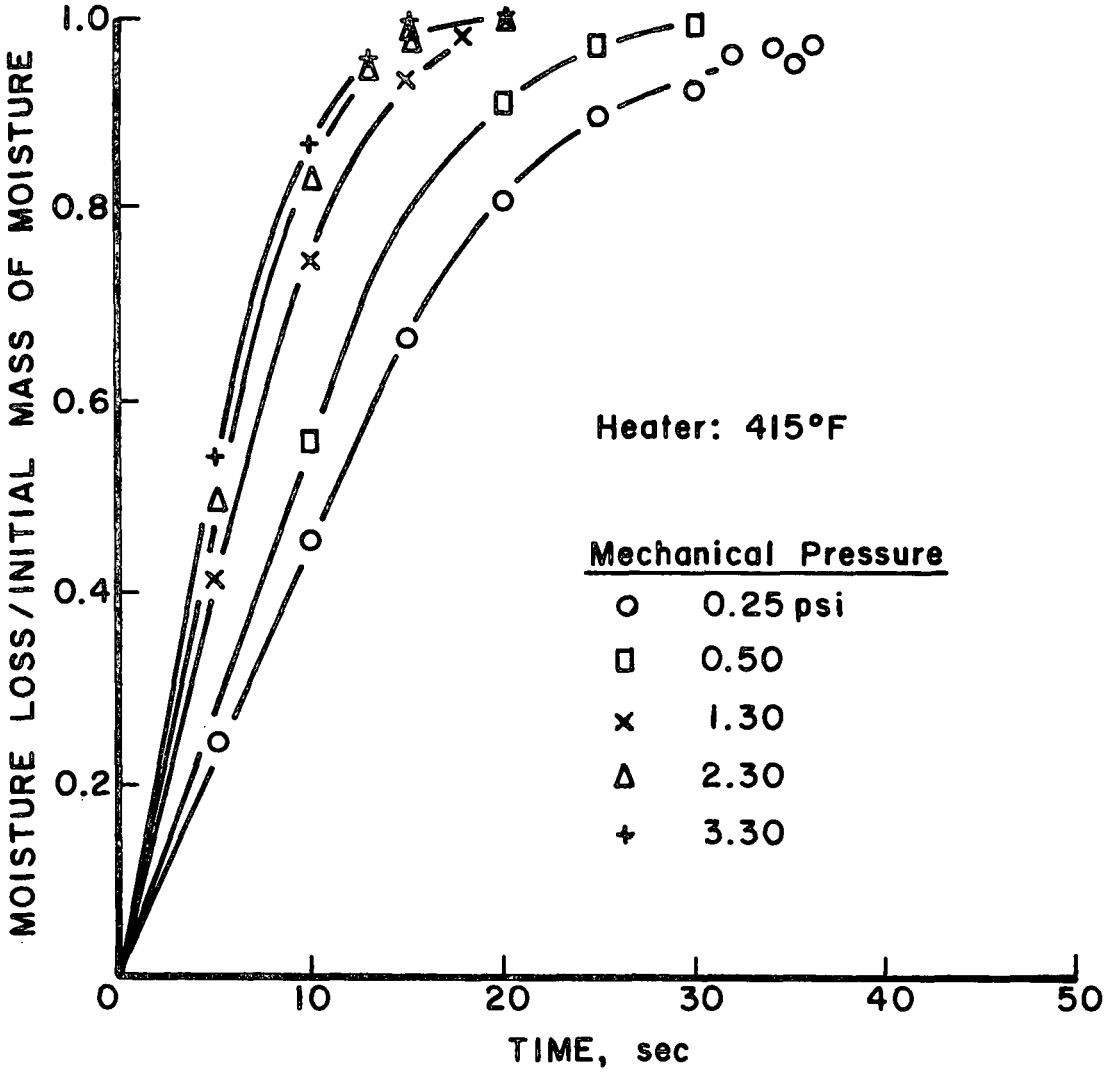

Figure II.3. Typical drying curves for unbleached southern softwood kraft handsheets: 42 lb/1000 ft^2, 570 CSF, 60% initial moisture.

Drying rate data from tests performed in the original experimental system are presented in Fig. II.4 and II.5. For comparison purposes, the approximate domain of conventional drying is indicated in Fig. II.4. It is seen that drying rates more than quadruple those of typical conventional dryers are possible at the maximum temperature/pressure conditions investigated.

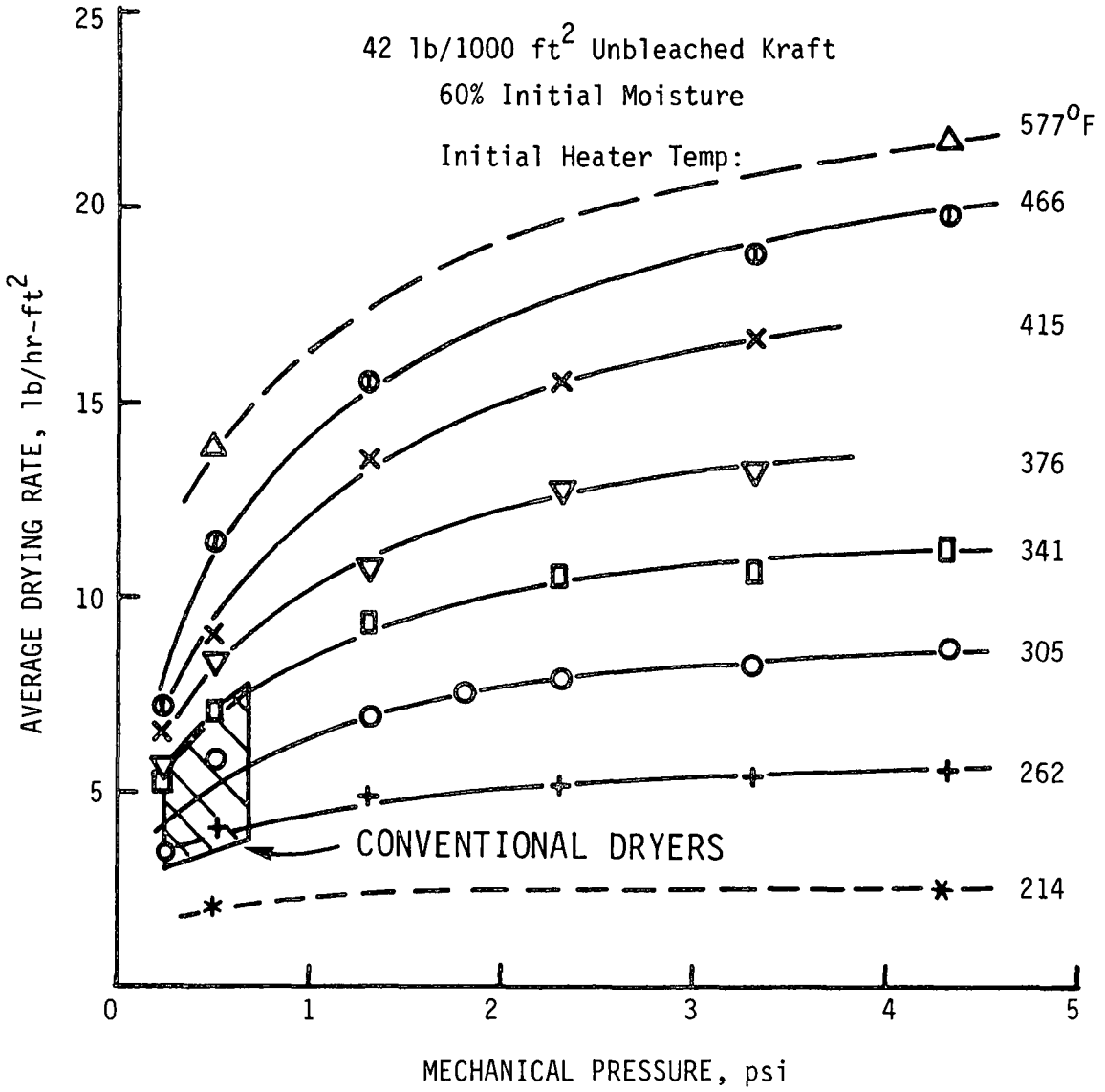

Figure II.4. Average drying rate at elevated temperature and moderately increased mechanical pressure. Unbleached southern softwood kraft, 42 lb/1000 ft^2, 570 CSF, 60% initial mositure.

Considering Fig. II.5 in more detail, it is noted that for a given pressure level the rate of increase of drying rate with heater temperature decreases as the heater temperature increases. This effect is more pronounced for the lower pressures. It is believed that these results are explained by the tendency for the vapor pressure at the web-heater interface to rise as the heater temperature increases, thus counteracting the applied pressure and tending to reduce the degree of contact between the hot surface and paper.

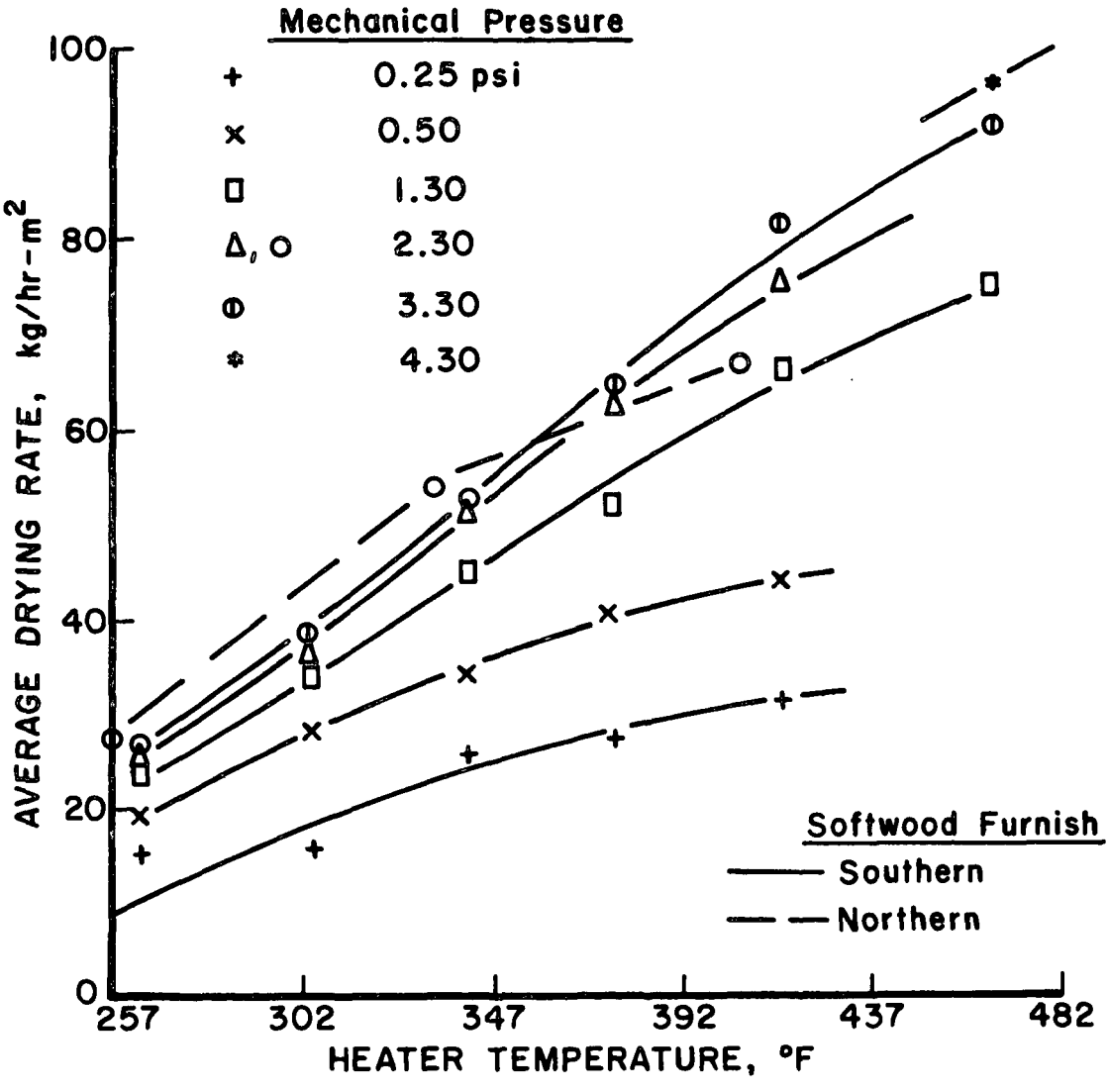

Figure II.5. Cross plot of data from Fig. II.4, with northern softwood kraft handsheet data added.

The limited data derived from tests of the northern softwood handsheets show a trend qualitatively similar to the other data, although the bending begins at a lower surface temperature level. This is possibly due to improved surface contact of the northern softwood handsheets (smoother surface). At lower surface temperature, higher interface temperatures result, and the onset of loss of good contact occurs. Of course, the difference in furnish may play some role as well.

Closer study of Fig. II.4 shows that the benefit of increasing mechanical pressure diminishes rapidly for lower heater temperatures, whereas it persists

to much higher pressures at higher temperature. The physical explanation given for the results shown in Fig. II.5 also explains this behavior. Thus, it can be concluded that to take full advantage of high surface temperature, sufficient web restraint must be used to overcome the tendency of the web to "lift off" from the surface.

The range of experimentally accessible mechanical pressures was extended to 200 psi using the apparatus depicted in Fig. II.2. In a Ph.D. thesis research project nearing completion at the Institute, Devlin[11] has used a heated hydraulic press to perform high-intensity drying experiments at pressures up to 1000 psi. Drying rates from tests in both of these systems are given in Fig. II.6. For reference, some data obtained from Fig. II.4 are also included in Fig. II.6. It is seen that the beneficial effect of pressure on drying rate prevails throughout the entire extended temperature/pressure regime. Maximum drying rates about 20 times typical conventional rates are implied by the 450°F surface temperature data, while rates nearly 100 times conventional ones are found at Devlin's most extreme operating conditions. Clearly, however, mechanical pressures several orders of magnitude greater than those normally associated with dryers are required to achieve these impressive drying rates. Also, high temperature levels are seen to be important to the attainment of very high rates.

It is interesting to note that the "conventional wisdom" (often stated in trade journal articles) is that there is no significant benefit to be gained from increased mechanical pressure in paper dryers. While the data in Fig. II.6 support the contrary conclusion, an element of support for this "wisdom" is displayed by the low temperature (below 300°F) data in Fig. II.4.

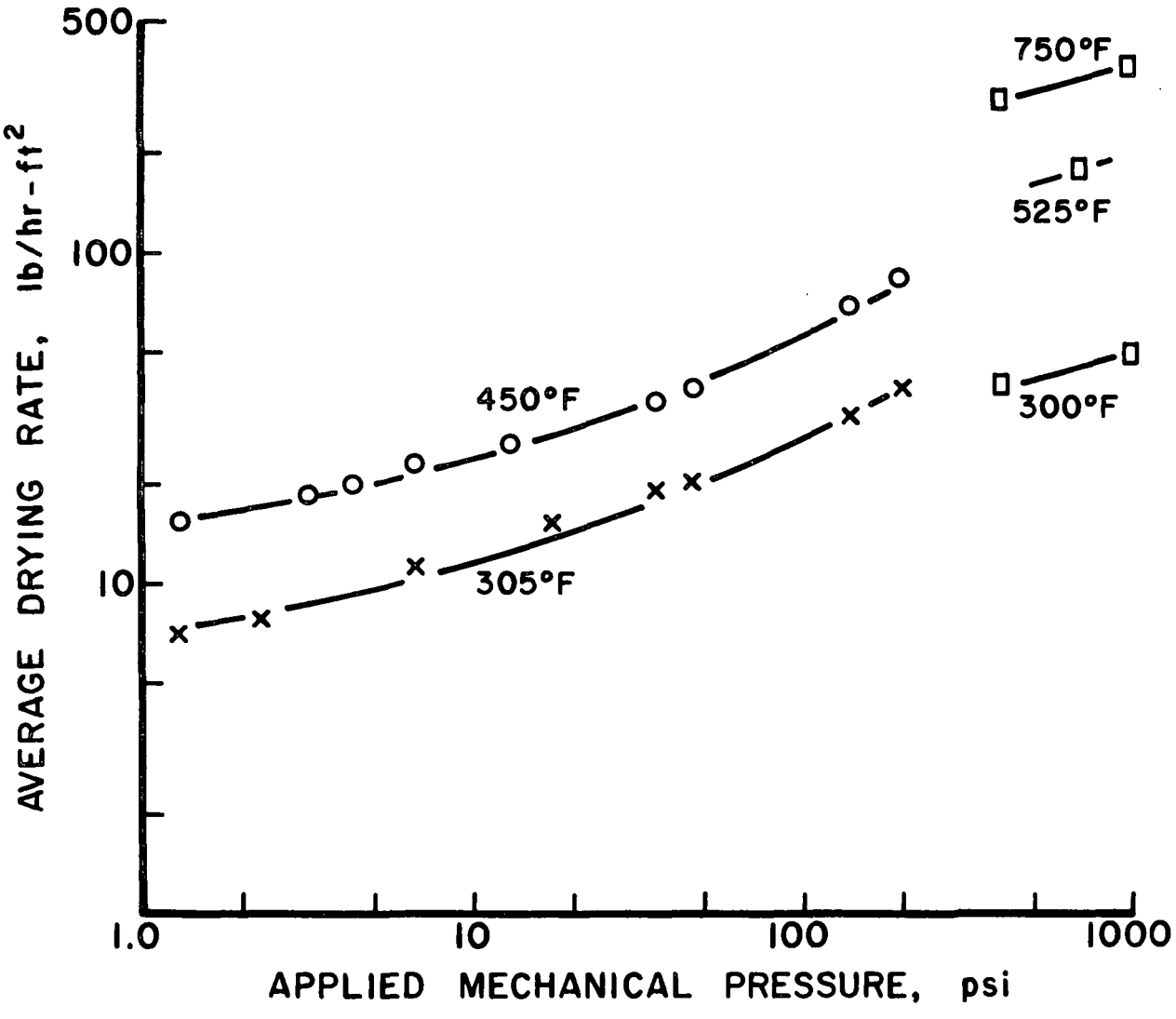

Figure II.6. Average drying rate at higher mechanical pressures. Unbleached southern softwood kraft, 42 lb/1000 ft^2. Data at pressures below 5 psi obtained from Fig. II.4. Data at pressures up to 200 psi: 570 CSF, 60% initial moisture. Data at pressures above 200 psi from Devlin (1984a): 650 CSF, 55% initial moisture content.

The influence of basis weight on drying rate in the elevated temperature/pressure regime has been briefly examined. The results are presented in Fig. II.7. For a given surface temperature, it appears that drying rate is independent of basis weight at low pressure and approaches an inverse proportionality to basis weight at large mechanical pressure. This behavior is explained by noting that the drying rate must be proportional to average heat input rate

(assuming the water removal is entirely by evaporation). Then, at low pressure (i.e., poor thermal contact between sheet and hot surface), the heat transfer is controlled by the contact resistance (which does not depend on basis weight). Conversely, at high pressure (i.e., excellent thermal contact), the heat transfer is controlled by the web internal thermal resistance (proportional to basis weight or caliper). The dependence on surface temperature indicated in Fig. II.7 is less easily explained, but might be due to improved conformability of the surface fibers to the hot surface at higher temperature. This would reduce the contact resistance for a given pressure level.

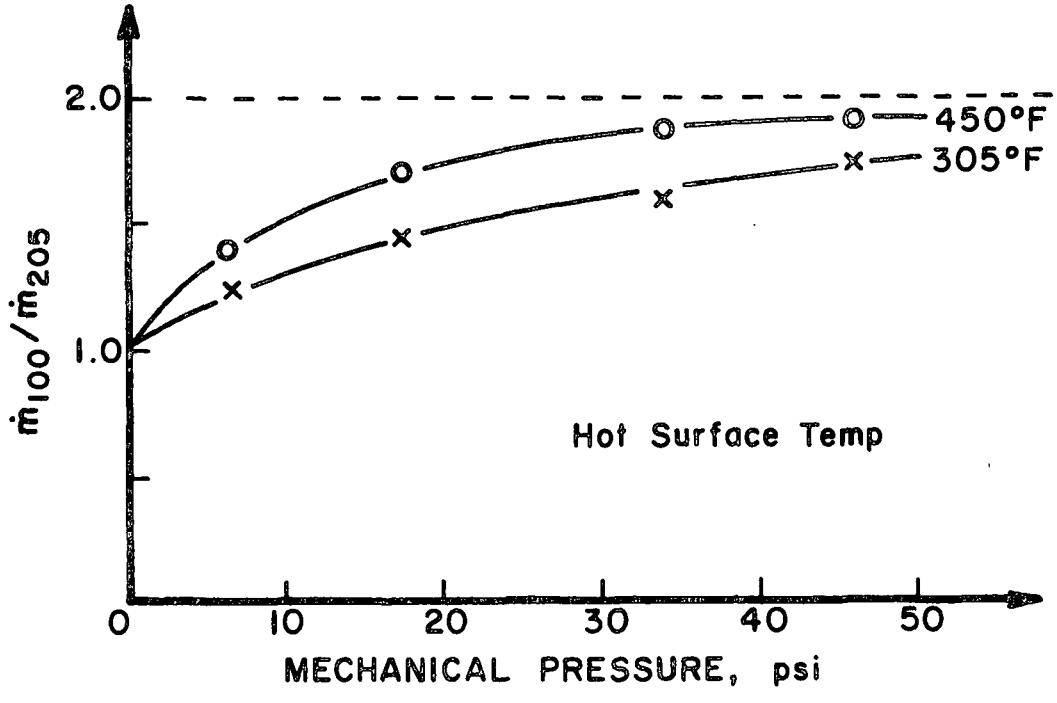

Figure II.7. Ratio of average drying rates for two basis weights, 205 g/m^2 (42 lb/1000 ft^2) and 100 g/m^2. Unbleached southern softwood kraft, 300 CSF, 60% initial moisture.

A very limited investigation of the effect of pulp freeness (300 mL CSF vs. 570 mL CSF) at pressures up to 50 psi was performed, using 205 g/m^2 sheets and a 450°F surface temperature. There was no observed difference in drying

rate over most of the pressure range. At the maximum pressure (and drying rate) the drying rates were still within 3 or 4% of each other, with the lower CSF pulp giving the lower drying rate. While it is expected that the differences should increase at higher pressure (high drying rate), due to internal flow resistance and heat transfer effects, no data are available to quantify this expectation.

Energy Use

The energy required for paper drying is a performance factor having a direct influence on operating cost. Using data from the surface thermocouple inserted in the heated copper block (see Fig. II.2), it is possible to calculate the total heat input to the web during the drying period. A discussion of the technique and its application to development of the process description are presented in the following section. Measured energy values for conditions within the extended temperature/pressure regime are given in Fig. II.8, for mechanical pressures up to about 50 psi. The theoretical energy transfer lines in this figure are based on the energy required for sensible heating of the fiber and water to the boiling point (212°F) and latent heat for evaporation of the water removed (at 212°F). Although there is appreciable scatter, there is fair agreement between theory and experiment. This indicates that within the low to moderate pressure range, the water removal is essentially a pure evaporation process.

Student work in progress, at the very high pressure conditions ascribed to Devlin in Fig. II.6, has yielded significantly lower energy measurements than those indicated in Fig. II.8. This suggests that some liquid-phase water removal occurs at high mechanical pressure. These results will soon be presented by Devlin in his Ph.D. thesis.

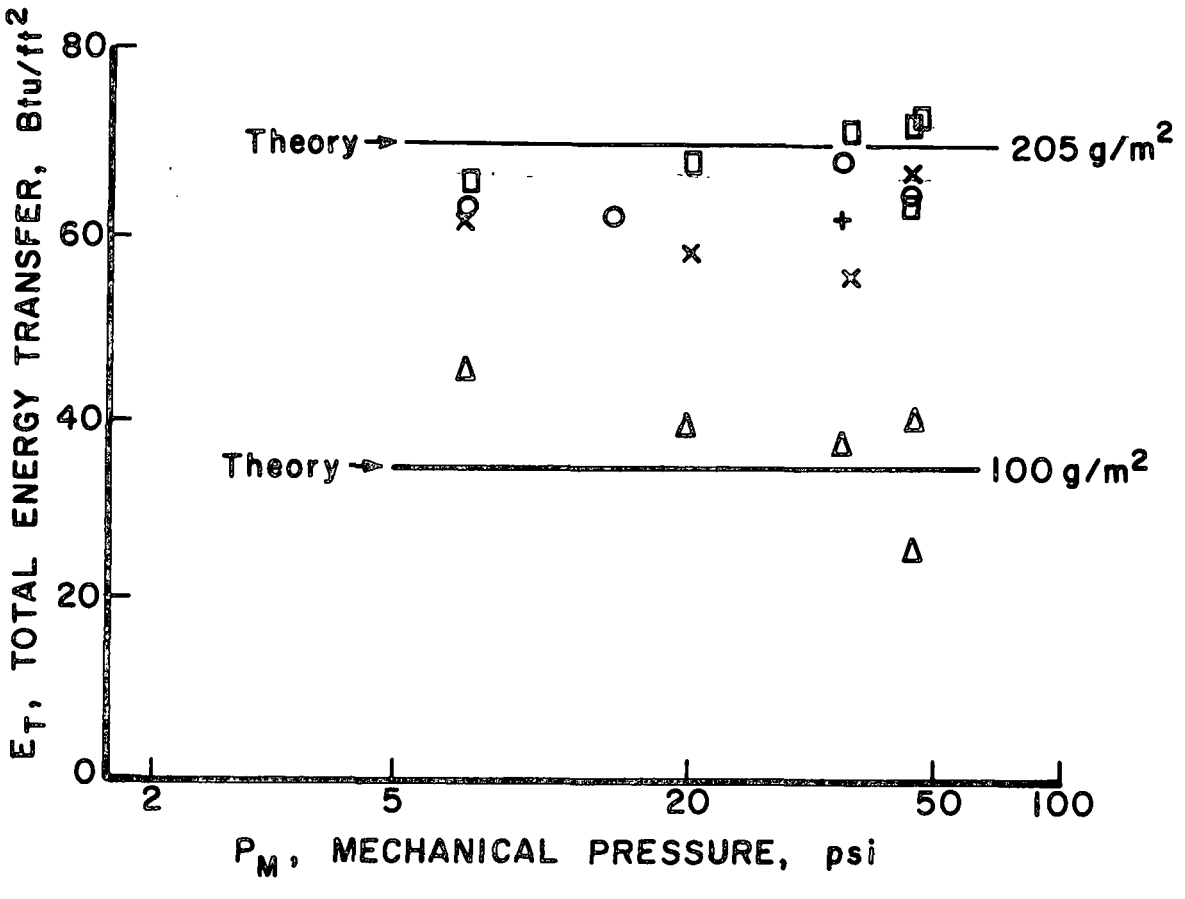

Symbol	Surface Temp.	Basis Weight	CSF
○	450°F	205 g/m^2	570
□	450	205	300
△	450	100	300
+	305	205	570
×	305	205	300

Figure II.8. Total thermal energy transfer to paper web during drying from 60 to 6% moisture content. Unbleached southern softwood kraft.

Properties

At the modest pressures studied with the original apparatus (Fig. II.1), below 5 psi, one would expect no significant effect on strength properties. This expectation was experimentally confirmed. In particular, the apparent

density, tear strength, tensile strength, and elongation were not affected by the combinations of temperature and pressure shown in Fig. II.4. As might be expected, the sheet roughness decreased with greater applied pressure; e.g., at 255°F surface temperature, the roughness decreased by about 40% as the pressure increased from 1.3 to 3.3 psi. In addition, the roughness also decreased with increasing temperature; e.g., at 1.3 psi the roughness decreased by about 45% as the temperature increased from 262 to 415°F.

The porosity measurements indicated that porosity is not affected by the pressure levels considered. However, the porosity slightly decreased as the dryer temperature increased; the decrease was about 12% as the temperature increased from 262 to 415°F.

Based on experiments involving very high pressures (400 to 1000 psi), it has been reported by Devlin[12] that high-intensity drying produces apparent densities on the order of 1.0 g/cm^3, with concomitant increases in tensile and compression strength properties (compared to standard control sheets). In general, the highest surface temperature studied (750°F) caused some degradation in paper properties compared to sheets dried at surface temperatures of 300 or 525°F but at similar pressure levels.

THERMAL/VACUUM DRYING

Experimental System

A bench-scale apparatus capable of providing thermally-induced vacuum operating conditions, including a provision for varying the mechanical pressure applied to the web, has been developed for this project. A simplified schematic diagram of this system is shown in Fig. II.9. The moist mat is dried within a chamber comprising a hot plate, a cylindrical housing, and a copper piston (heat

sink). O-rings are used to provide vacuum seals, and the housing is clamped to the hot plate. The housing, machined from an epoxy/glass fiber composite, has an inside diameter of about six inches. The copper piston is two inches thick and has a hole to facilitate air removal and admission. It is usually operated at room temperature and has a negligible temperature rise during a test, even though it serves as the site for condensation of the vapor removed from the web. The filler material attached to the piston is a stack of plastic screens, approximately one-inch thick. The hot plate is made of copper and is electrically heated. The hot plate contains a pressure tap to permit pressure measurement prior to or during a drying experiment. An earlier version of the system was based on a hot-oil-heated plate, but it proved to be inadequate with respect to surface temperature control.

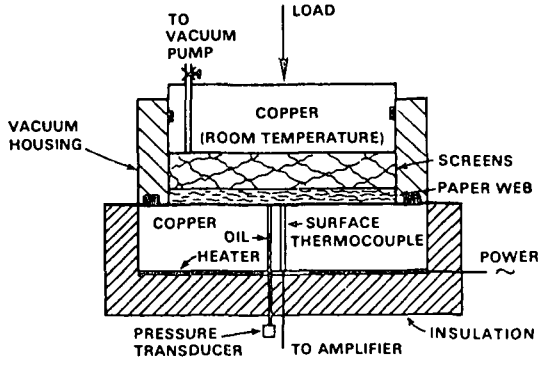

Figure II.9. Schematic diagram of thermal/vacuum drying apparatus, showing configuration during an experiment. For initial evacuation prior to an experiment, the upper copper block, support screens and web are separated from the heated block.

The handsheets are about five inches in diameter. Prior to a test, one is attached to the filler screens with fine threads. The drying test procedure used is as follows. First, the lower copper block is preheated to the desired initial temperature. Then, after attaching a moist handsheet to the filler screens, the piston/filler/handsheet assembly is partially inserted into the

housing, such that the O-ring seal is engaged, but with the mat about one inch above the hot plate. The piston is held in this position for about 30 seconds, during which the vacuum pump removes the air from the system. Next, the vacuum valve is closed and the piston is released. The piston, exposed to a pressure difference of approximately 1 atmosphere, rapidly moves toward the hot plate, initiating the drying period. The effective mechanical pressure applied to the sheet during drying is controlled by means of air cylinders connected between the piston and a load frame (not shown in Fig. II.9). After a desired amount of drying time, the vacuum valve is opened to permit atmospheric air to reenter the chamber. The piston is then rapidly removed and the mat is retrieved and weighed. By also determining the initial and oven-dry weights of the sample, the amount of water removal during the test can be found. For a given hot surface temperature, a series of drying tests having different time durations is performed, so that a drying curve (relative moisture loss vs. time) can be established.

It was found that a small amount (e.g., about 5%) of the initial mat moisture evaporates during the chamber evacuation period. Since this does not constitute true drying, the test data are corrected for this effect.

Water Removal

The paper webs dried in the thermal/vacuum drying study were similar to and prepared in the same manner as the southern softwood kraft handsheets described in Section II.B.2. A single basis weight, 42 lb/1000 ft^2, was used in the test other basis weights and furnishes were deferred in favor of placing project emphasis on the impulse drying process.

For given basis weight and furnish and processing conditions prior to drying, the drying rate should depend on the ambient pressure (thermal/vacuum

vs. atmospheric), the hot surface temperature, and the mechanical pressure pressing the paper web against the hot surface. Due to the reduced boiling point, thermal/vacuum operation is expected to exhibit a higher drying rate than conventional drying for a given surface temperature. However, the mechanical pressures utilized in conventional drying are also considerably lower (less than one psi) than the value (nearly 14.7 psi) which occurs naturally in the thermal/vacuum system (as a result of the atmospheric pressure transmitted to the wet web by means of the piston). In order to clarify the individual roles of the vacuum environment and of the increased mechanical pressure in affecting the thermal/vacuum drying rate, several drying tests have been performed. Tests were done using the thermal/vacuum apparatus at the nominal mechanical pressure, as well as at net mechanical pressures of 3.3 and 41 psi, using an air cylinder to apply a retarding or assisting force which combines with the nominal 14.7 psi loading. Tests were also done in the atmosphere, with a mechanical pressure of about 14.7 psi, using the basic thermal/vacuum setup without the vacuum housing in place.

The combined data from these experiments and from some previous atmospheric tests (reported in Section II.B) are shown in Fig. II.10. Before commenting on the effects of the operating variables, the two most important implications of these data should be emphasized; namely, maximum thermal/vacuum drying rates of up to one order of magnitude greater than conventional rates have been demonstrated and drying rates up to four times conventional are indicated even at surface temperatures below those typically employed in today's dryers!

The data in Fig. II.10 clarify the relative contributions of mechanical pressure and of ambient pressure on the drying rate vs. hot surface temperature relationship. To a rough approximation, the family of thermal/vacuum curves is similar to the atmospheric drying curves with respect to pressure dependence and

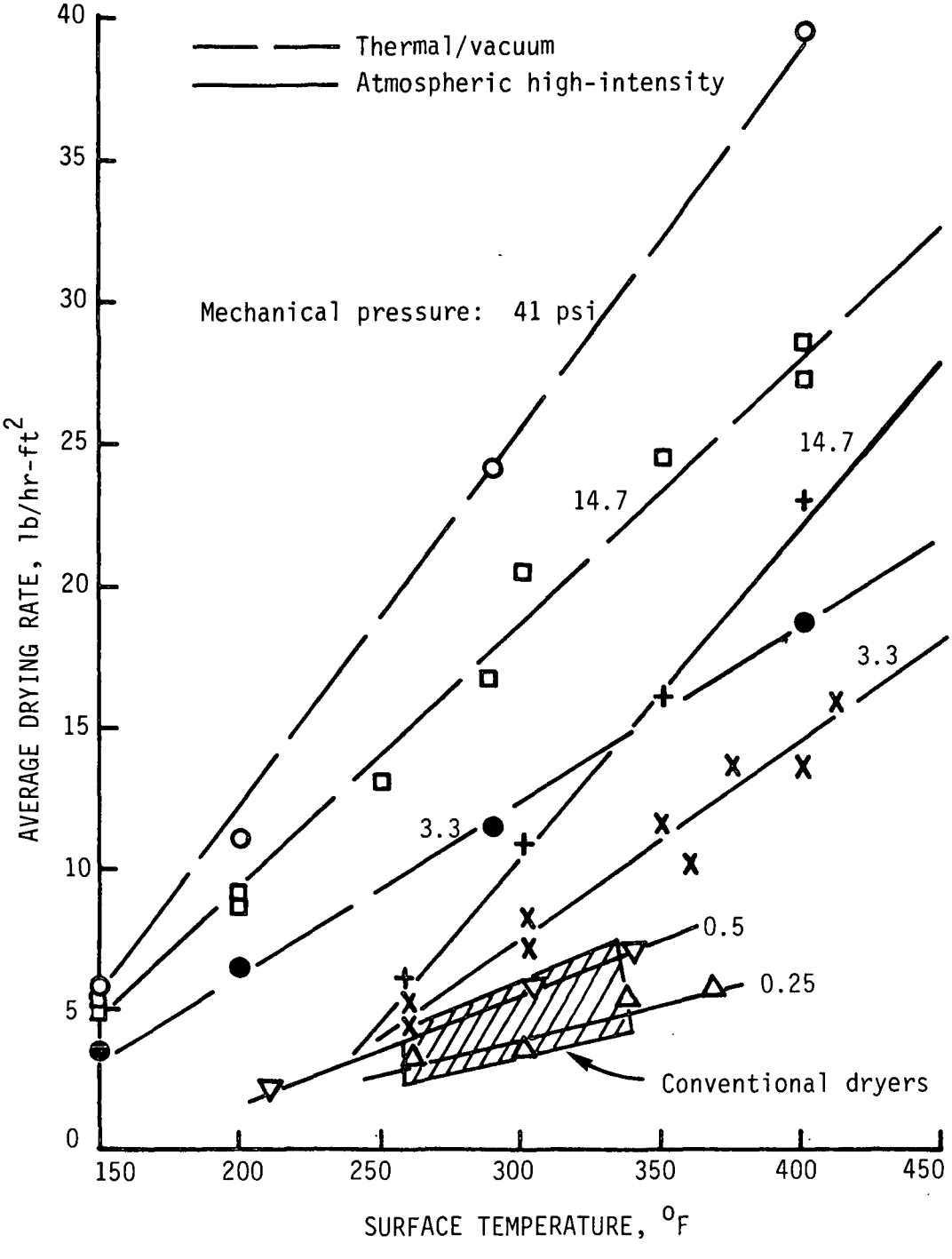

Figure II.10. Experimental average drying rates for southern softwood kraft handsheets (42 lb/1000 ft^2, 570 mL CSF, 60% initial moisture, 6% final moisture - wet basis), under thermal/vacuum and atmospheric high-intensity operating conditions, for various mechanical pressures.

shape, but the curves are simply shifted uniformly to lower temperatures. The amount of temperature shift is in fair agreement with the reduction in boiling point caused by the vacuum. A further discussion of the character of these curves, in the light of a simple theory (two-zone model), will be presented in the following section. For now, suffice it to say that the results in Fig. II.10 are compatible with the idea that thermal/vacuum and atmospheric elevated temperature/pressure drying are conceptually and mechanistically the same high-intensity drying process, only occurring at different ambient pressures.

One of the potential disadvantages of thermal/vacuum drying is the need for preventing a significant quantity of air from entering the drying/vacuum zone. The presence of air would tend to impede the vapor condensation on the cooled surface, tending to raise the effective ambient pressure and, thus, the boiling point in the web. In order to quantify the deleterious effect of air in the system, a series of tests was run for which the air pressure in the vacuum chamber just prior to initiation of drying was varied. The air pressure is set by first evacuating the chamber as in a normal air-free run and then admitting air through the vacuum valve until the desired total pressure and, therefore, air partial pressure is obtained. The drying rate results are presented in Fig. II.11. It should be noted that no external load apart from atmospheric pressure was applied to the piston during these tests. Therefore, when the air pressure is greater, the net mechanical pressure is also lower. Therefore, the decrease in drying rate with air pressure indicated by the Fig. II.11 data may actually be partly due to poorer contact and partly due to increased boiling point (reduced heat input rate). Since, for most of the conditions shown in the figure, the net mechanical pressure exceeds 0.5 atmosphere, it is believed that the change in boiling point is the primary factor causing the observed results. In

any case, the results underscore the need for creating and maintaining low air concentrations if thermal/vacuum drying is to be successfully implemented.

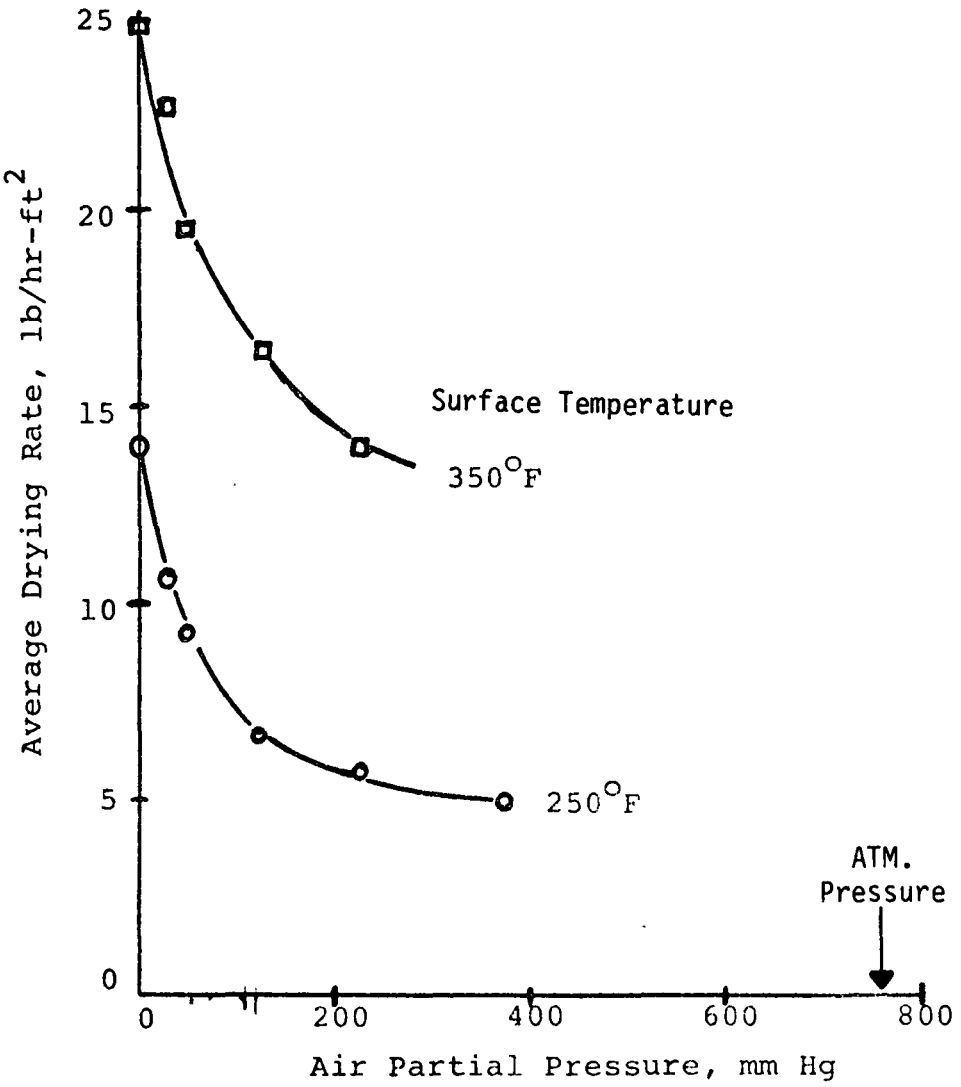

Figure II.11. Effect of vacuum level on average thermal/vacuum drying rate. Southern softwood kraft, 42 lb/1000 ft^2, 570 mL CSF.

Energy Use

Direct thermal energy input measurements, of the type presented in Fig. II.8 for the elevated temperature/pressure regime, were not performed during the thermal/vacuum study. However, in view of the strong similarity of drying rate behavior for the two regimes, discussed above, it seems entirely reasonable to

expect that the energy requirement would also correspond closely with the theoretical amount needed for sensible heating and purely evaporative vapor removal. Other energy-related aspects of thermal/vacuum drying are discussed later in the report.

Properties

The effect of the thermal/vacuum drying process on paper properties has not been thoroughly investigated during this study. The limited tests which were performed agree qualitatively with the findings of Lehtinen,[9] that density (and, thus, strength and stiffness) and surface smoothness are increased over those properties for conventionally-dried sheets. Table II.1 gives a comparison of the density among handsheets dried at typical conventional conditions and at three levels of hot surface temperature in the thermal vacuum system. The increased density resulting from the higher mechanical pressure in thermal/vacuum drying appears to be independent of the surface temperature. This suggests that the potential energy cost benefit of low temperature operation for thermal/vacuum drying will not be offset by adverse property development, due to reduced bonding effectiveness.

Table II.1. Final densities for conventional and thermal/vacuum drying conditions. Southern softwood kraft handsheets, 60% initial moisture content, 42 lb/1000 ft^2, 570 mL CSF.

	Conventional	Thermal/Vacuum with ≈ 14.7 psi		
	290°F, 0.5 psi	150°F	290°F	400°F
TAPPI Density, g/cm^3	0.47	0.61	0.59	0.60

To further evaluate the influence of the vacuum drying process on final density, some drying runs were made for which the drying time and applied pressure were held constant. In each case, this required a higher surface temperature

for atmospheric drying than for thermal/vacuum drying. Two sets of results of such experiments are given in Table II.2. These results do indicate a slight density reduction at lower temperature (vacuum) conditions, but the effect decreases in importance at higher applied pressure (Case II). This is the expected condition in any practical implementation of thermal/vacuum drying.

Table II.2. Final densities for atmospheric and thermal/vacuum drying at fixed mechanical pressure and drying time. Southern softwood kraft hand sheets, 42 lb/1000 ft^2, 570 mL CSF, 60% initial moisture content.

	Case I (3.3 psi)		Case II (14.7 psi)	
	Vacuum, 150°F	Atmosphere, 245°F	Vacuum, 150°F	Atmosphere, 250°F
TAPPI Density, g/cm^3	0.50	0.53	0.58	0.57
IPC Density, g/cm^3	0.53	0.56	0.72	0.74

It should be noted that the amount of density change produced by the higher-than-conventional mechanical pressure levels associated with thermal/vacuum drying is probably greatly overstated by the data in Table II.1 and 2. This is because the handsheets were prepared at TAPPI standard pressing conditions rather than at typical wet pressing pressure levels. Therefore, the impact of thermal/vacuum drying on properties would probably be quite modest, in practice.

IMPULSE DRYING

Experimental Systems

Heated Drop Press

Since impulse drying refers to the process of water removal and web consolidation within a heated press nip, a modified version of the Wahren-Zotterman "press simulator" (a drop-press) is an obvious choice for use in the

study of this process. Most of the early data were derived from experiments performed in the heated drop press shown schematically and photographically in Figs. II.12 and 13, respectively. A Variac connected to the electrical heater is used to set the temperature of the block at the desired level (usually between 300 and 900°F) prior to a test. The carriage, sometimes carrying extra weight in addition to the heated block assembly, is released to initiate a test run. Three variables - the initial carriage height and weight, and the rubber pad thickness - can be adjusted to obtain the desired peak pressure and nip residence time combination. The details of the pressure-time pulse are obtained from the output of a load cell in the pedestal on the base of the apparatus. In practice, it is difficult to achieve nip residence times greater than about 15 ms with this system. Longer times can be achieved by attaching interspersed layers of weight and rubber pads to the carriage or by connecting an air spring between the pedestal/felt and the base plate.

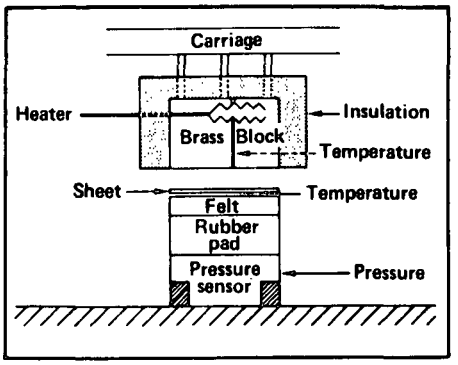

Figure II.12. Typical version of the heated drop press used in impulse drying study. Other versions employed copper and steel heated blocks.

Heated Roll Press

In order to significantly extend the nip residence times and peak pressures experimentally available for the impulse drying study, as well as to

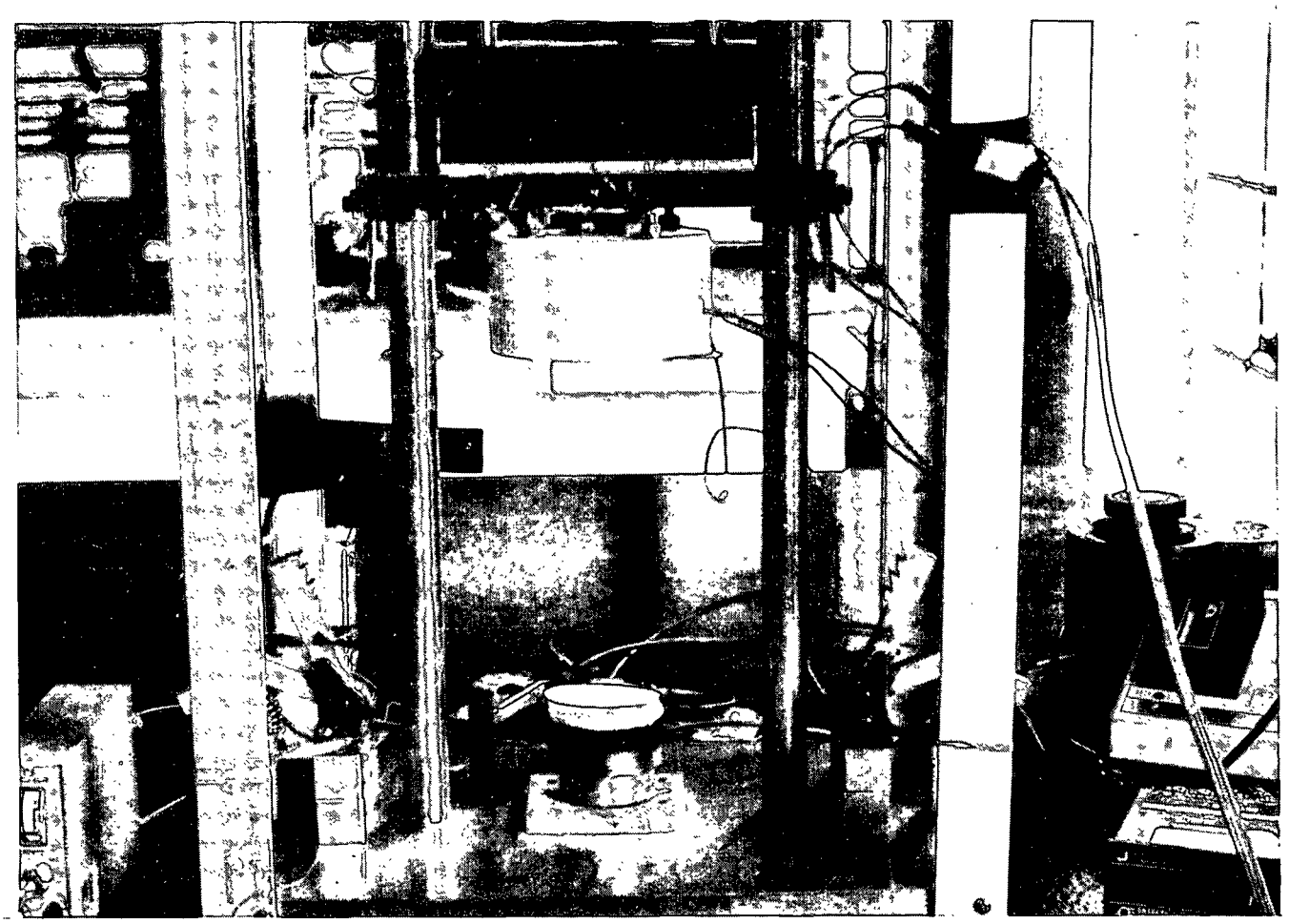

Figure II.13. A heated drop press used in impulse drying study.

demonstrate the concept in a press roll configuration, the heated roll system depicted in Fig. II.14 was constructed. The hot roll is preheated with a bank of gas burners. Temperature levels up to 800°F are readily achieved in the present configuration. A "test sandwich" is employed in drying experiments, comprising a moist web/felt* sandwich having a 3-inch width. This is fed through the rolling nip. Within the range of practical forces in the apparatus, nip loadings up to about 880 pli are readily applied by means of the air

*The felt used initially was an Albany International high temperature-resistant felt called DURAPLANE™; its web is of Du Pont Nomex fibers. The felt weight is 4.5 ozs/ft^2.

cylinder. The small-diameter, hard rolls, combined with the typical test sandwich, result in nip widths of approximately 0.5 inch. Thus, average pressures up to about 1760 psi can be applied to the web during impulse drying with the present configuration. Using the variable-speed drive and two variations of the pulley system, a range of nip residence times from 10 to 200 ms has been employed in the drying experiments performed in this system.

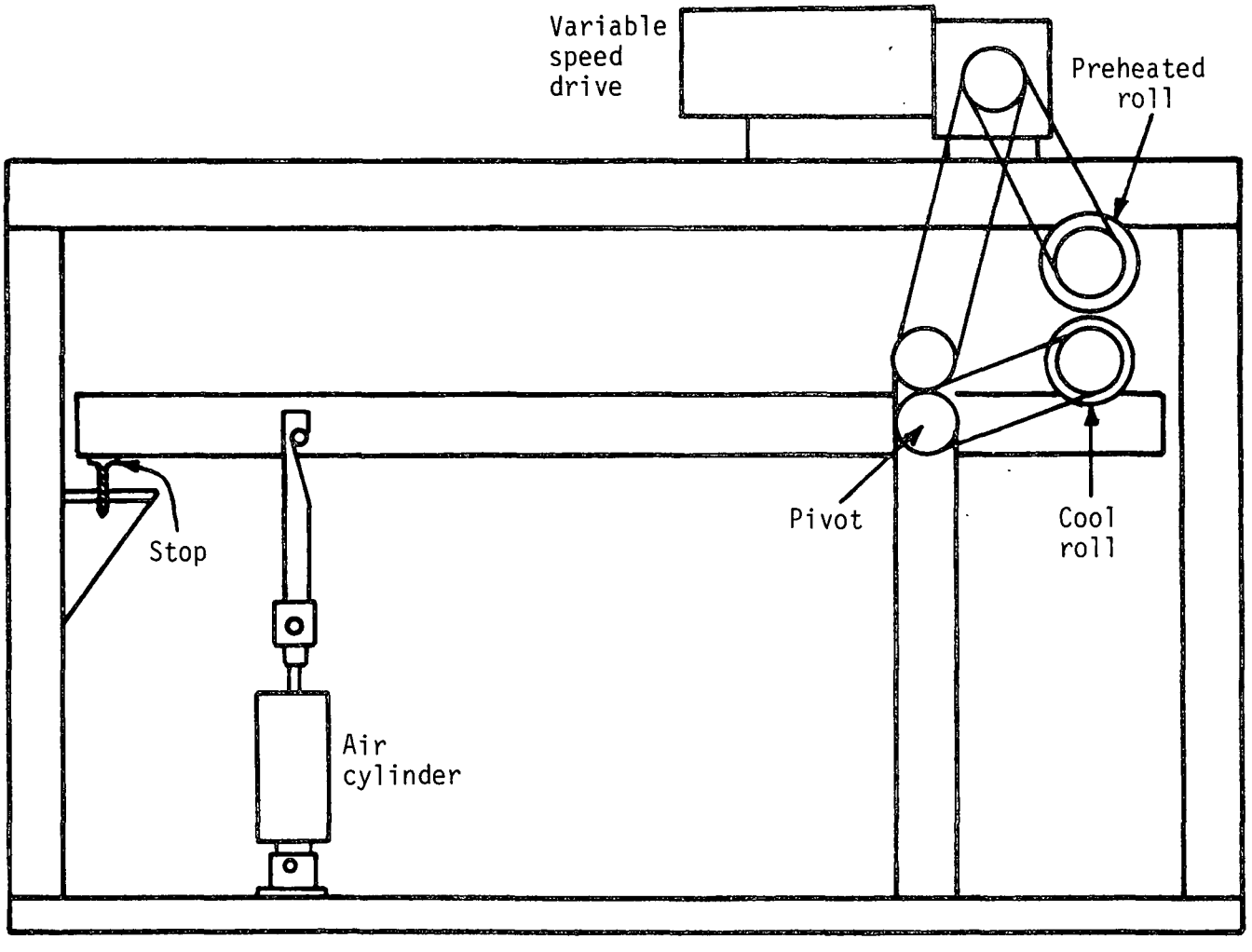

Figure II.14. Schematic diagram of heated roll impulse dryer.

Water Removal

As with the other two drying regimes investigated, the impulse drying research completed so far has tended to emphasize water removal performance.

Numerous experiments have been performed in both the heated drop press and the heated roll systems. Before considering results of these experiments, it is worth noting an important (but somewhat arbitrary) distinction between the impulse drying concept and other drying methods, that leads to a differnce in the mode of presentation of water removal results. That is, impulse drying is identified with the use of pressinglike equipment, for which "nip residence time (NRT)" constitutes a meaningful "independent variable," with the resulting sheet moisture loss (or RMR) becoming a dependent variable. The other two regimes, elevated temperature/pressure and thermal/vacuum drying, are more identifiable as extensions to conventional drying technology, thus making total moisture removal a meaningful independent (and, ususally, fixed) parameter, with drying time (or, equivalently, drying rate) becoming a dependent variable.

Early impulse drying experiments were performed to clarify the differences between impulse drying and conventional pressing and drying, by determining the effects of initial sheet moisture content (or dryness), surface temperature (hot vs. room temperature), and furnish variables on water removal. Some results of these experiments are given in Fig. II.15-17. Data in the first of these figures indicate that significant dryness changes (e.g., 10 to 20%) are possible with a hot press nip and reasonable nip residence times. As would be expected, performance is better for higher freeness sheets.

Figures II.16 and 17 emphasize the great increases in water removal for impulse drying as compared to that for room temperature pressing. The increases are much greater than have ever been reported for the usual "hot pressing" (heated web) operation.

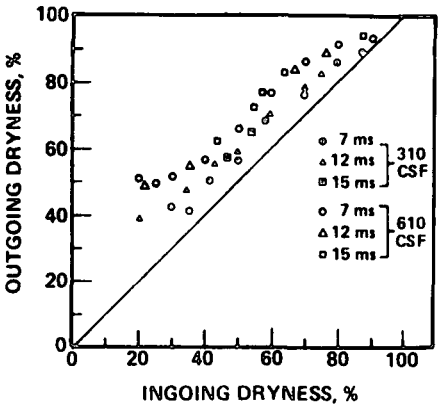

Figure II.15. Outgoing sheet dryness after one impulse as a function of ingoing dryness, bleached kraft, 45 g/m^2, peak pressure 400 psi, hot surface temperature 600°F.

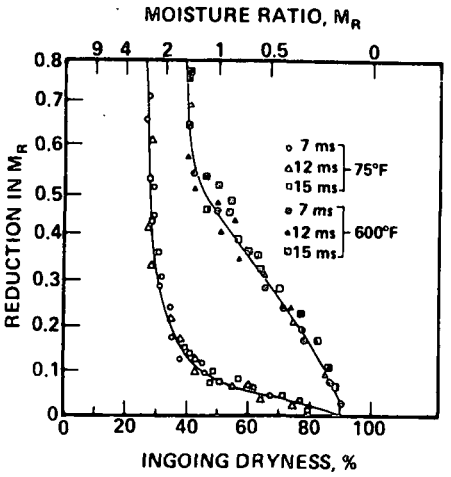

Figure II.16. Reduction of moisture ratio as a function of ingoing dryness for three nip residence times. Bleached kraft, 45 g/m^2, 610 CSF, maximum pressure 400 psi.

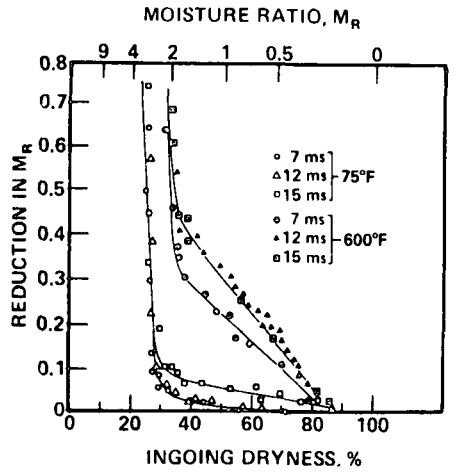

Figure II.17. Reduction of moisture ratio as a function of ingoing dryness for three nip residence times. Bleached kraft, 45 g/m^2, 310 CSF, maximum pressure 400 psi.

If one converts data on the quantity of water removed by impulse drying to an apparent water removal rate (based on nip residence time), extremely large values are found, even at ingoing dryness values normally associated with dryer section operation. Figures II.18 and 19 exhibit the apparent water removal rates for two initial drynesses and two furnishes; the effects of surface temperature and peak pressure are indicated. It is not really valid to compare these rates with the average drying rates presented earlier in this report because of differences in basis weight and final dryness (both of which favor a higher drying rate for the impulse-dried sheets). However, it is still worth noting that even the 45% initial dryness results are orders of magnitude greater than any paper drying rates heretofore observed for this dryness and basis weight range. It is certainly fair to conclude that major breakthroughs in water removal technology can be expected based on the impulse drying principle.

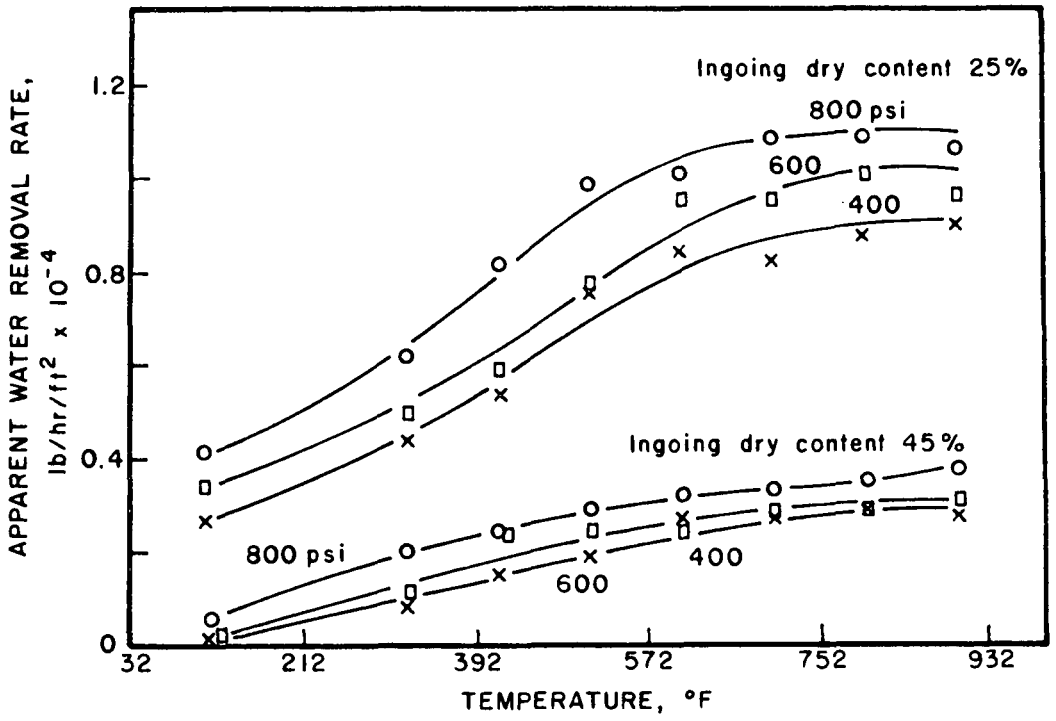

Figure II.18. Effect of initial hot surface temperature and peak pressure on the apparent rate of water removal for two levels of dryness of the sheet prior to impulse drying. Basis weight 45 g/m^2, reslushed newsprint. Nip residence time 4.5 ms.

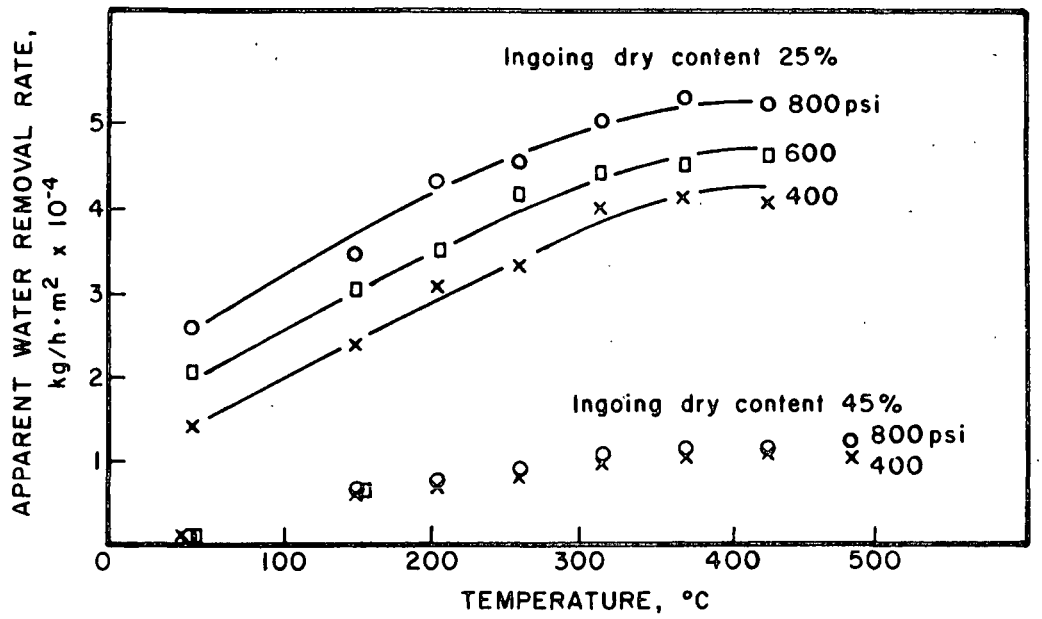

Figure II.19. Effect of initial hot surface temperature and peak pressure on the apparent rate of water removal for two levels of dryness of the sheet prior to impulse drying. Basis weight 45 g/m^2, bleached kraft at 140 CSF. Nip residence time 4.5 ms.

Most of the impulse drying data discussed so far were obtained in experiments in which the paper sample was "strapped" to the pedestal/felt. Eventually, it was suspected that this technique was not adequately holding the samples to the pedestal. The result would be a tendency for adhesion of the sheet to the hot block during part of the rebound. If correct, this would mean that the actual contact time would exceed that measured from the applied pressure pulse record. The remaining data to be presented (from both the drop press and the roll press) were obtained, except where noted otherwise, from experiments in which a thin coating of a releasing agent (usually silicone) had been previously applied to the hot surface. It is believed that a more well-defined release of the sheet from the surface occurs when using this method. This is supported by the fact that the more recent water removal results tend to be slightly lower, but more reproducible than the earlier values when similar test conditions are

considered. The issue of adhesion has obvious practical ramifications; a further examination of adhesion is discussed later in this section.

One series of experiments was performed with the goal of quantifying the heat transfer rate and total heat input to the web as a function of surface temperature. The energy-related results are discussed later in this section, but the corresponding water removal data are given here (Fig. II.20) for future reference. The data in this figure indicate that at the highest temperature level over half the water in the sheet can be removed in a single impulse of reasonable duration (11 ms).

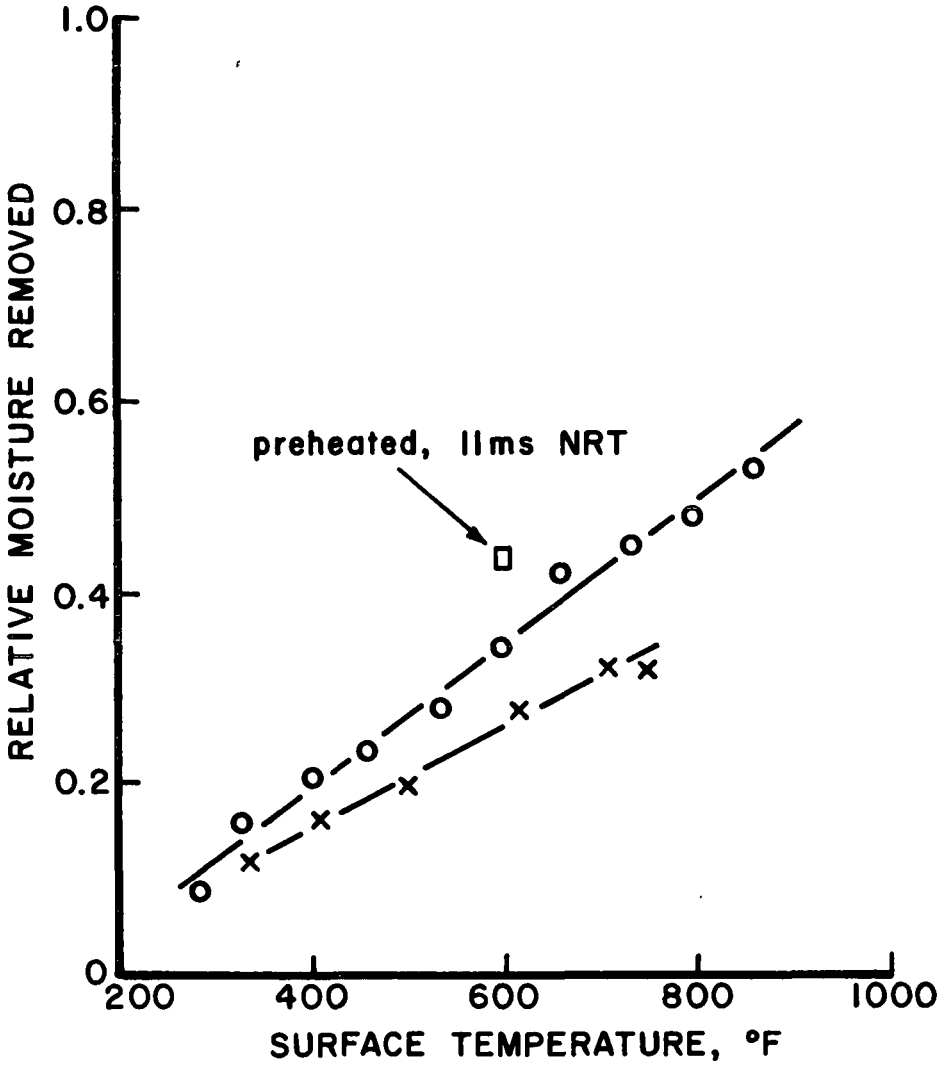

Figure II.20. Water removal in impulse drying. Primary linerboard stock, 600 mL CSF, 50 g/m^2, 40% initial dryness. Peak pressure: 800 psi, nip residence times: x = 8 ms, o = 11 ms. Steel heated block with 0.1 mil chrome-plated surface.

A very exciting finding is also indicated in Fig. II.20. If the web is preheated (e.g., by low pressure steam) to a temperature near the boiling point (~ 210°F), a considerable enhancement in water removal results. It is likely that this phenomenon occurs because all the heat transfer to the preheated web is immediately useful for producing a water removal effect, with no initial time delay while web heatup occurs. Since a presteaming operation would be comparatively easy to implement, it appears that this would be a preferred feature of an impulse drying system. Some additional preheating experiments have been performed, with the results summarized in Table II.3. All of the preheating test results confirm that an extra 10% or more of the water initially in the web can be removed during a given impulse if this technique is employed.

Tabel II.3. Effect of web preheating (to ~ 210°F) on water removal in impulse drying. Conditions: 50 g/m^2 sheets, 40% initial dryness, 750-800 psi peak pressure, 600°F surface temperature, 9-11 ms nip residence time.

	RMR, % (nonpreheated)	RMR, % (preheated)
1. Unbleached southern softwood kraft, 570 mL CSF	40.3	51.6
2. Bleached northern softwood kraft, 300 mL CSF	34.9	47.8
3. Bleached northern softwood kraft, 680 mL CSF	64.7	75.9

During the exploratory study, a limited investigation of water removal from lightweight, tissuelike samples was performed. The results are presented in Fig. II.21. For the case of a dry felt and 60% ingoing dryness, it is seen that complete drying can be accomplished with a 5 ms nip residence time and a surface temperature of at least 450°F. Unfortunately, the effect of a moist felt, common in tissue production, has not as yet been investigated. Furthermore, because of the high machine speeds in tissue-making, the 5 ms nip residence

time corresponds to a rather wide press nip. Finally, it should be mentioned that the impulse drying produced sheet with a smooth, glossy surface.

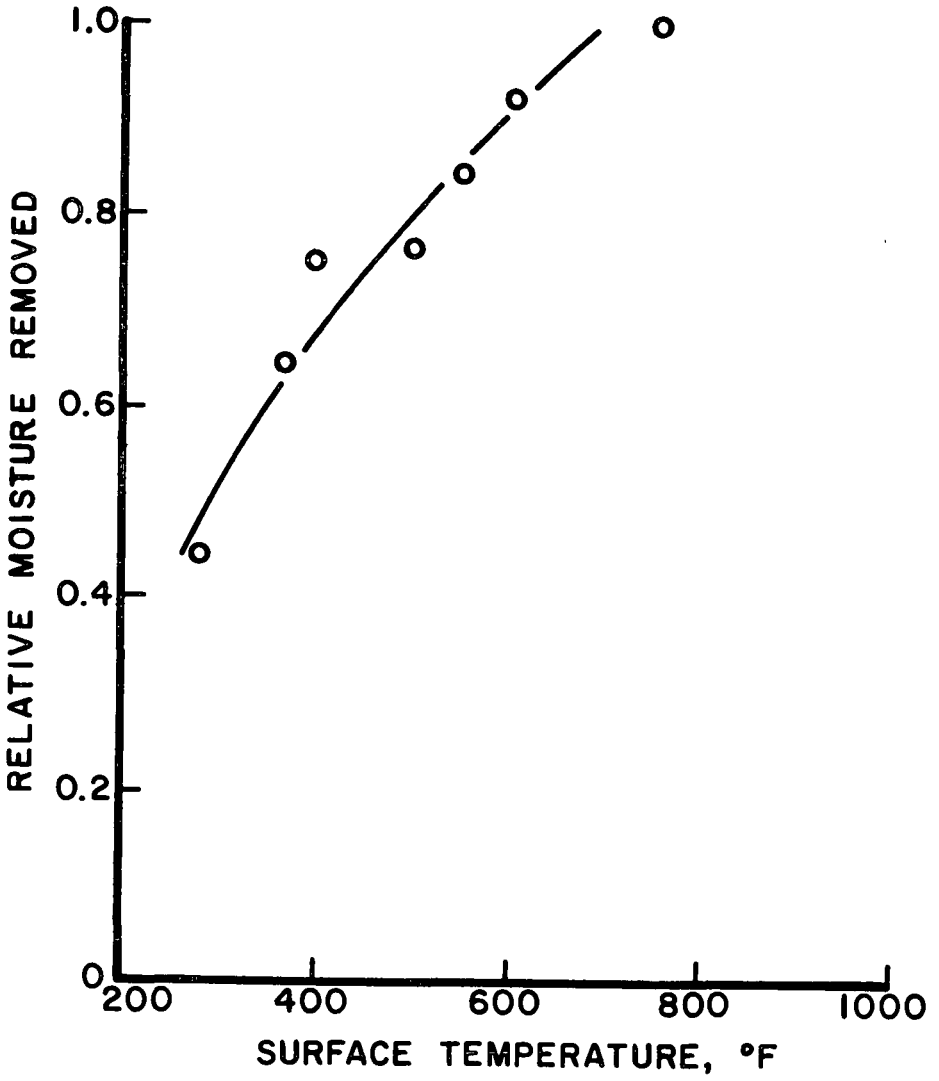

Figure II.21. Impulse drying of tissue. Bleached southern softwood kraft, 400 mL CSF, 12 g/m^2, 60% initial dryness. Peak pressure: 625 psi, nip residence time: 5 ms, dry felt.

Whereas nearly all of the impulse drying experiments performed during the exploratory study involved single impulse application, one preliminary test of a two-impulse process was run. The objectives were to determine the extra amount of water removal resulting from the second impulse (applied immediately after

inverting the sheet on the pedestal of the drop press) and to examine the appearance of the sheet after drying. Using sheets and test conditions similar to those described in Fig. II.20, a surface temperature of 600°F, and a 12 ms nip residence time per impulse, it was found that the RMR is 41% after the first impulse and a total RMR of 66% after the second. Thus, about 60% as much water is removed during the second impulse as during the first. Interestingly, this result is in fair agreement with expectations based on application of data in Fig. II.16. This implies that the smooth surface attained in the first impulse does not materially impede water removal in the second impulse relative to that which would occur with a "fresh" sheet. With regard to final sheet appearance, it was found that some of the smooth, glossy texture of the side first pressed against the hot surface is lost when it is subsequently pressed against the felt; the opposite side does attain considerable gloss and smoothness. The net result of the two-impulse process is a sheet with two relatively similar surfaces. Overall, the two-impulse test results suggest that a dryer system involving two (or more) impulse steps should prodcue no adverse effects, compared to use of a single (longer time) impulse application. This further implies that considerable latitude in the engineering design of impulse drying system will be available.

Compared to the heated drop press, the heated roll impulse dryer (Fig. II.14) permits longer nip residence time experiments at higher peak pressures to be conveniently performed. Consequently, impulse drying of heavier basis weight sheets can be more adequately studied with this system. Sheets of 100 g/m^2 basis weight have been tested extensively in the heated roll system; the water removal results are presented in Figs. II.22-25. While the maximum

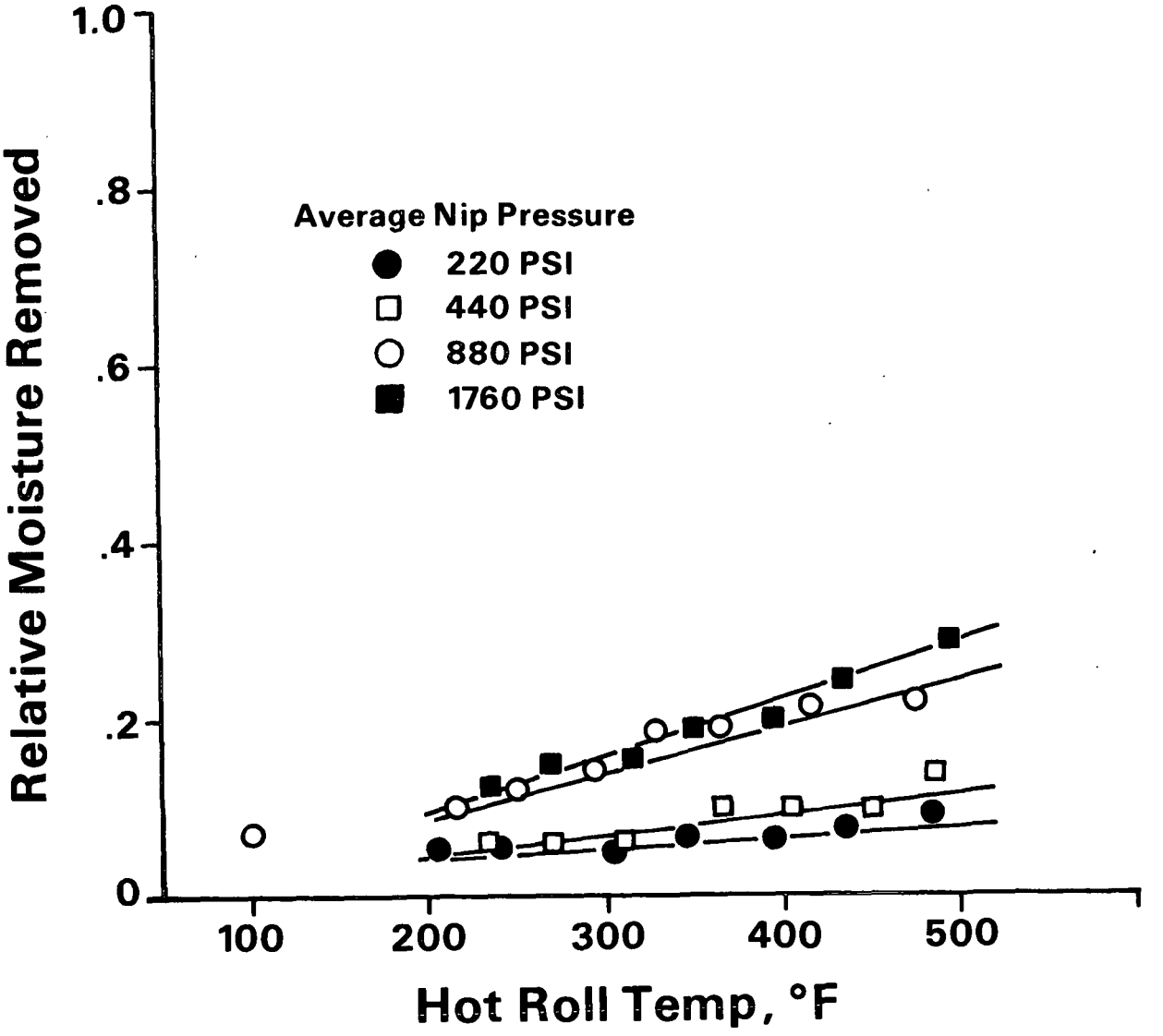

Figure II.22. Relative moisture removed vs. hot roll temperature for 100 g/m^2 sheets at 10 ms nip residence time. Unbleached southern softwood kraft, 570 mL CSF, 58-60% initial moisture content.

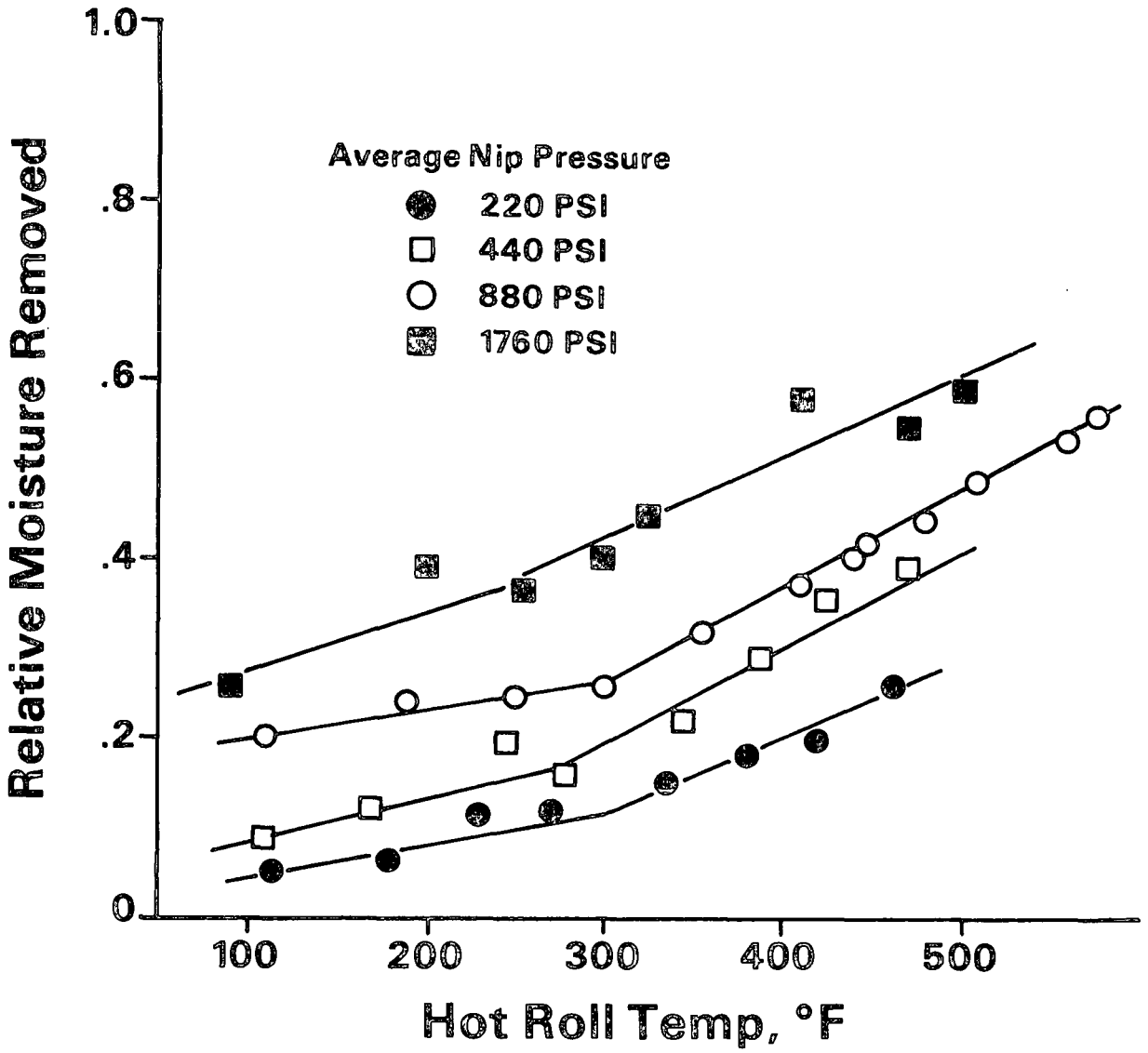

Figure II.23. Relative moisture removed vs. hot roll temperature for 100 g/m^2 sheets at 40 ms nip residence time. Unbleached southern softwood kraft, 570 mL CSF, 58-60% initial moisture content.

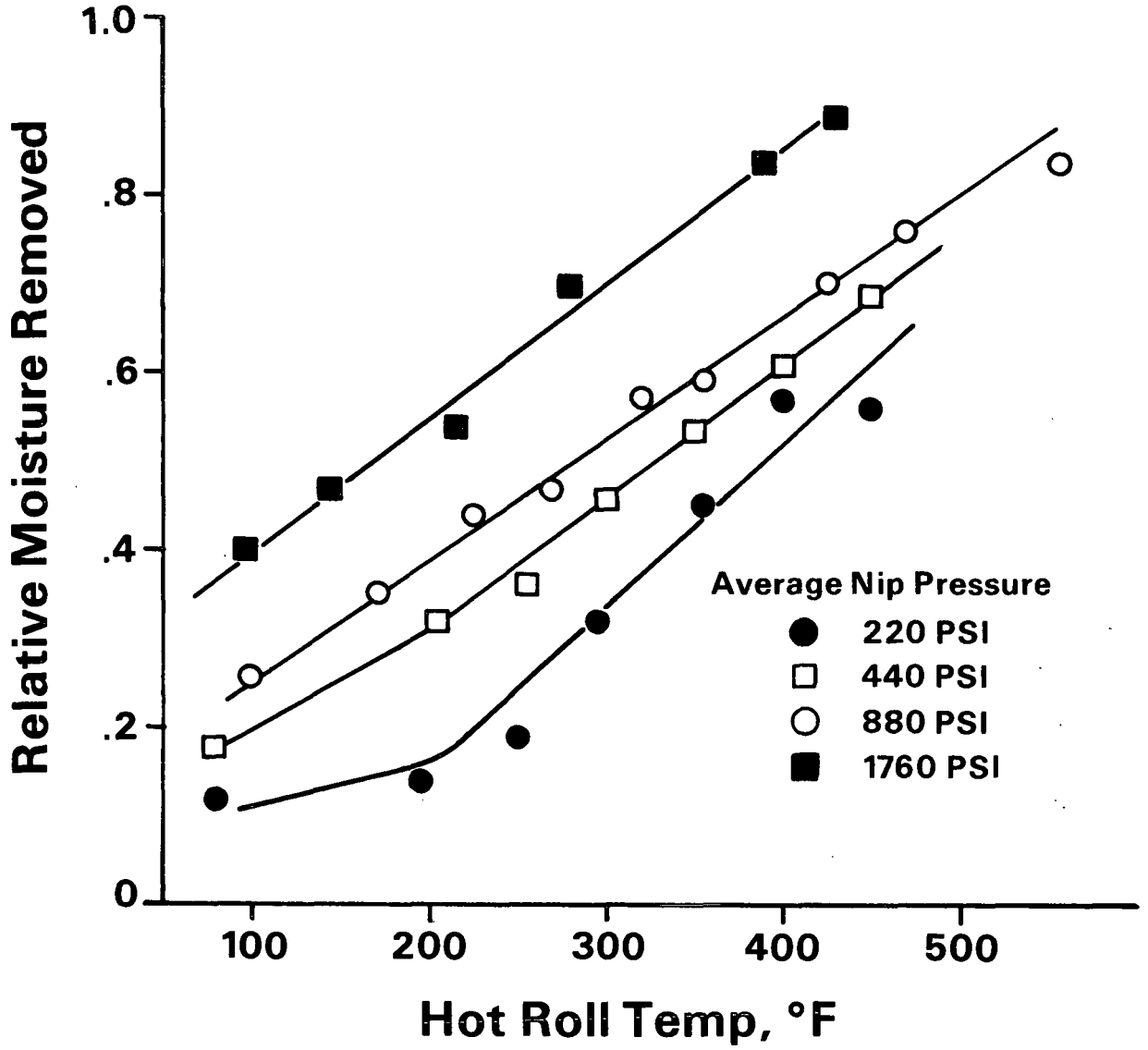

Figure II.24. Relative moisture removed vs. hot roll temperature for 100 g/m^2 sheets at 100 ms nip residence time. Unbleached southern softwood kraft, 570 mL CSF, 58-60% initial moisture content.

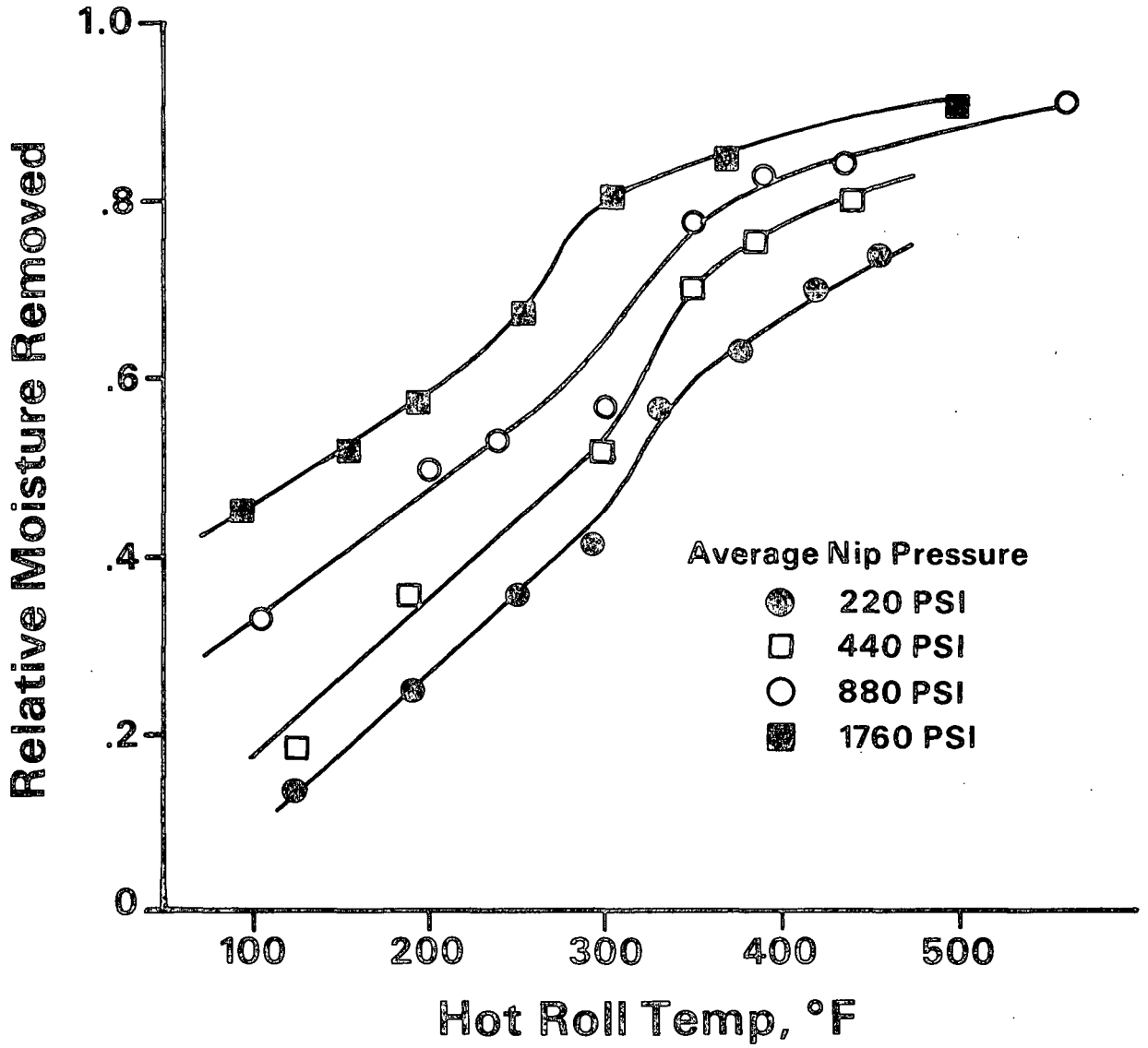

Figure II.25. Relative moisture removed vs. hot roll temperature for 100 g/m^2 sheets at 180 ms nip residence time. Unbleached southern softwood kraft, 570 mL CSF, 58-60% initial moisture content.

average pressure and nip residence time encompassed in these tests (1760 psi and 180 ms) certainly exceed practical values, it is established in Fig. II.25 that a fairly heavy sheet can be almost completely dried in a single impulse at these conditions, using a reasonable surface temperature.

In order to facilitate the consideration of temperature-nip residence time tradeoffs, data from tests at temperature levels up to 800°F have been used to develop the performance maps shown in Fig. II.26 and 27. It is seen that for very high pressure and temperature the majority of the water in the sheet can be removed in times commensurate with those prevailing in an extended nip (e.g., 20 to 30 ms).

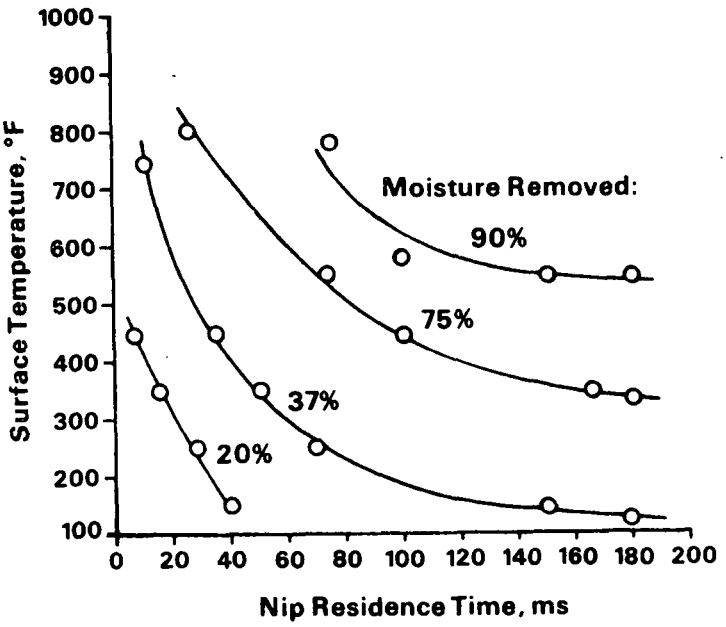

Figure II.26. Relative moisture removed during impulse drying: 100 g/m^2 unbleached softwood kraft handsheets (570 CSF) at 58% initial moisture content, with 880 psi average mechanical pressure applied.

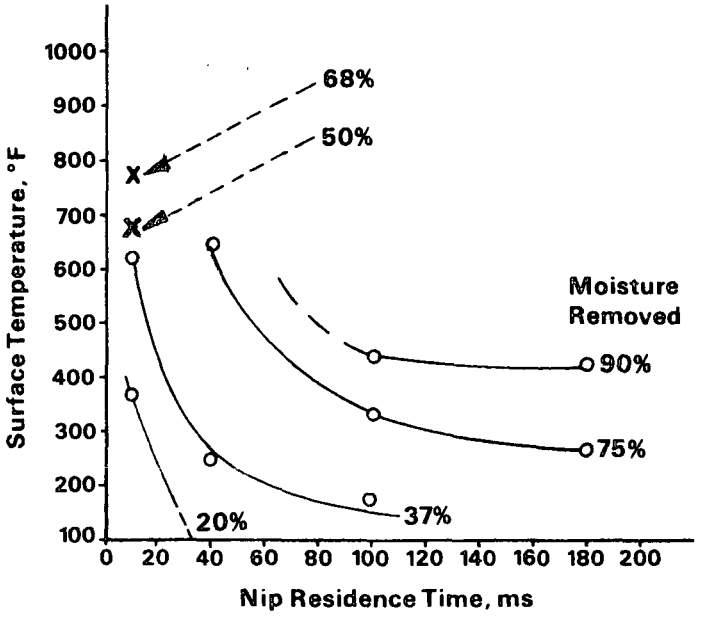

Figure II.27. Relative moisture removed during impulse drying: 100 g/m^2 unbleached softwood kraft handsheets (570 CSF) at 58% initial moisture content, with 1760 psi average mechanical pressure applied.

A final point worth noting about the long nip residence time experiments in the heated roll system is that they involved pressure-time pulses qualitatively similar in shape to those in the drop press (i.e., a "bell-shaped" curve). However, in practice, a long nip residence time would probably be produced in an extended nip configuration having a more "square" pulse shape. Thus, experiments to delineate the effect of pulse shape on impulse drying are needed.

While the results of heated roll experiments discussed so far were based on use of a releasing agent (silicone oil) on the hot roll, one test series was used to explore the effect of postnip contact, which would occur if adhesion between the sheet and the hot surface takes place. Tests were run with the location of a doctor blade as a variable (or, equivalently, the postnip contact time). Control tests involved use of the releasing agent. The results are given in Fig. II.28. It is evident that the majority of the water removal

results from the effect of the hot nip alone. However, an appreciable portion (e.g., 30%) results from the extra contact, in spite of the fact that there is no applied pressure during this time.

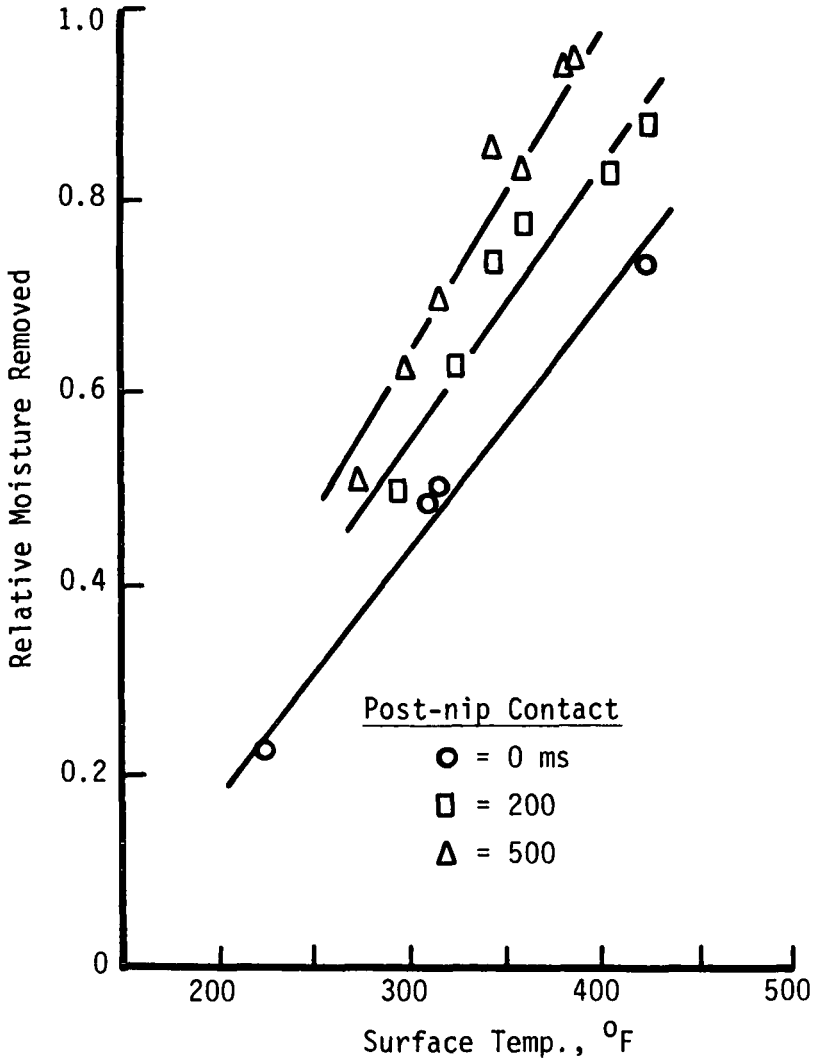

Figure II.28. Effect of postnip contact between sheet and hot surface on water removal in impulse drying. Unbleached southern softwood kraft, 570 mL CSF, 100 g/m^2, 58-60% initial moisture, 100 ms nip residence time, 883 psi average pressure.

Energy Use

In addition to the excellent water removal performance of impulse drying, it appears that this process will also be advantageous with respect to energy

utilization. Using a surface thermocouple in the heated block of the drop press system as a means for the measurement of heat transfer into the web, the data shown in Fig. II.29 were obtained. The trends of increased energy transfer with increasing nip residence time and increasing surface temperature are as expected from physical considerations. In particular, the variation with surface temperature is compatible with the idea that the overall driving force for heat transfer is the difference between the surface temperature and the initial web temperature (≈ room temperature for all but one of the data points shown).

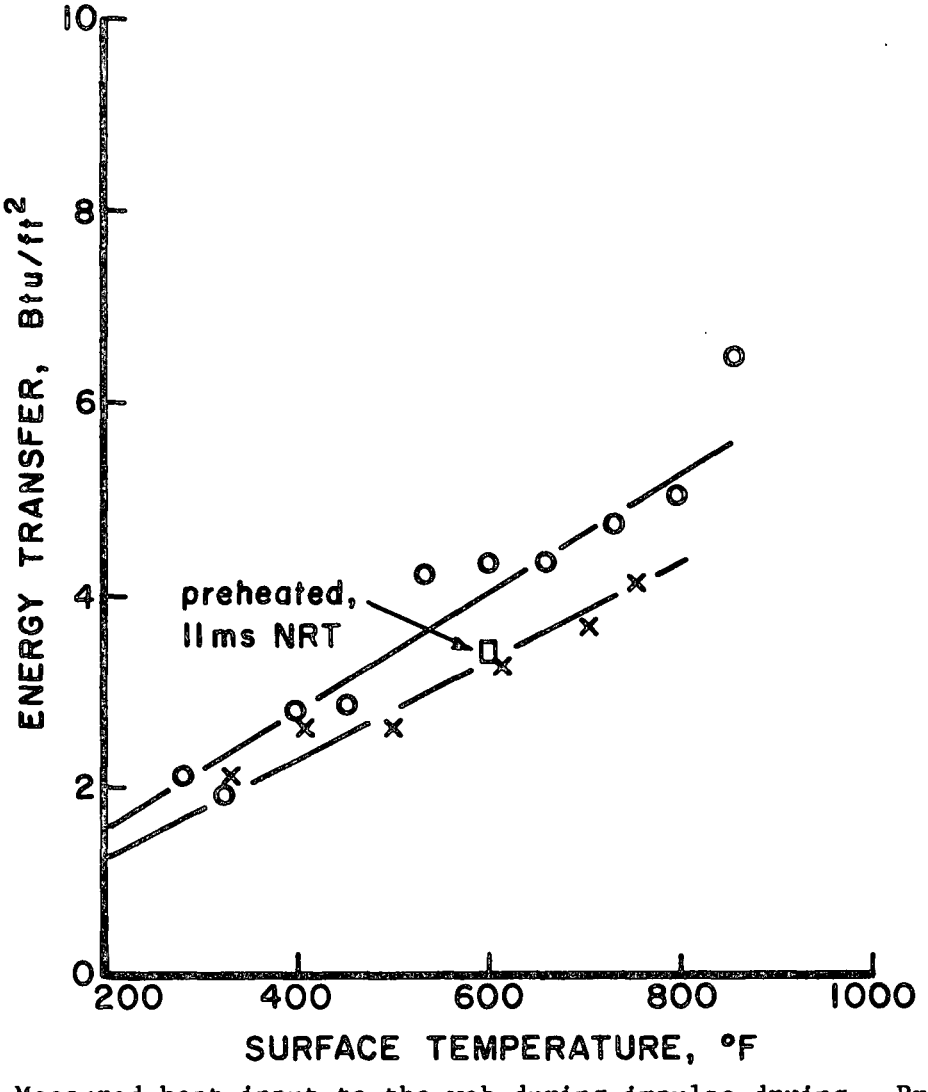

Figure II.29. Measured heat input to the web during impulse drying. Primary linerboard stock, 600 mL CSF, 50 g/m^2, 40% initial dryness. Peak pressure: 800 psi, nip residence times: x = 8 ms, o = 11 ms. Steel heated block.

The potential energy-related benefits of impulse drying can be defined clearly by combining the energy transfer data with the water removal data from Fig. II.20. The resulting performance measure, energy transfer per unit mass of water removed, is shown in Fig. II.30. For comparison, "theoretical" energy use curves are displayed. The "theoretical" curves represent the behavior to be expected for a true drying process and are calculated as being the sum of three contributions: sensible heating of all the fibers and water initially in the web to the boiling point (taken as 210°F), evaporation of all the water lost from the web during impulse drying, and further sensible heating of the web to a temperature midway between the boiling point and the surface temperature. This third contribution is nearly negligible.

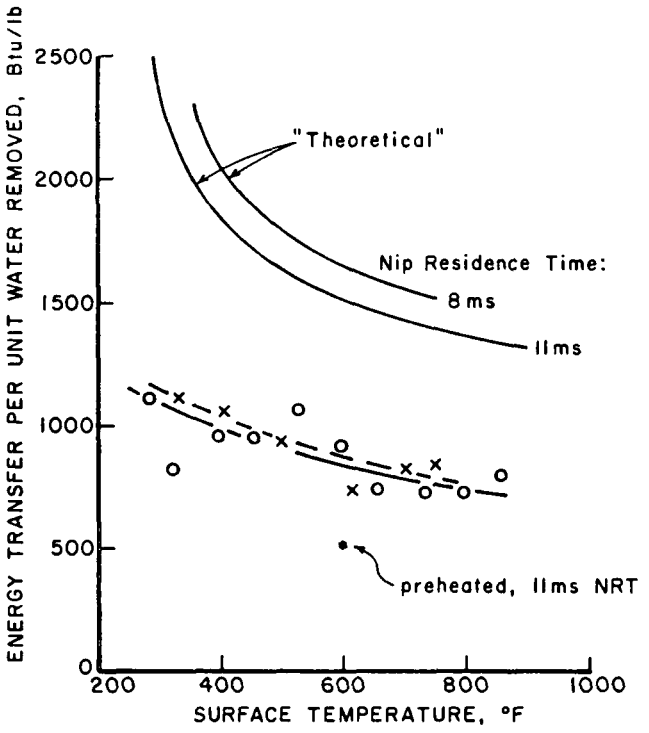

Figure II.30. Measured heat input during impulse drying per unit water removal, compared to theoretical amount required for sensible heating and evaporation (using RMR values from Fig. II.20). Primary linerboard stock, 600 mL CSF, 50 g/m^2, 40% initial dryness. Peak pressure: 800 psi, nip residence times: x = 8 ms, o = 11 ms.

The information in Fig. II.30 suggests that only slightly more than half the energy expected for an "ordinary" drying process is needed for water removal by impulse drying. The probable explanation of these results is that impulse drying, being a hybrid pressing and drying process, gives rise to a very significant component of liquid-phase dewatering. In the following section further experimental and theoretical support for this conclusion are also presented.

The single data point in each of Figs. II.29 and 30 labeled "preheated" represents a web that was preheated with low pressure steam (to approximately 200°F) just prior to the experiment. The initial sensible heating of the web was thus not done by the heated block in this case, as confirmed by the lower energy input value. From a thermodynamic and economic standpoint, the implications of the "preheated" result should be emphasized. That is, the use of a sizeable amount of more costly, high grade energy needed for transfer from the high temperature surface has been replaced by the use of the same quantity of less expensive, low pressure "steam heat." Of course, as shown earlier (Fig. II.20 and Table II.3), the greater water removal for preheated webs yields the additional benefit of reduced capital equipment size and cost. This benefit is all the more clear if one realizes that the size of an impulse dryer cylinder is likely to be dominated by the surface area required to put heat <u>into</u> the cylinder wall at the needed rate. The "preheated" data point in Fig. II.30 thus suggests a size reduction of about 50% compared to an impulse dryer processing nonpreheated webs! A final conclusion from the preceding discussion is that, if one measures both water removal and energy transfer in the laboratory over a range of test conditions, one has the information needed to begin the engineering of an impulse drying system. A test program aimed at gathering such data and paper properties as well has recently been initiated. This work will be discussed in a future report.

Properties

The conditions of pressure and temperature in an impulse drying situation are indeed intense. It is to be expected that paper subjected to these conditions will be significantly denser and smoother than paper pressed and dried in the usual manner. Investigations of these effects and of those resulting paper properties meaningful to particular grades are in progress, and results will be reported in the near future. It is anticipated that potential properties-related benefits at least as important as the water removal and energy benefits of impulse drying will be established. Student research (S. Burton) on the fundamentals of property development in impulse drying is also well underway and soon will be reported in the form of a Ph.D. thesis. An overview of property development issues is also presented in the following section.

Relatively little work related to properties has been performed as part of the exploratory study of impulse drying. However, since strength properties are known to correlate well with the apparent density of the dry sheet, a brief investigation was performed to determine the final densities that result from various impulse drying conditions. For comparison, densities of sheets pressed at room temperature and (immediately) dried at "conventional" (i.e., very low) mechanical pressure conditions were obtained. In both cases, density variations were obtained by varying the applied impulse (product of average pressing pressure and nip residence time); tests were performed in the heated roll system. Using a fixed roll speed (corresponding to a 100 ms nip residence time), the impulse applied to the room temperature sheets was varied through a combination of average pressure variation and use of multiple passes through the nip. For the impulse drying case, impulse variation was attained from pressure variation only, and a single pass through the nip was employed. Since only partial drying

was accomplished in this case, final drying was performed at conventional conditions. The test results are given in Fig. II.31. For a given level of press impulse, a much larger density is found for impulse-dried sheets than for conventionally dried ones. An increase in density with surface temperature is also noted. The limited testing of paper properties, such as breaking length, zero-span breaking length and tear strength, produced no conclusive evidence of independent effects of temperature, while density changes did tend to produce property changes, as expected.

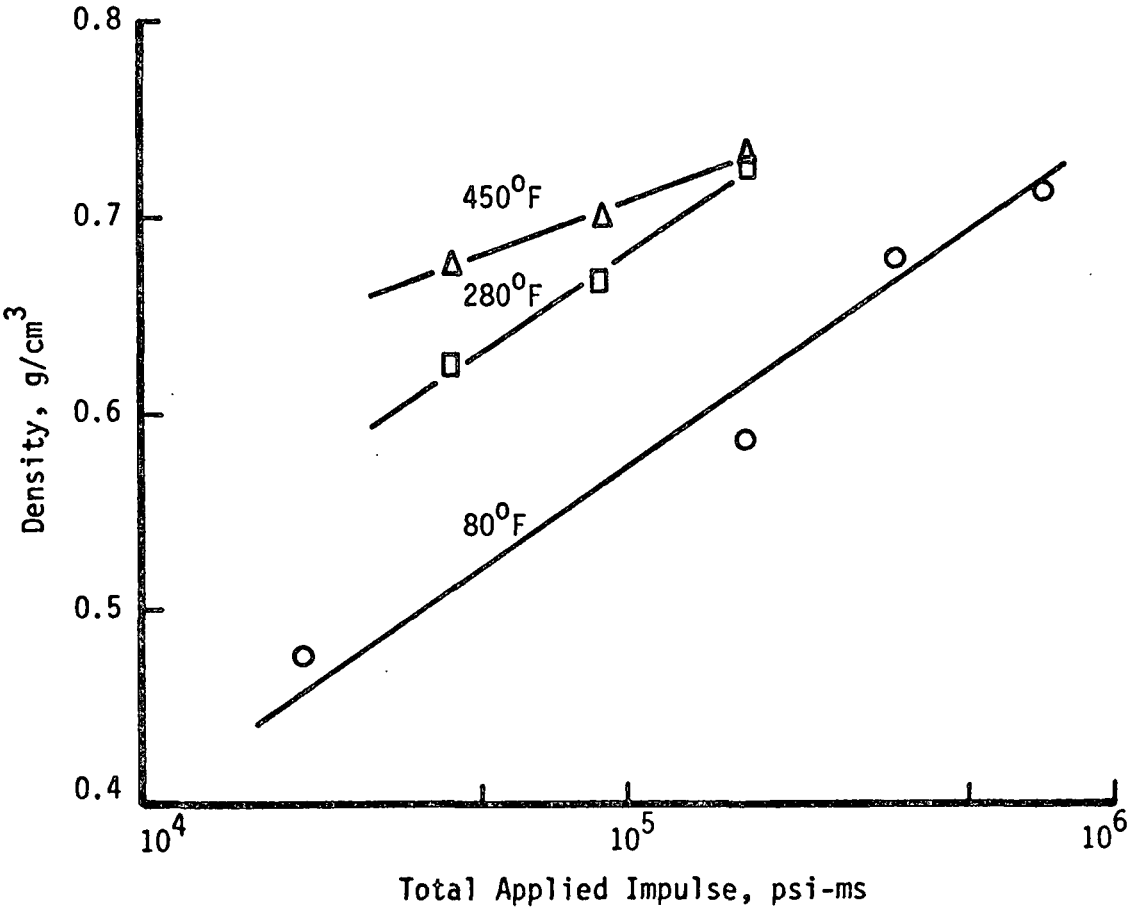

Figure II.31. Effect of pressing and of impulse drying on final sheet density. Unbleached southern softwood kraft handsheets, 570 mL CSF, 100 g/m^2, 40% initial dryness. Experiments performed in heated roll press.

While the density-related effects referred to above suggest that impulse drying may give rise to a favorable impact on properties, not unlike that of "press drying," it must be acknowledged that some combinations of basis weight, freeness, and operating conditions can produce detrimental effects, too. In particular, examples of sheet delamination or blistering have been observed in some operating regimes. It is believed that these effects occur in cases where the mechanical pressure is relieved while there is still a relatively high vapor pressure inside the hot, damp web. A possible contributing factor may be a tendency for the sheet to adhere to the hot surface during nip expansion. While a better definition of operating limits imposed by this phenomenon is needed, experience so far suggests that a wide scope for favorable impulse drying operation does exist.

CONCLUDING REMARKS ON EXPLORATORY PERFORMANCE STUDIES

It seems surprising that a mature technology such as paper drying has a large potential for improvement. However, the high-intensity drying processes which have been discussed, encompassing very broad ranges of surface temperature, applied pressure and ambient pressure, have indeed demonstrated great potential. Drying systems using these processes will be significantly smaller (per unit production rate) and, presumably, less expensive than conventional systems, will be advantageous with respect to energy utilization, and (in the case of impulse dyring, at least) will have a beneficial effect on paper properties. More specific comments concerning each of the three regimes which have been studied are given below.

The elevated temperature/pressure regime covers about three orders of magnitude in applied pressure, beginning with pressures only a few times greater than those applied with felt tension in today's dryers. The water removal data

presented in this section indicate that relatively modest increases in felt tension and steam pressure (surface temperature) could be used to achieve moderate drying rate increases (perhaps up to 50%), with corresponding equipment size reductions. (The implementation of those conditions, however, could present major engineering challenges.) The resulting systems would tend to be more energy efficient, due to reduced size and due to the lack of dependence of drying rate on vapor partial pressure in the air surrounding the paper, which implies a reduced air heating and circulation requirement and more effective energy recovery from the humid exhaust (due to reduced air contamination). Based on the available data, drying in such a system would have no real impact on paper properties. While the data in the intermediate pressure portion of this regime (e.g., 5 to 200 psi) show much greater impact on water removal, it is difficult to visualize real equipment that would implement the conditions over the necessary drying time durations. Finally, the implementation of the high pressure and temperature conditions corresponding to the extreme part of this regime would, in practice, seem to suggest the use of impulse drying equipment (e.g., involving a heated roll in an extended nip press). The impulse drying regime is discussed later in this section.

The thermal/vacuum drying process has been shown, based on the exploratory data presented here, to offer the possibility of dryers only about 10% the size of conventional dryers if slightly elevated hot surface temperature levels are employed. Alternatively, dryers about the same size as today's dryers would result if an inexpensive, low-temperature heat source is utilized. In either case, the condensation of the steam driven from the sheet, an integral part of the process, permits easy recovery of the drying energy. Thus, these dryers would have a very high energy use effectiveness. In fact, very energy efficient

cascaded systems are conceivable.[10] No detrimental effect of lower temperature thermal/vacuum drying on paper properties was indicated by the exploratory study; no significant property benefits can be expected either.

The engineering implementation of the thermal/vacuum process will be difficult. Particular challenges will be the need for a moving vacuum seal, the removal of the condensate from the cooled surface, and the need to maintain a low temperature heat sink (condensing) surface (if low heat source temperature and high drying rate are desired).

The impulse drying results which have been presented are the most interesting of all. It appears that very small water removal equipment, reduced energy use (perhaps half that of conventional dryers), and favorable properties effects will all result from implementation of this concept. The use of web preheating (before the impulse) was shown to be important to further reducing the dryer size and (high-grade) energy requirement. The implementation of impulse drying should be feasible using extended nip pressing ideas. The only major apparent "disadvantage" of this process is the need for high surface temperatures, requiring nontraditional heating methods. Options include direct heating by combustion gases or electricity, and indirect infrared or liquid heating.

The overall outcome of the exploratory studies of high-intensity drying is very encouraging. Plans for the further development and application of these principles are given later in the the report.

PROCESS DESCRIPTION

INTRODUCTION

In the preceding section, the results of exploratory studies of high-intensity drying performance have been presented and discussed. That work emphasized the water removal characteristics of high-intensity drying processes, but also dealt with energy use and possible impacts on paper properties. The results indicate that major breakthroughs in water removal equipment and costs can be anticipated. However, since the high-intensity drying processes (especially, impulse drying) depart so dramatically from the drying process in a conventional dryer section, a fundamental understanding and description of their principles is needed to assure the success and maximize the benefits of their commercial application. Experimental and analytical investigations directed toward this need are the subject of this section. Major student contributions to this work, leading to separate theses and reports, are mentioned for completeness. As with the performance studies, much of the completed work has been oriented toward water removal (and related energy aspects), but a discussion of recent work related to property development is included.

EXPERIMENTAL STUDIES

Experiments and measurements performed in support of developing an understanding and a description of high intensity drying performance pertain to the characteristics of the heat input process, the vapor pressure developed at the hot surface, the quantity of liquid-phase dewatering, the internal web thermodynamic conditions during drying, and the sheet structure during and after drying. A review of work and interpretation of results in each of these areas follows.

Heat Transfer

High-intensity drying covers a wide range of operating coditions. In the low-to-moderate pressure portion of the "elevated temperature/pressure regime" and in the thermal/vacuum regime, available evidence indicates that water removal is entirely the result of evaporation and vapor outflow. In the high pressure part of the elevated temperature/pressure regime and in impulse drying, some of the water apparently leaves the sheet in the liquid state and some (probably most) leaves as vapor. Throughout the entire high-intensity drying region, therefore, the process of heat transfer into the web, which governs the rate of evaporation, is of central importance. The heat transfer, in turn, should be influenced by the degree of contact between the web and the hot surface, the distributions of moisture, temperature and porosity near the hot surface, etc. Thus, the experimental determination of the heat transfer rate should provide insight into the nature of the drying process.

Overall Heat Transfer

A simple overall indication of the character of the heat transfer process can be established if the water removal is entirely in the vapor phase. In this case, and if heat losses are negligible, the average heat flux ($\bar{q}$) into the web is related to the average drying (evaporation) rate ($\dot{m}_D$) by the energy balance relation:

$$\bar{q} = \Delta h \cdot \dot{m}_D \qquad (1)$$

where Δh is an enthalpy rise per unit of water evaporated that represents both sensible heating of the water and fibers and the latent heat of vaporization. Since the evaporating water in the web at a temperature (T_B) near the ambient boiling point represents the ultimate sink for the heat entering the web, it is

reasonable to a define an apparent, time-average, overall heat transfer coefficient by the equation:

$$\bar{q} = \bar{U} (T_H - T_B) \tag{2}$$

Combining Eq. (1) and (2) yields:

$$\bar{U} = \Delta h \, \dot{m}_D / (T_H - T_B) \tag{3}$$

Using Eq. (3), values for $\bar{U}$ have been calculated for the drying data in Fig. II.4. These results are given in Fig. III.1. It is felt that $\bar{U}$ characterizes the intrinsic heat transfer benefits of operating at higher than normal surface temperature and mechanical pressure, since it removes the obvious effect of increased thermal driving force from consideration. The quantity $\bar{U}$ represents the combined effects of two processes: heat transfer across the interface between the heater and web, and heat transfer through part of the web thickness. For the low mechanical pressure conditions of Fig. III.1, the increase in $\bar{U}$ with mechanical pressure reflects primarily the improved contact which occurs, while the drop in $\bar{U}$ with increasing hot surface temperature may reflect a buildup of vapor pressure at the interface which partially destroys contact. These results demonstrate that, to achieve full drying rate benefit from high surface temperature operations, higher pressures must be applied to the web.

Drying rate data from the higher pressure part of the elevated temperature/pressure regime and from the thermal/vacuum process have been used to evaluate the average overall heat transfer coefficient ($\bar{U}$) for higher applied pressures than those represented in Fig. III.1. The results are given in Fig. III.2, together with some values for lower pressure from Fig. III.1. It is seen that as pressure increases to the 10-100 psi range the previously noted tendency for a reduced $\bar{U}$ value at higher temperature and low pressure is eliminated. The increase of thermal conductivity and decrease of web thickness due to increased applied pressure are believed to account for the increasing $\bar{U}$ values in this range.

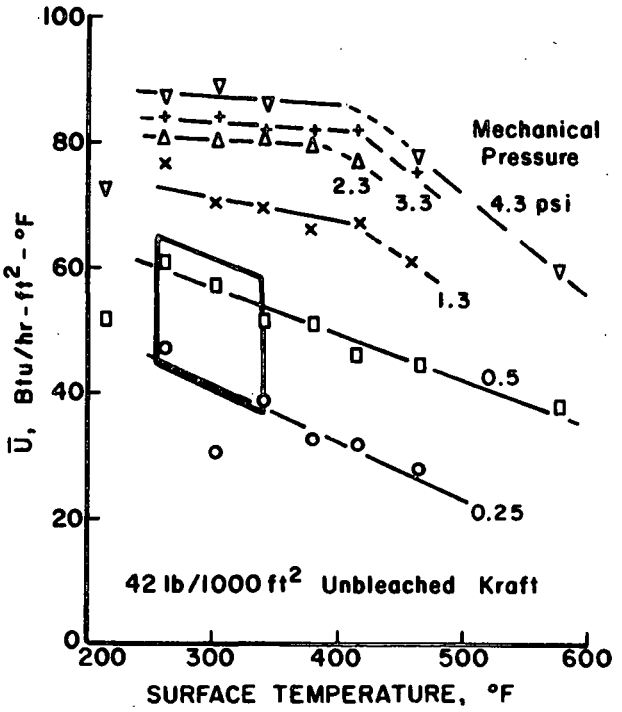

Figure III.1. Apparent time-average overall heat transfer coefficient, $\bar{U}$, between heater surface and web. Values based on drying data in Fig. II.4, for 42 lb/1000 ft^2 sheets. Box indicates approximate region of operation for conventional dryers.

The "Conduction Upper Bound" indicated in Fig. III.2 represents the thermal conductance of a fully-compressed (zero-porosity) fiber mat of half the actual sheet basis weight. It is shown for reference purposes because it represents the limiting average conductance value (for infinite applied pressure) predicted by the simplified "two-zone model" presented later in this section. It appears that this conduction limit is approximately the value toward which the trend curve of the low-to-moderate pressure $\bar{U}$ values tend when extrapolated to very high pressures. However, the points in the higher pressure range deviate upward considerably from this trend. Since the $\bar{U}$-values were calculated from water removal rate data under the assumption of a pure evaporation process, these higher-than "expected" values may indicate the presence of a rapid (i.e., not limited by heat transfer rate) liquid-phase dewatering component to the drying process at high pressure. This explanation is supported to some

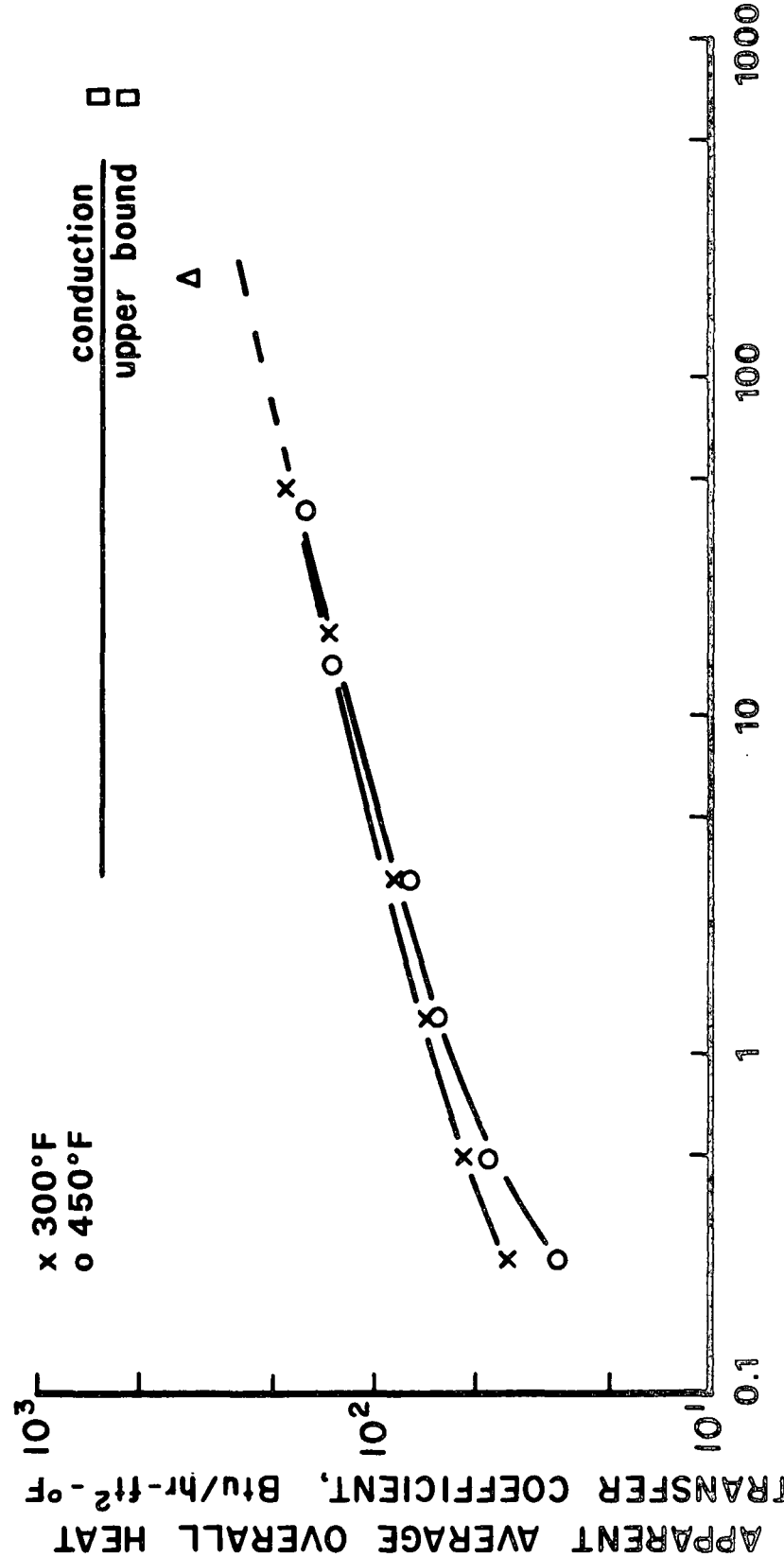

Figure III.2. Apparent average overall heat transfer coefficient ($\bar{U}$) between hot surface and web. Based on drying data in Fig. II.4, 6, 10 for 42 lb/1000 ft^2 sheets. Points at 700 psi based on drying data from Devlin (1984a).

degree, by observations of liquid dewatering in impulse drying, to be discussed later. However, it is also possible that these high $\bar{U}$ values at high pressure are in part indicative of an augmentation of the heat transfer mechanisms which were dominant at low to moderate pressure.

Instantaneous Heat Transfer

While the overall average heat transfer parameter ($\bar{U}$) inferred from water removal data provides some insight into the nature of the heat transfer process (or, at least, the effects of operating conditions) in high-intensity drying, a more detailed understanding can be expected from examination of data on the instantaneous heat flux (q) into the web. Furthermore, the time-integral of the heat flux represents the thermal energy used in drying.

The rapid-response surface thermocouple installed in the heated block of the drying system (see Fig. III.3) provides the only signal required for the heat flux measurement technique employed. The technique is based on application of the law of transient heat conduction in the heated block material and works as follows. Prior to a drying experiment, the insulated block is electrically heated to a desired temperature level. The heater is then switched off so that the block and thermocouple tube can attain an essentially uniform temperature. The rapid-response surface thermocouple measures the surface temperature transient which occurs once the wet web makes contact with the heater, initiating the experiment. The particular thermocouple design shown in the figure is supplied by the Medtherm Corp. It features a junction formed by the very thin layer of constantan ($\sim 10^{-4}$ inch thick) covering the end of the thermocouple tube, which is flush mounted. The thermocouple tube material is chosen to have similar thermal properties to the block material. If it is assumed that the block (including the thermocouple tube) thermal behavior obeys the one-dimensional

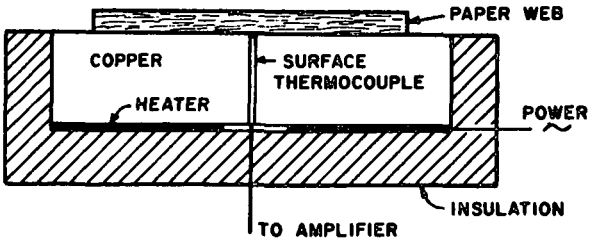

(a)

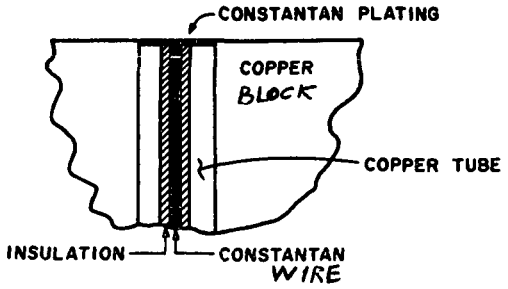

(b)

Figure III.3. (a) Typical heated block with surface thermocouple.
(b) Detail of surface thermocouple configuration (wire and insulation diameters greatly exaggerated). Heater block and thermocouple tube shown as copper, but brass and steel blocks and iron tubes were used in some impulse drying experiments.

form of the heat conduction equation for a slab which loses heat only to the web, it is possible to use the measured surface temperature history to calculate the instantaneous heat flux into the paper. The analysis involves use of Duhamel's theorem in the form:

$$U(x,\tau) = T(x,\tau) - T_o = \int_0^\tau V(x,\tau-\tau') \frac{dT_s}{d\tau'} d\tau' \qquad (4)$$

where $U(x,\tau)$ is the departure from the initial temperature, T_o, occurring at any position x, at time τ, due to the variations in surface temperature, T_s, occurring at all earlier times τ'. The function V is called the fundamental solution, and

represents the dimensionless temperature response of the slab to a unit step change in surface temperature occurring at time $\tau = 0$. The heat flux conducted from the block into the web can be evaluated from Fourier's law:

$$q(\tau) = - k_B \left. \frac{\partial T}{\partial X} \right|_{x = x_s} \tag{5}$$

where k_B is the thermal conductivity of the block material and x_s is the coordinate of the block surface. Combining Eq. (4) and (5) yields:

$$q(\tau) = - k_B \int_0^\tau \frac{\partial V}{\partial X} (x_s, \tau-\tau') \frac{dT_s}{d\tau'} d\tau' \tag{6}$$

Two useful fundamental solutions (V) are available (e.g., see Myers[13]) for implementation of numerical heat flux computations based on Eq. (6). One is the solution for the case of a finite slab insulated on the back side and is needed for long drying time experiments in which the block temperature changes throughout its thickness during an experiment. The other is the solution for the case of a semi-infinite medium; it is adequate for short duration impulse drying tests and yields a much faster-running computer program for the heat flux computations.

Heat flux measurements have been made for experiments in both the elevated temperature/pressure and the impulse drying regimes. A typical example from the first category is given in Fig. III.4 (the vapor pressure curve will be discussed later). It is seen that the heat flux very quickly reaches a large peak value, comparable in magnitude to boiling heat transfer values, followed by a continuous decline throughout the drying period. Since, following an initial web heatup period, the vapor removal rate due to evaporation must be approximately proportional to the heat transfer rate, one can conclude that there is no constant rate period in high-intensity drying. This suggests that wicking of liquid

water toward the hot surface, which accounts for the constant rate period in conventional drying, plays a reduced role in the present situation. One would expect this to be the case because any temperature gradient through the web would impose a vapor (total) pressure gradient onto the liquid water, tending to oppose capillary action. It follows from this argument that a continuously increasing dry region should develop near the hot surface. Thus, the thermal resistance between the hot surface and the evaporation zone continuously increases, accounting for the declining heat transfer rate into the web.

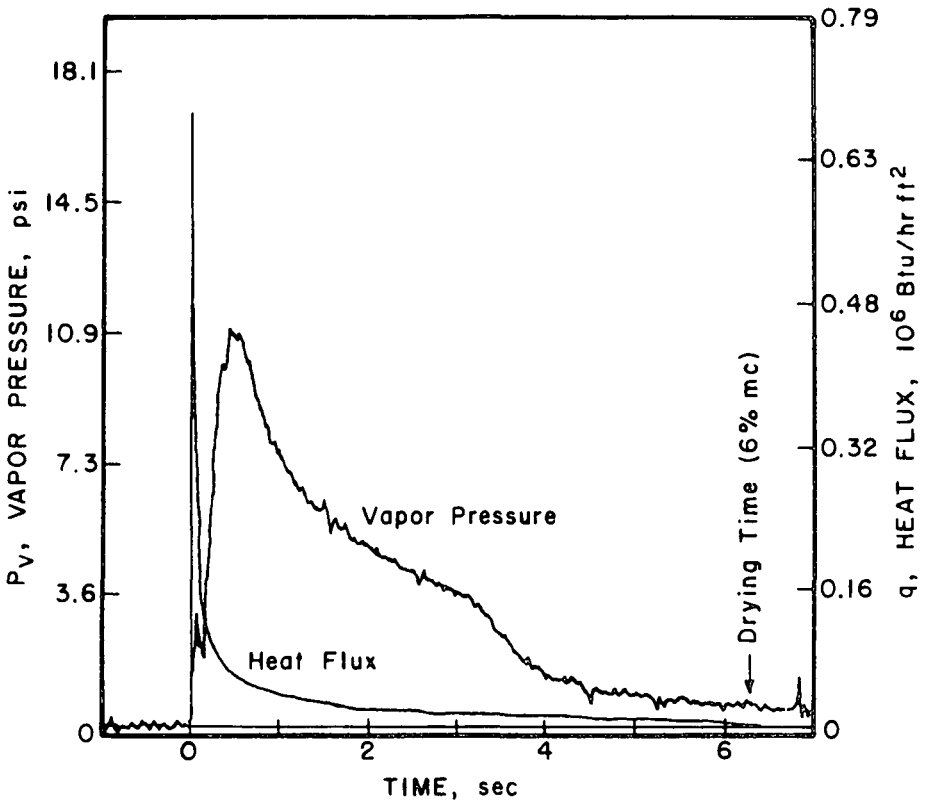

Figure III.4. Typical instantaneous heat flux and vapor pressure during high intensity drying. Unbleached southern softwood kraft, 42 lb/1000 ft^2, 570 CSF, 60% initial moisture content. Surface temperature: 450°F; applied pressure: 34.6 psi.

Figure III.5 gives an example of a situation with higher paper web vapor flow resistance (lower CSF) and relatively light mechanical loading. In this

case the high evaporation rate (and, thus, flow rate through the wet zone) early in the process induces a vapor pressure comparable in magnitude, but opposed to, the applied mechanical pressure. This appears to cause a "lift-off" phenomenon. An insulating vapor film is formed at the hot surface/paper interface. The small values of heat flux during this period suggest the corresponding loss in thermal contact. These detailed data explain the decrease in $\bar{U}$ at high temperature exhibited in Fig. III.1, and support the interpretation of Fig. II.4 and 5 given in the preceding section. The practical implication of these data is that applied loads considerably in excess of the vapor pressure must be used in order to avoid loss in drying performance due to poor thermal contact.

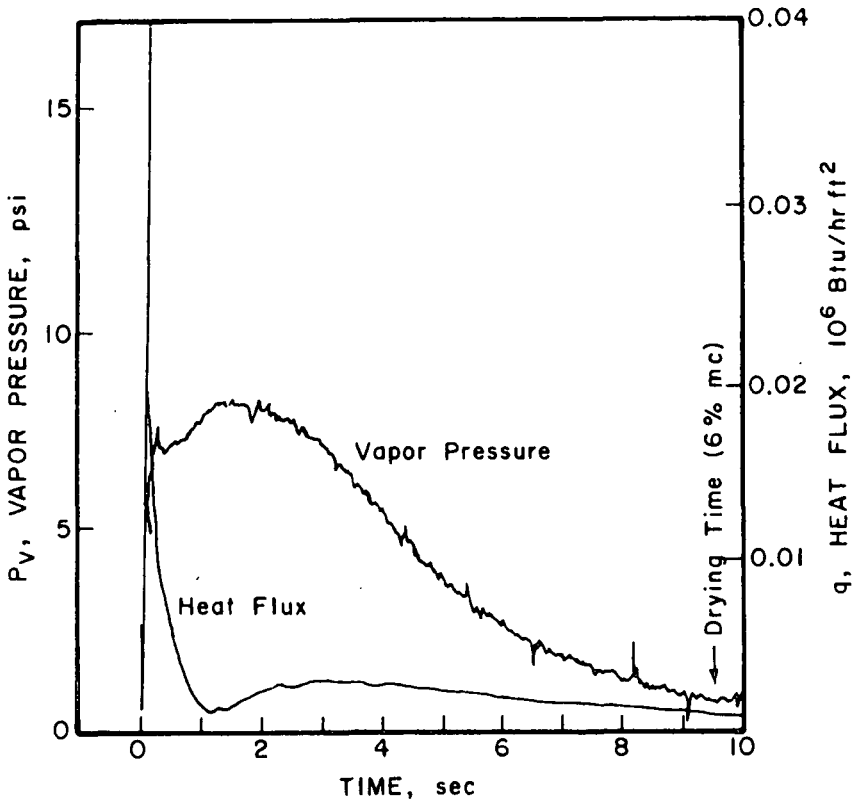

Figure III.5. Instantaneous heat flux and vapor pressure at low freeness and low applied pressure. Unbleached southern softwood kraft, 42 lb/1000 ft^2, 300 CSF, 60% initial moisture content. Surface temperature: 450°F; applied pressure: 6.7 psi.

The peak heat flux values resulting from the experiments in the elevated temperature/pressure regime are presented in Fig. III.6. These values

are found to be, for a given pressure level, approximately proportional to the difference between surface temperature and boiling point, relatively independent of basis weight and freeness, and to increase with increasing pressure. These findings appear to be compatible with the peak heat flux being associated with a rapid evaporation (boilinglike) process occurring at the hot surface side of the web. In particular, the temperature difference driving force is typical of an evaporative process, the near independence from basis weight and freeness effects is indicative of a surface process, and the increase with pressure may be the result of greater water availability at greater compression levels and the improved contact between the web surface and the heated block.

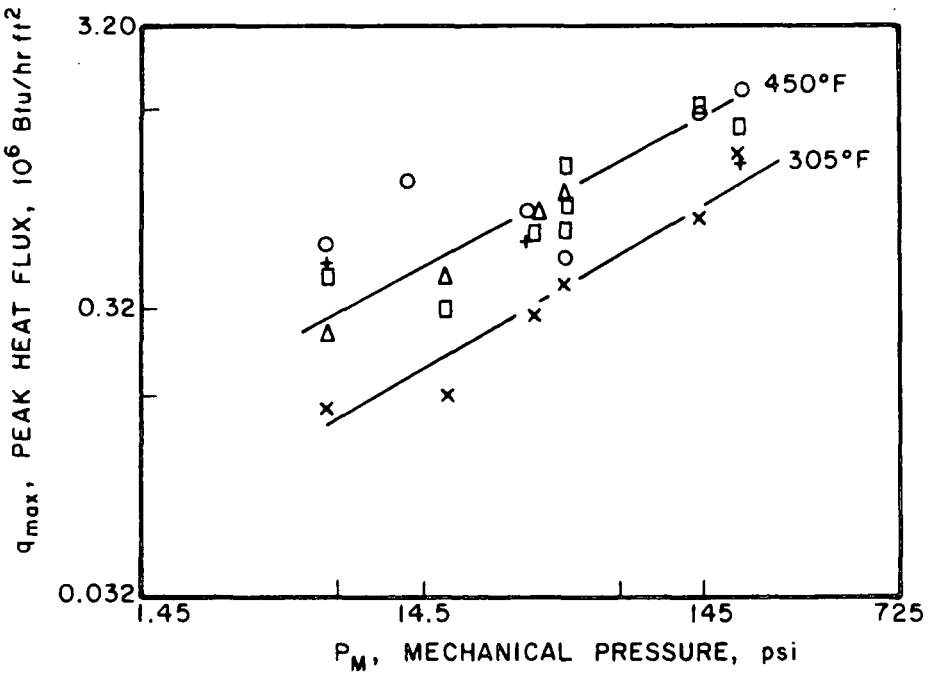

Figure III.6. Peak heat fluxes during high-intensity drying of unbleached softwood kraft paper webs at 60% initial m.c. in atmospheric ambient. Copper heated block.

Symbol	Surface Temp., %	Basis Wt., g/m^2	CSF, mL
○	450	205	570
□	450	205	300
△	450	100	300
+	305	205	570
×	305	205	300

Instantaneous heat flux measurements under impulse drying conditions have also been obtained. Fairly typical examples are given in Fig. III.7 and III.8 for the cases of webs initially at room temperature and preheated to about 210°F, respectively. For perspective, the measured applied mechanical pressure histories are also shown. In these examples, the nonpreheated web gives rise to a heat flux response that, relative to the preheated web case, is slightly delayed but has a somewhat higher peak value as well as significantly larger values in the expansion part of the impulse. Futhermore, the total energy transfer (area under the heat flux curve) is about 30% greater for the nonpreheated web experiment, even though the water removal is about 30% less. A possible interpretation of the differences cited is as follows. Since the preheated web initial temperature is close to the boiling point, evaporation of surface water begins immediately upon contact with the hot surface. One effect of this could be a more rapid dryout of the surface region, causing the earlier occurrence and reduced magnitude of the peak heat flux, as well as the lower heat flux magnitudes during expansion, compared to the nonpreheated case. In both cases, the initial continuous decline in heat flux after the peak is rather similar to that observed in the elevated temperature/pressure regime and is, therefore, probably due to an increasing thermal resistance (dry layer) near the hot surface. The steeper rate of decline later in the expansion is probably the result of poorer thermal contact between the web and hot surface at lower mechanical pressure levels. Finally, the greater water removal for the preheated web may be the result of three factors: the energy put into the web is all used for evaporation (not partly for web heatup); a high vapor pressure at the hot surface may develop sooner, giving a longer-duration driving force for liquid water removal; and the higher average web temperature may promote a greater "wet-pressing" effect.

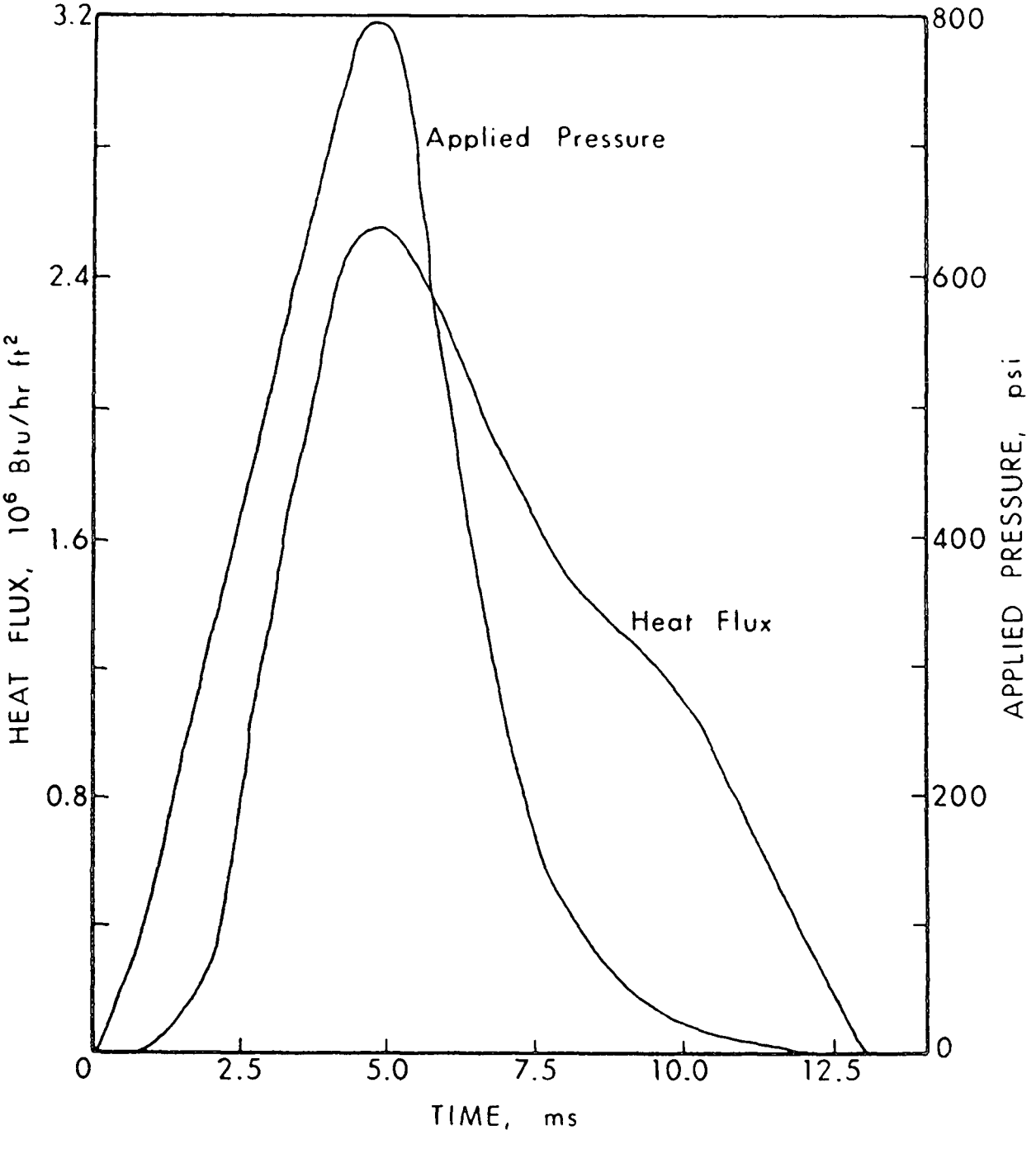

Figure III.7. Instantaneous heat flux in impulse drying. Primary linerboard stock, 600 mL CSF, 50 g/m^2, 40% initial dryness. Steel heated block; surface temperature: 600°F. Total energy transfer: 4.3 Btu/ft^2; RMR = 34%.

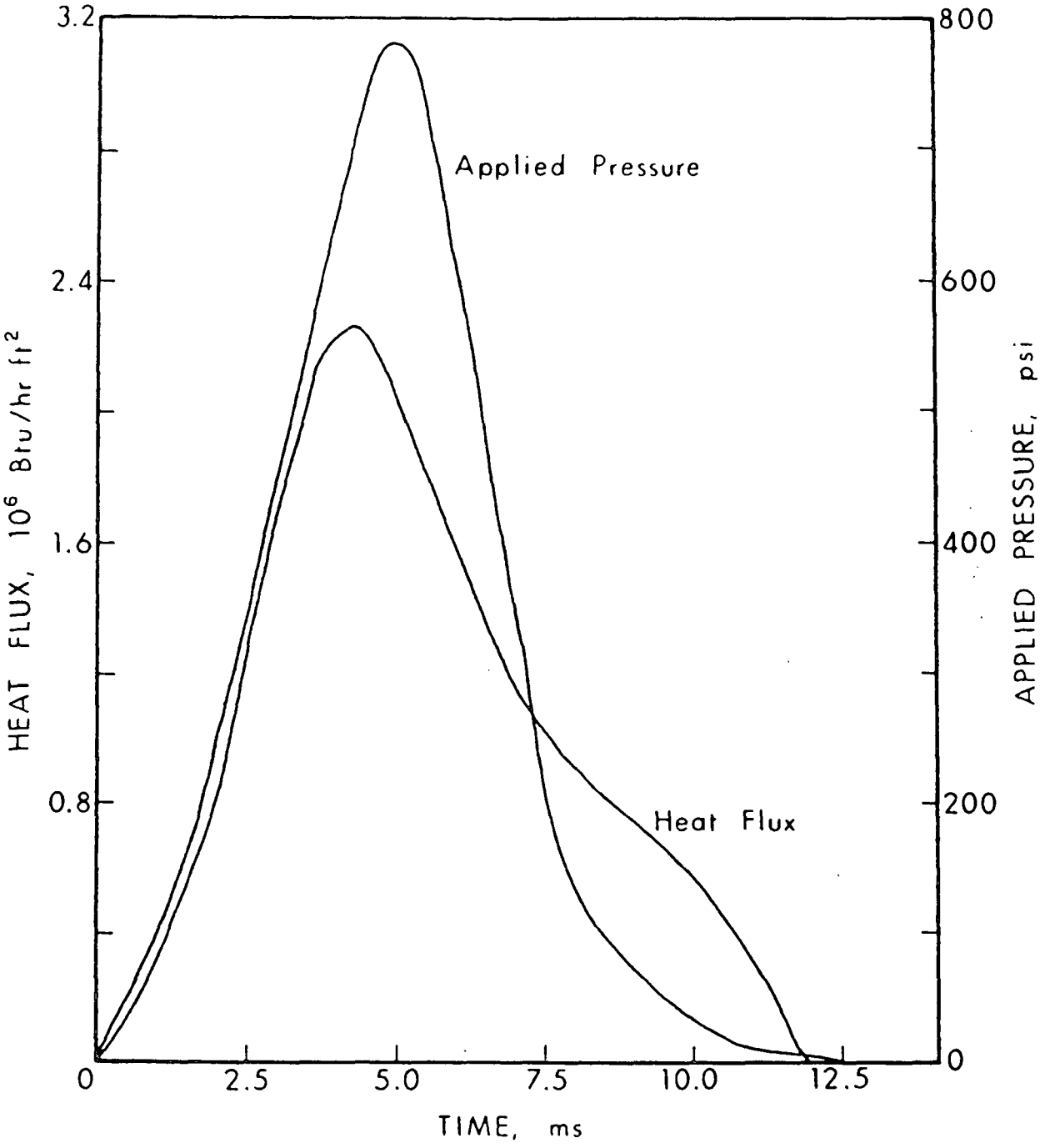

Figure III.8. Instantaneous heat flux in impulse drying. Primary linerboard stock, 600 mL CSF, 50 g/m^2, 40% initial dryness. Preheated web. Surface temperature: 600°F. Total energy transfer: 3.4 Btu/ft^2; RMR = 43%.

The peak heat fluxes found from impulse drying experiments are presented in Fig. III.9. Interestingly, the values corresponding to surface temperatures of 305°F and 450°F are in fair agreement with values projected from Fig. III.6 for the same pressure level, although the peak heat fluxes vary less with temperature than expected from the Fig. III.6 data. The slight tendency for the shorter nip residence time to yield a higher peak might be the result of a reduced hot surface dryout prior to the time that the peak pressure occurs for this case.

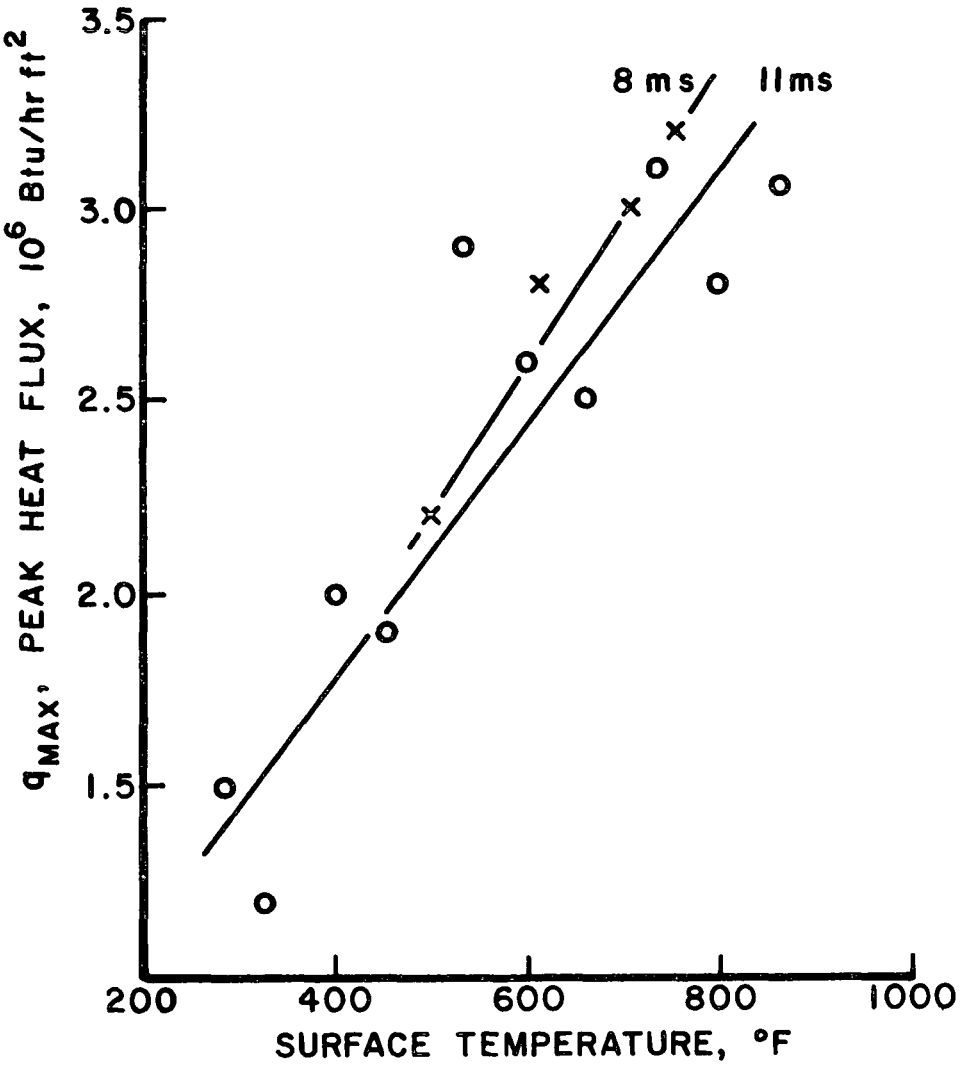

Figure III.9. Peak heat flux in impulse drying. Primary linerboard stock, 600 mL CSF, 50 g/m^2, 40% initial dryness. Peak pressure: 800 psi, nip residence times: x = 8 ms, o = 11 ms. Steel heated block. Nonpreheated webs.

Vapor Pressure at the Hot Surface

In high-intensity drying, the intensive heat input must generate, in the vicinity of the hot surface, web temperatures equal to or exceeding the ambient boiling point. Therefore, a vapor pressure equal to or exceeding the ambient pressure must develop at the hot surface. The difference between the vapor pressure at the hot surface and the ambient pressure (i.e., the vapor pressure difference across the sheet) is a significant quantity. It is the driving force for vapor removal from the sheet and is potentially capable of driving liquid water from the sheet as well. It also represents a force that tends to oppose the sheet compression promoted by the applied mechanical pressure. The magnitude of the vapor pressure reflects the temperature level in the evaporation region for which a balance exists between the heat transfer rate into and the total rate of energy removal including that carried by vapor flowing from this region.

In several high-intensity experiments, measurement of the instantaneous vapor pressure has been performed using a pressure tap/transducer arrangement as shown in Fig. II.9. Preliminary trials were performed during thermal/vacuum drying experiments; an example vapor pressure curve is given in Fig. III.10. The majority of the vapor pressure measurements have been made during atmospheric ambient, elevated temperature/pressure regime, experiments. The response presented in Fig. III.4 and the one in Fig. III.11 are typical examples of the results.

The response presented earlier in Fig. III.5 is an untypical response; it corresponds to a situation in which the applied pressure was "too low" to withstand the vapor pressure generated at the hot surface, causing a "liftoff" phenomenon. Under liftoff conditions the spatial (area) average vapor gage-pressure at the sheet/hot surface interface must balance the applied pressure. Since the pressure tap is at the diametral center of the sheet, radial flow effects cause the measured vapor pressure to slightly exceed this average value.

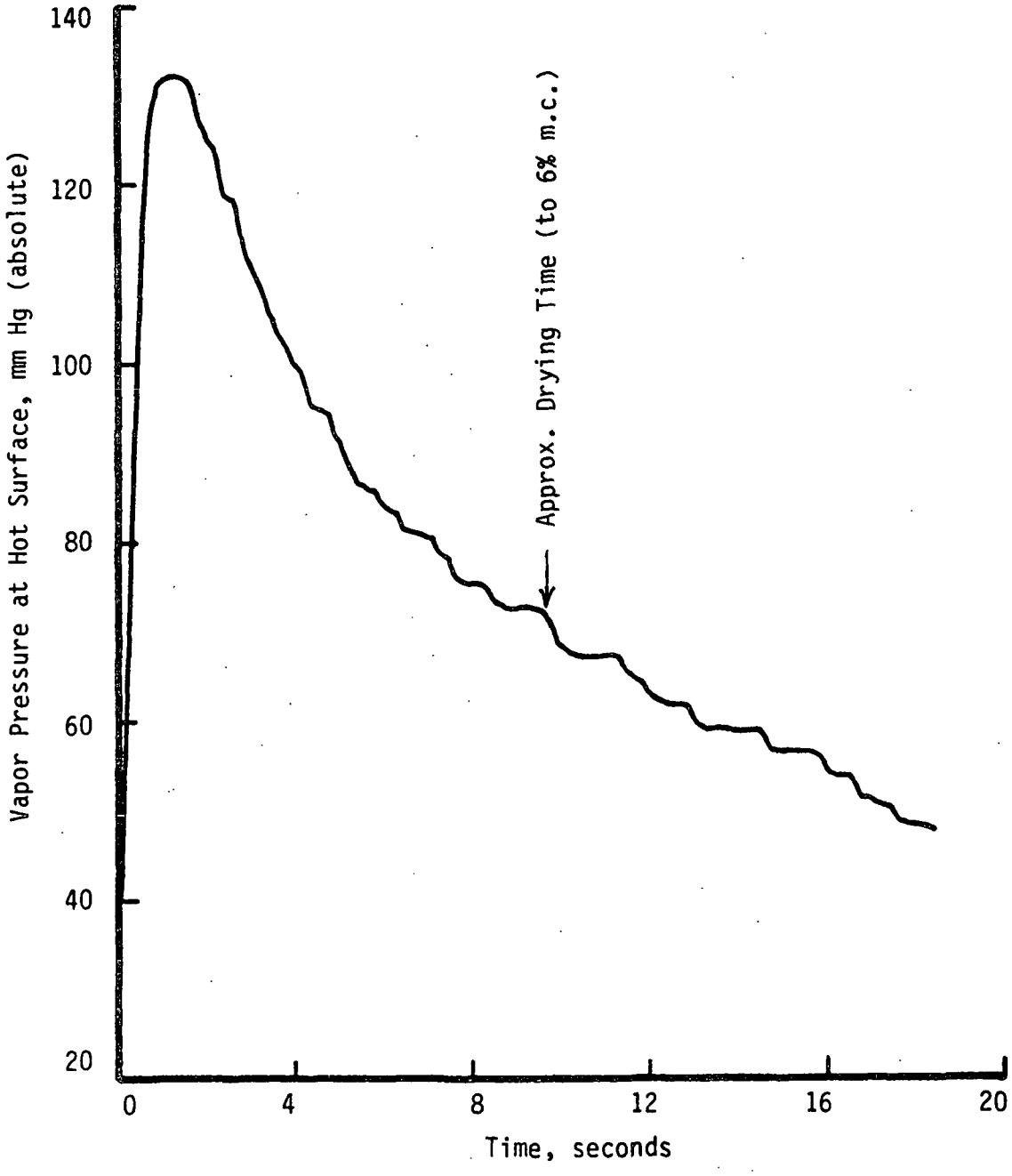

Figure III.10. Absolute vapor pressure response at hot surface in thermal/vacuum drying. Unbleached southern softwood kraft, 42 lb/1000 ft^2, 570 mL CSF, 60% initial moisture. Surface temperature: 400°F, applied mechanical pressure: 14.7 psi (nominal). Nominal ambient prssure (based on cold block temperature): 30 mm Hg (abs.) 51.7 mm HG = 1 psi.

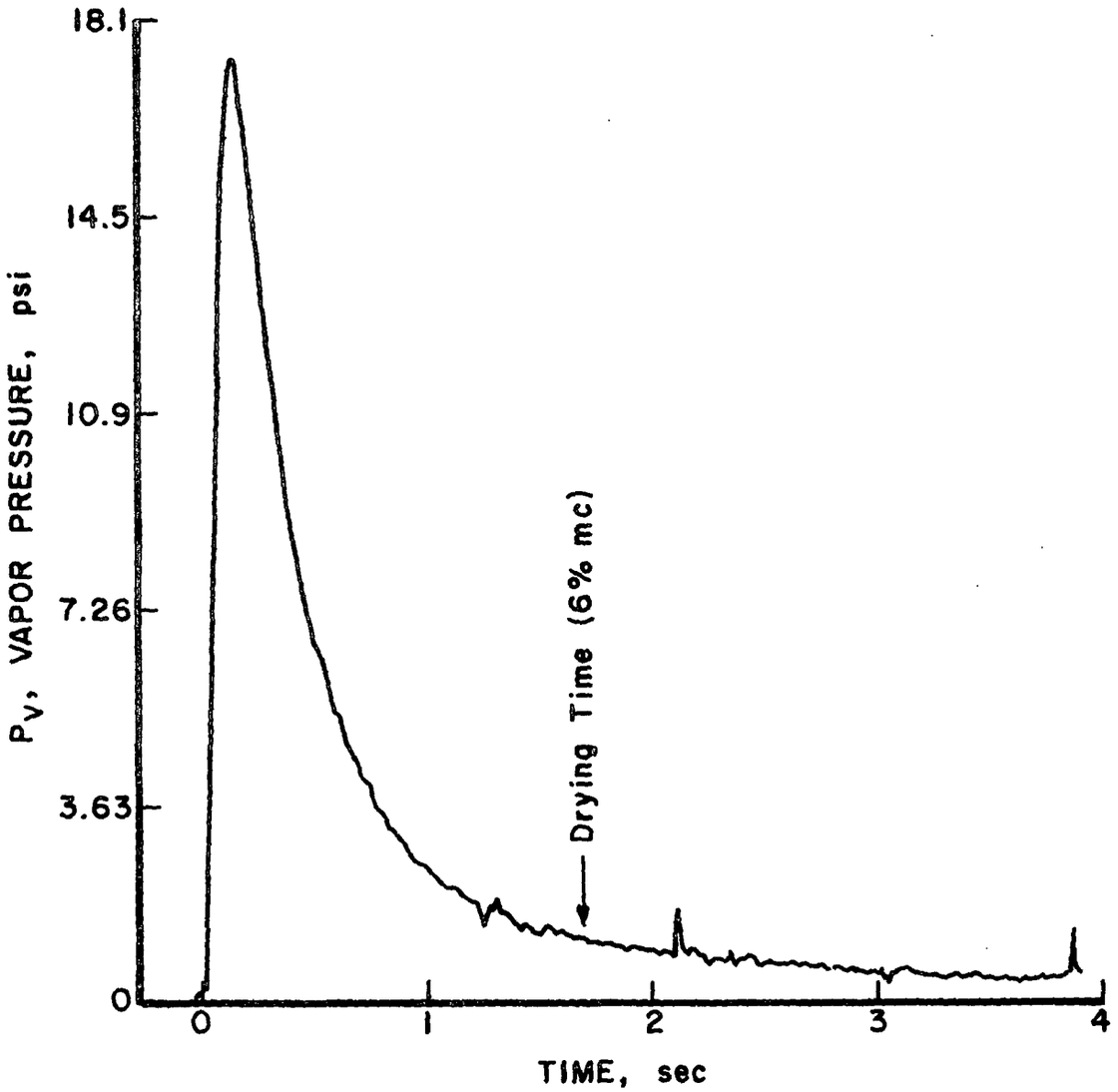

Figure III.11. Vapor pressure gage at hot surface. Unbleached southern softwood kraft, 100 g/m^2, 60% initial moisture content, 300 mL CSF. Surface temperature: 450°F; applied pressure: 46.5 psi.

The shapes of all three of the typical vapor pressure curves (Fig. III.4, III.10, and III.11) are qualitatively similar to the instantaneous heat flux behavior which has been discussed. That is, the vapor pressure rapidly reaches a peak and then declines continuously during the rest of the drying process. Since the vapor flux from the sheet should be proportional to heat flux,

and since the pressure difference, in turn, is roughly proportional to the product of vapor flux and flow pathlength (assuming a Darcy's law description to be valid), the observed behavior is reasonable. Furthermore, the declining temperature of the evaporation region with time, implied by the vapor pressure curve (after the peak) together with the declining heat flux, supports the earlier explanation for the declining heat flux being the result of an ever-increasing thermal resistance (dry layer) between the hot surface and the evaporation site (moist region) of the sheet.

The peak vapor pressures from various experiments in the elevated temperature/pressure regime are given in Fig. III.12. These pressures are found, for fixed freeness and basis weight, to be nearly proportional to the difference between surface temperature and boiling point at low vapor pressure, strongly dependent on freeness (and, therefore, sheet flow resistance), inversely proportional to basis weight, and strongly dependent on mechanical pressure. These effects are all compatible with the heat input/vapor outflow discussions given above. The strong variation with mechanical pressure is attributed to the increase in vapor flux through the sheet (due to the higher heat flux) and to the increased flow resistance as the sheet becomes more compressed.

There are two limitations to the peak vapor pressure value. First, it cannot exceed the applied mechanical pressure, except for the small radial flow effect under "liftoff" conditions, mentioned earlier in connection with discussion of Fig. III.5. A few of the low freeness, high basis weight points in Fig. III.12 also exhibit this small effect. Second, the vapor pressure cannot exceed the saturation pressure corresponding to the hot surface temperature. Within the allowable range of vapor pressure values, however, the data suggest that at high mechanical pressures and high temperatures, such as are typical of the

impulse drying process, driving forces sufficient to produce appreciable liquid-phase dewatering can be expected. Research by Institute Ph.D. candidate S. Burton, in progress, confirms this expectation.

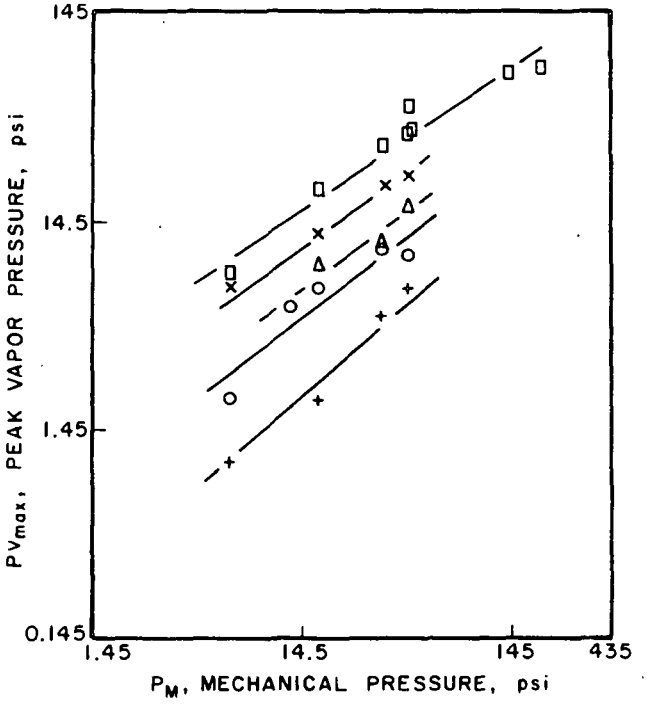

Figure III.12. Peak vapor pressures (gage) during high-intensity drying of unbleached softwood kraft paper webs at 60% initial m.c. in atmospheric ambient.

Symbol	Surface Temp., °F	Basis Wt., g/m^2	CSF, mL
×	450	205	570
□	450	205	300
△	450	100	300
+	305	205	570
○	305	205	300

Liquid-Phase Dewatering in Impulse Drying

Several features of impulse drying - the very high water removal rate, the low energy input per unit of water loss, and the high vapor pressure

difference across the web - suggest that some of the water removal must occur in the liquid phase. Certainly, direct physical reasoning also leads to this conclusion. However, to further substantiate this conclusion and to quantify the amount of this component of water removal some experiments involving a water soluble chemical tracer have been performed.

The tracer (LiCl in most cases, but sodium fluorescein in the initial tests) is added to the fiber/water slurry in a known concentration during the handsheet making process. This provides a known concentration of tracer in the water within the sheet prior to the test. After the experiment, the felt is soaked in a known volume of water. Analytical evaluation of the amount of tracer in this solution then provides sufficient information to calculate the amount of water that left the sheet as liquid. This assumes that the water leaving the sheet contains the same tracer concentration as the original concentration.

The results of some impulse drying experiments using chemical tracers are presented in Fig. III.13. Based on the LiCl results, it is seen that more than one-third of the water removal is in the liquid phase for nonpreheated sheets, with still greater liquid dewatering fractions for preheated webs. In fact, examination of the data reveals that the additional liquid water removal that occurs with preheated webs is equal to or slightly greater than the total additional water removed. It is surmised that this large effect is mainly due to the earlier occurrence of high vapor pressure at the hot surface in the pre-heated web case, causing a greater tendency for liquid-phase dewatering of the web while it is compressed. The observed behavior is physically reasonable because the heat transfer to the sheet (responsible for the vapor removal that occurs) is about the same or slightly less when drying the preheated sheets, as compared to the heat transfer to nonpreheated sheets.

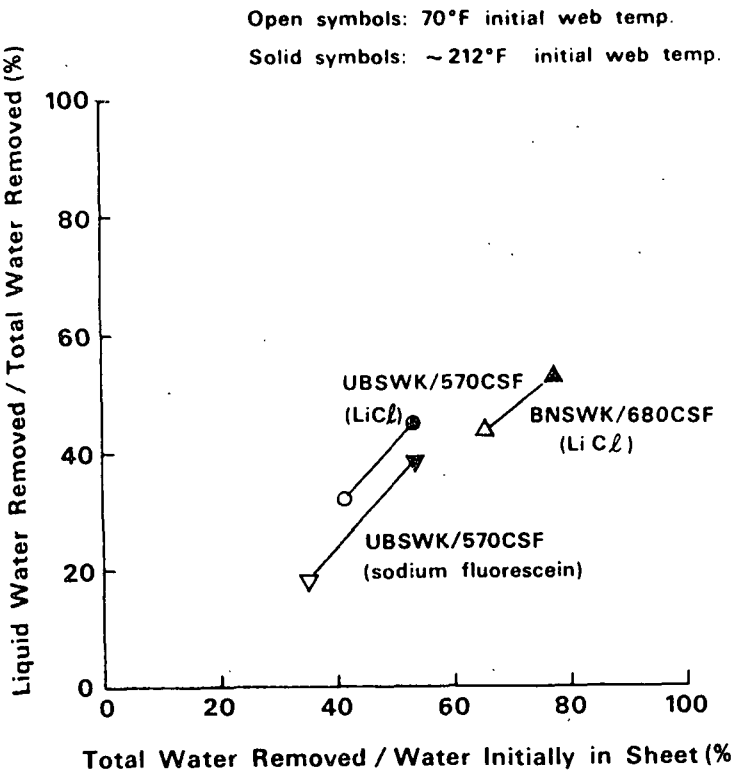

Figure III.13. Total and liquid water removal in impulse drying. Liquid transfer based on chemical tracer transfer from sheet to felt. Conditions: 50 g/m^2 sheets at 40% initial dryness, 750-800 psi mechanical pressure, 600°F surface temperature, 9-11 ms nip residence time.

The results of a limited investigation of the effect of surface temperature on liquid water removal for nonpreheated webs are presented in Fig. III.14. With the furnish employed, the magnitudes are somewhat lower than those in Fig. III.13. However, the trend of increased liquid water removal fraction at higher surface temperatures is encouraging because it indicates a probable reduction in drying energy (per unit water removal) at high temperature, implying a positive impact on dryer size (cost) and operating cost.

Internal Web Behavior

The heat flux, vapor pressure and liquid dewatering measurements discussions given above have all been attempts to identify important features of the

high-intensity drying process in terms of physical effects occurring at the sheet surface. In this subsection, results of experiments dealing with moisture and temperature variations inside the web are briefly reviewed; the following subsection covers internal behavior relevant to property development for the case of impulse drying.

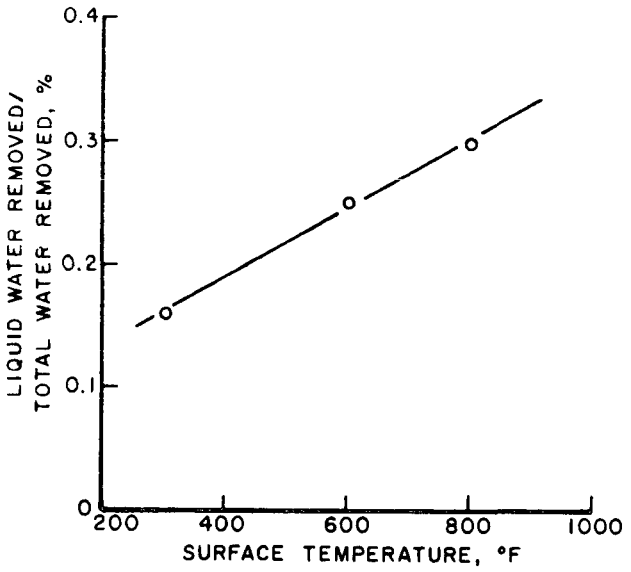

Figure III.14. Liquid water removal in impulse drying. Primary linerboard stock, 600 mL CSF, 50 g/m^2, 40% initial dryness. Peak pressure: 800 psi; nip residence time: 11 to 12 ms.

During the study of drying in the elevated temperature/pressure regime, a few experiments were performed using handsheet produced from three plies, or sublayers, which were pressed together. By interrupting the drying process at various times in a series of test runs and quickly delaminating the sheets it was possible to develop moisture removal curves for each ply and for the sheet as a whole, based on weight measurements. Fig. III.15 gives an example of the results. The data tend to convey a picture of a progressive dryout from the hot surface side toward the open side of the sheet. This is compatible with the heat flux and vapor pressure measurements discussed earlier. The water removal curve for the sheet as a whole (labelled "total") exhibits the continuously

decreasing slope that indicates the absence of a "constant rate period," also compatible with the progressive dryout/declining heat flux picture. Finally, it is worth noting in regard to the Fig. III.15 results that any moisture redistribution in the sheet between the termination of the test run and the completion of delamination would tend to make the observed moisture distribution more uniform than that in the undisturbed sheet as it dries.

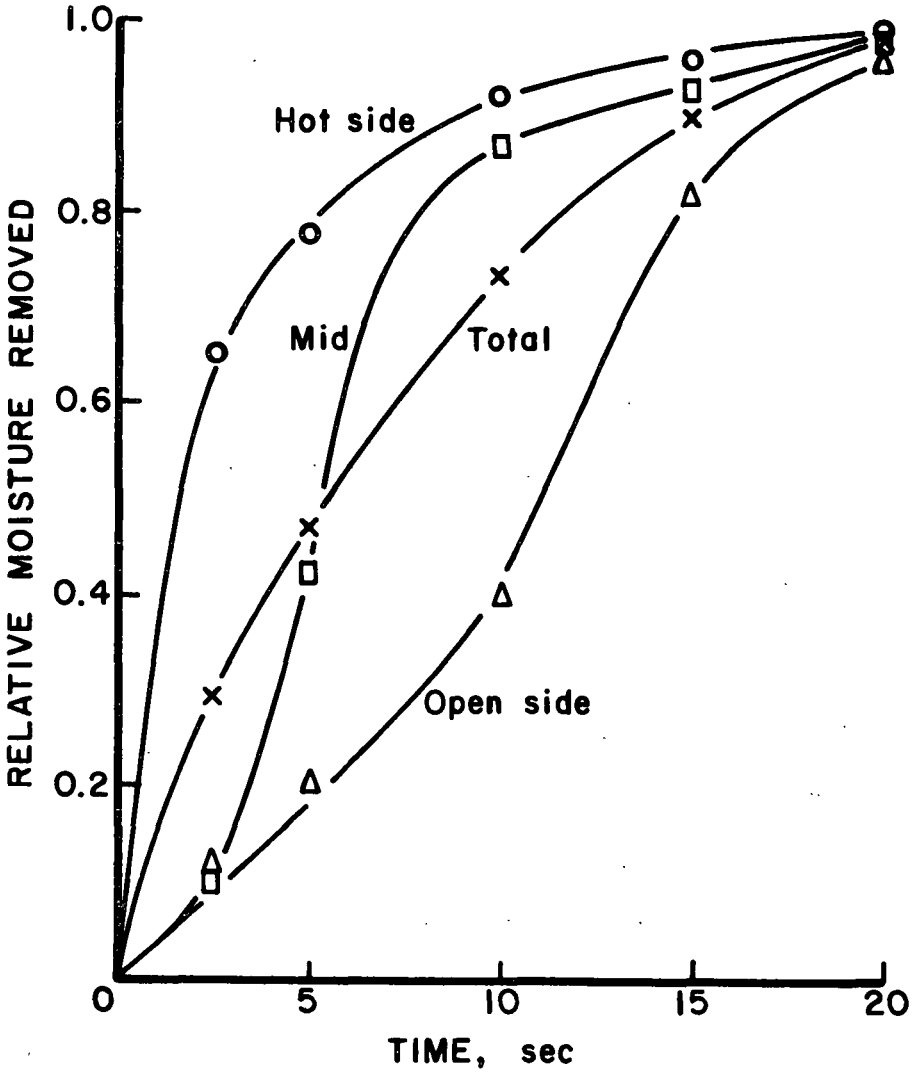

Figure III.15. Water removal for sublayers in elevated temperature/pressure regime. Unbleached southern softwood kraft, 570 mL CSF, 60% initial moisture content, 42 lb/1000 ft^2 sheet. Applied pressure: 1.3 psi, surface temperature: 415°F. Each sublayer is one-third the basis weight of total sheet.

The only other quantitative internal moisture-related data obtained in the high-intensity drying regimes covered by this report have been obtained by Institute student C. Devlin, as part of his doctoral research. These relate to the migration of liquid water within the web during the early part of an intense elevated temperature/pressure drying event, and will be included in his forthcoming thesis.

On a qualitative basis, a few impulse drying experiments were performed (with a surface temperature of 550°F, nip residence time of 30 ms and at 883 psi average pressure) using a 100 g/m^2 basis weight, high freeness sheet containing dyed water. It was found that, following an experiment, the dye was concentrated on the open side and rather dilute on the hot side, again suggesting the relative unimportance of capillary action. For comparison, tests run at "conventional" drying conditions did indeed show the expected high dye concentration at the hot surface side of the sheet.

Various internal temperature measurements in high-intensity drying have also been obtained. Examples of results for elevated temperature/pressure and thermal/vacuum operating conditions are given in Fig. III.16 and III.17, respectively. These cases are qualitatively very similar. Both are characterized by rapid heatup of the sheet until the outer surface reaches the ambient boiling point. The rapidity of heatup is undoubtedly the result of an evaporation/bulk vapor flow/condensation mechanism within the web. The outer layer then remains at the boiling point until dryout begins to occur there, after which it rises toward the hot surface temperature. Meanwhile, the temperature nearer to the hot surface reaches a plateau (of short duration), which probably persists until the moisture at that location is evaporated, after which it rises toward the hot surface temperature. These results again suggest the progressive dryout picture

discussed earlier. Furthermore, the higher evaporating temperatures nearer the hot surface are of such a magnitude as to correspond well with the vapor pressure measurements discussed earlier.

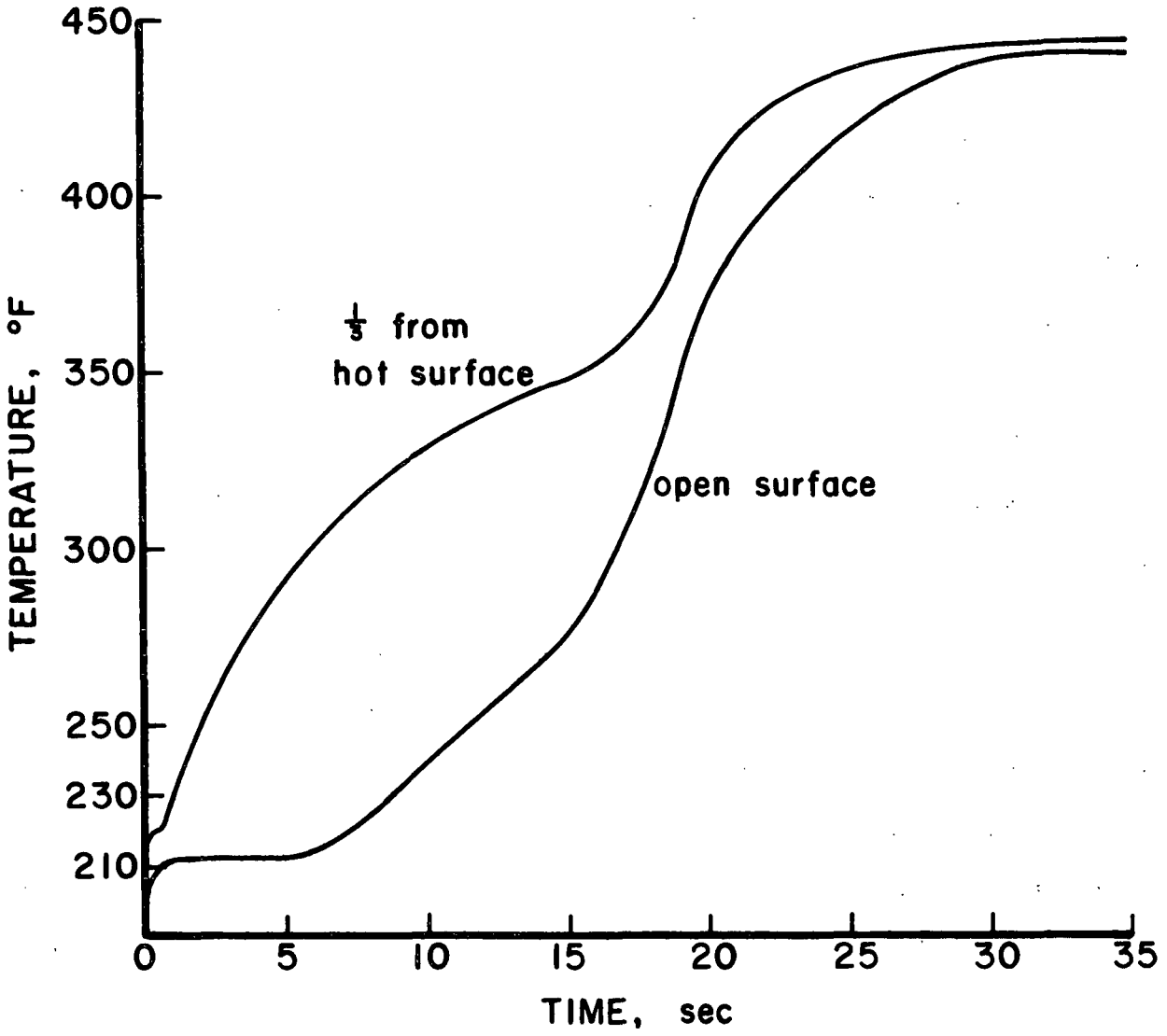

Figure III.16. Typical web temperatures during elevated temperature/pressure drying. Unbleached southern softwood kraft, 570 mL CSF, 42 lb/1000 ft^2, 60% initial moisture content. Surface temperature: 466°F; applied pressure: 3.3 psi.

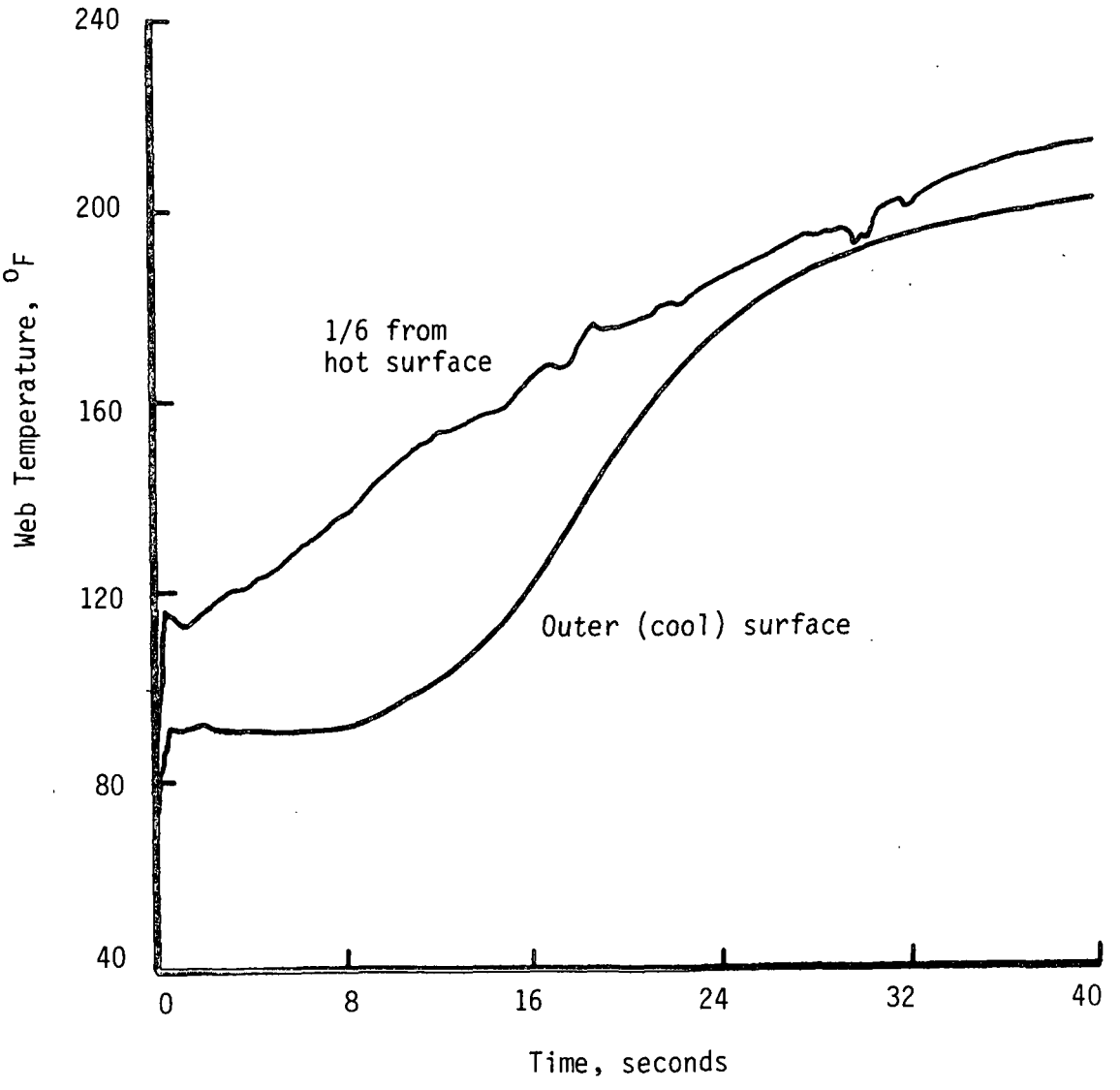

Figure III.17. Typical web temperatures during thermal/vacuum drying at surface temperature and 14.7 psi applied pressure. Unbleached southern softwood kraft, 570 mL CSF, 42 lb/1000 ft^2, 60% initial moisture content.

It should be noted that the forthcoming thesis of C. Devlin will include internal web temperatures from experiments at much more intensive operating conditions. These results indicate the presence of significantly higher evaporating temperatures (and, by implication, higher internal vapor pressures). This appears to be the result of increased vapor flow resistance for the more highly-compressed webs.

The temperature at the open surface (web/felt interface) during impulse drying has been measured by Institute student S. Burton. The results are given in Fig. III.18. These demonstrate that temperatures at least as high as the ambient boiling point can under some conditions occur while the web is experiencing the impulse. This could only happen if hot steam flows rapidly through the web from the hot surface region. This certainly suggests that the observed liquid-phase dewatering in impulse drying is driven by a steam pressure flow flow effect. More detailed internal temperature data will be included in the forthcoming Ph.D. thesis of S. Burton.

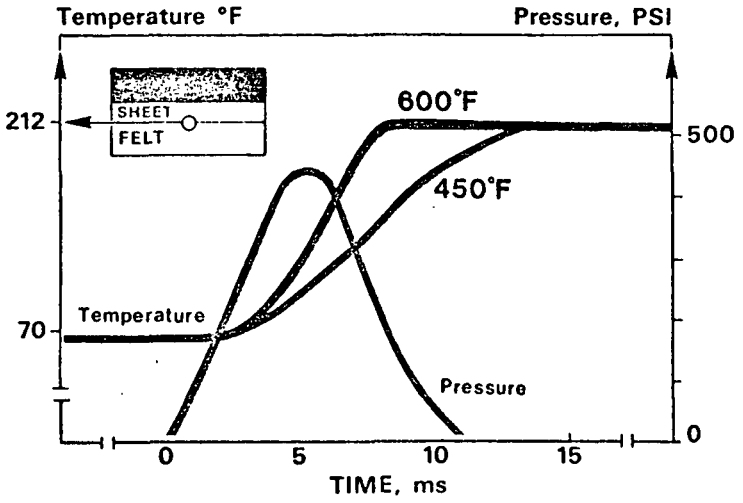

Figure III.18. Typical recordings of total nip pressure and temperature at the sheet/felt interace in impulse drying, for two temperature of the hot surface (450 and 600°F). Unbleached kraft, 550 mL CSF, 50 g/m^2.

MATHEMATICAL MODELS

The experimental data discussed so far in this report, both performance-related and more detailed process-description-oriented, indicate important features of the high-intensity drying processes and provide some hints as to their causes. The student work in progress should provide further useful data to aid in developing understanding of these processes. Interestingly, the

available information suggests the relative simplicity associated with the low to moderate pressure portion of the elevated temperature/pressure regime and with thermal/vacuum drying, and the extreme complexity of the impulse drying process. Several efforts at developing mathematical models of these processes, based on fundamental physical principles and concepts have been made. This work, and particularly the process of comparing model predictions with experimental observations, offers a way of establishing the adequacy of the physical understanding of high-intensity drying that has been accumulated. These efforts, in turn, are helpful in identifying aspects requiring additional research. An ultimate goal of the mathematical model development is to provide a process description sufficient to be useful in the engineering design of technically and economically successful water removal equipment based on high-intensity drying principles. A review of the mathematical modeling work follows. As with the experimental studies, much of the modeling to date has been related more to water removal than to property development.

Zone Models

Two approaches to mathematical analysis/modeling of complex heat and mass transfer processes are common in the engineering literature. One involves the attempt to write (and solve) general mathematical descriptions containing appropriate terms to represent all the potentially important physical phenomena involved in the process. Application of this approach to high-intensity (e.g., impulse) drying would lead to a model capable, in principle, of predicting the continuous temporal and spatial variations of temperature, moisture, and fiber concentration in the web, and of course, the vapor and liquid removal rates, etc. Unfortunately, there are numerous impediments to the success of this approach.

The other approach is to make major assumptions and idealizations that lead to the formulation of (admittedly) less exact models, but ones which are far more tractable and "understandable." In the present context, this approach can lead to the development of zonal models.

Simplified two-zone model

The simplest model which has been developed represents an attempt to explain/describe some of the most significant features of high-intensity drying in the least complex part of the domain - the low-to-moderate pressure portion of the elevated temperature/pressure regime and the thermal/vacuum regime. Because of its simplicity, the model is presented in detail.

The paper is assumed to comprise two zones (Fig. III.19). A growing dry zone, initially of zero thickness, adjacent to the hot surface, and a wet zone of gradually decreasing thickness adjacent to the open surface. The primary assumptions employed in developing the model are listed in Table III.1. Assumptions 1, 2, 3, 6, and 7 are all supported by experimental evidence discussed earlier in the report. Based on these assumptions, the model is thus described by a series of algebraic equations and one first order ordinary differential equation. It is clear that impulse drying cannot be adequately described by this model, in view of Assumptions 2, 3, 6, and 9.

The instantaneous heat flux density through the dry zone is*:

$$q(t) = U(t)\ (T_H - T_B) \qquad (1)$$

where U(t) is the overall heat transfer coefficient and can be expressed by:

*Nomenclature for the model is defined in Table III.2.

$$\frac{1}{U(t)} = \frac{1}{h_c} + \frac{\delta(t)}{k_D} \tag{2}$$

The energy balance at the dry-wet zone interface is:

$$q(t) = \dot{m}_D \, \Delta h \tag{3}$$

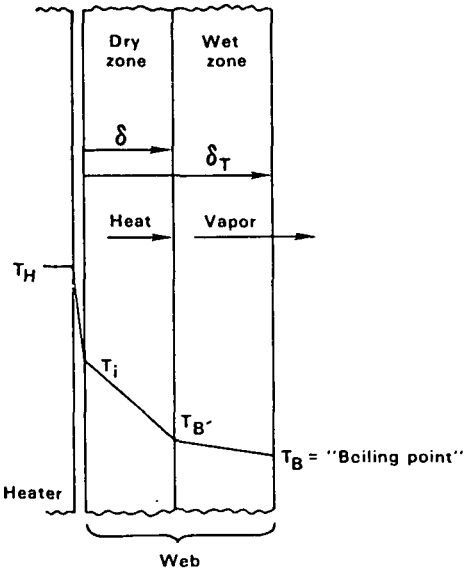

Figure III.19. Idealized two-zone model of high-intensity drying process.

Table III.1. Assumptions in two-zone model.

1. Sheet has distinct dry and wet zones
2. Temperature difference across wet zone is small ($T_B' \approx T_B$)
3. Heatup time is negligible
4. Quasi-steady heat transfer through dry zone (i.e., negligible energy storage in dry zone)
5. Moisture is uniformly distributed within the wet zone
6. No liquid flow occurs
7. Sheet open surface is at the ambient boiling point (T_B)
8. No heat loss (by conduction) at open surface
9. Constant properties in each zone
10. All shrinkage occurs at wet zone/dry zone interface[a]
11. Negligible hygroscopic effects

[a] δ_{T_i} = initial (wet) sheet thickness
δ_{T_f} = final (dry) sheet thickness

Table III.2. Nomenclature for two-zone model.

Symbol	Definition
Bi	Biot number, defined in text
h_c	contact heat transfer coefficient between hot surface and paper web, assumed constant
k_D	thermal conductivity of the dry zone
$K_a\overline{K}_v$	effective vapor permeability in wet zone, expressed as product of absolute permeability of porous structure and vapor relative permeability
$\dot{m}_D$	instantaneous drying rate (per unit area)
$\langle\dot{m}_D\rangle$	average drying rate
M_o	initial mass of water in web, per unit area
Δh	latent heat of vaporization of water, evaluated at the boiling point temperature
ΔM	cumulative water loss, mass per unit area
$\Delta\overline{M}$	relative water loss, defined in text
$\Delta\overline{P}_v$	dimensionless vapor pressure, defined in text
ΔP_v, p_v	vapor pressure (gage, relative to ambient pressure) at hot surface/paper web interface - assumed equal to vapor pressure at dry zone/wet zone interface
q	heat flux into dry zone
$\overline{q}$	dimensionless heat flux, defined in text
t	time
T_H	hot surface temperature
T_B	boiling point temperature
$T_{B'}$	temperature at dry zone/wet zone interface
U	overall heat transfer coefficient between hot surface and dry zone/wet zone interface
δ	dry zone thickness
δ_T	total paper web thickness
ΔT_f	final paper web thickness (dry)
ρ_{ℓ_e}	effective liquid density at the wet-dry interface

The instantaneous drying rate can be expressed by the velocity of the advancement of the dry zone (via a mass balance at the interface):

$$\dot{m}_D = \rho \ell_e \frac{d\,\delta(t)}{dt} \; ; \quad \delta(o) = 0 \tag{4}$$

Combining Eq. (1)-(4) and solving the first order differential equation yields the relative moisture loss as a function of time:

$$\Delta\overline{M} \equiv \Delta M/M_o = \delta(t)/\delta_{T_f} = \sqrt{\frac{1}{Bi^2} + \tau} - \frac{1}{Bi} \tag{5}$$

The dimensionless time is

$$\tau = \frac{2\ k_D\ (T_H - T_B)\ t}{M_o\ \Delta h\ \delta_{T_f}} \tag{6}$$

The Biot-number in Eq. (5) is based on the final thickness of the dry paper.

$$Bi = \frac{h_c \cdot \delta_{T_f}}{k_D} \tag{7}$$

The average drying rate and the (dimensionless) instantaneous heat flux can also be derived from the above equations:

$$\langle \dot{m}_D \rangle = \frac{2\ k_D \cdot (T_h - T_B)}{\delta_T \cdot \Delta h} \cdot \frac{Bi}{2 + Bi} \tag{8}$$

$$\overline{q} = \frac{q}{\left(\frac{k_D\ (T_H - T_B)}{\delta_{T_f}}\right)} = \frac{1}{\sqrt{\frac{1}{Bi^2} + \tau}} \tag{9}$$

Knowing the instantaneous drying rate and the vapor permeability of the wet zone, the vapor pressure needed for the vapor to leave the sheet can be deduced by application of Darcy's law. According to Darcy's law the mass flow through the wet zone is

$$\dot{m}_D = \frac{\rho_v \cdot K_a \bar{K}_v}{\mu_v} \frac{\Delta P_v}{(\delta_T(t) - \delta(t))} \tag{10}$$

Assuming the initial and final sheet thicknesses are known the instantaneous thickness can be expressed as

$$\delta_T(t) = \delta_{T_i} - \left(\frac{\delta_{T_i}}{\delta_{T_f}} - 1\right) \delta(t) \tag{11}$$

If Eq. (10), (11) and the derivative of Eq. (5) are combined, the vapor pressure at the hot surface (in dimensionless form) follows:

$$\Delta \bar{P}_v = \frac{\Delta P_v}{\left(\frac{\mu_v k_D (T_H - T_B) \delta_{T_i}}{\rho_v \cdot K_a \bar{K}_v \cdot \Delta h \, \delta_{T_f}}\right)} = \frac{1 + \frac{1}{Bi}}{\sqrt{\frac{1}{Bi^2} + \tau}} - 1 \tag{12}$$

The equations above, derived from the two-zone model, have been used to develop comparisons with experimental data.

Some example data on cumulative moisture loss *vs.* time are shown in Fig. III.20, together with model predictions for several values of the Biot number (a measure of the thermal contact between the hot-surface and paper web). One would expect the contact coefficient (and, thus, the Biot number) to increase with applied mechanical pressure. The data points confirm this; the higher pressure data coincide with the high-Bi part of the graph.

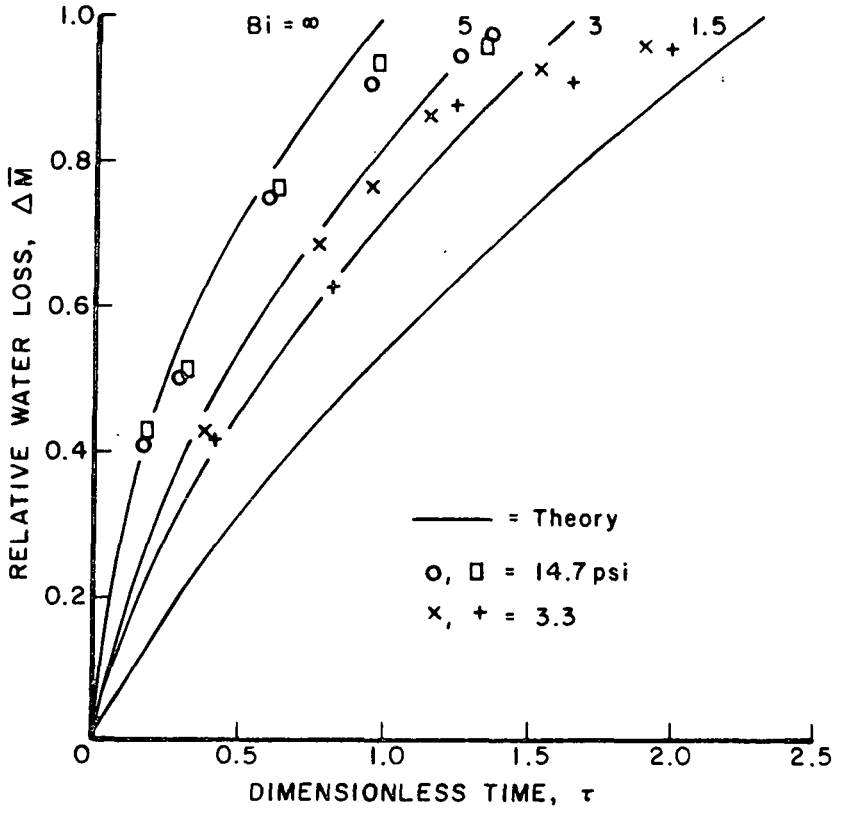

Figure III.20. Examples of drying behavior: 205 g/m^2 unbleached softwood kraft paper webs at 570 CSF and 60% initial m.c. (wet basis).

Symbol	Ambient	Surface Temp., °F	Mechanical Pressure, psi
o	atm.	320	14.7
□	vac.	230	14.7
×	atm.	338	3.3
+	vac.	255	3.3

It is also evident from Fig. III.20 that data from runs at two different ambient pressures collapse onto essentially the same curve for each of the mechanical pressures indicated. Since the data are plotted in terms of a dimensionless time variable, this confirms its suitability (in particular, the use of $T_H - T_B$) for correlating data. Some difficulty was experienced, however, in defining T_B for the vacuum drying runs. Although the nominal boiling point was room temperature (i.e., the temperature of the copper piston on which the vapor condensed), it was found that corrections for condensate layer thermal resistance, effects

of residual air in the condensing zone, etc., were appreciable (e.g., 15 to 40°C, depending on drying rate).

The experimental data trends and the theoretical curves in Fig. III.20 have about the same shapes until the paper reaches the high-dryness range ($\Delta\bar{M} >$ 0.9). Discrepancies at high dryness are probably due to hygroscopic effects not accounted for in the model. Empirically, however, it is found that the theoretical drying time for complete evaporation agrees rather well with the experimentally determined drying time to 6% moisture content. Interestingly, the slopes of the moisture loss curves continuously decrease, showing that no "constant rate regime" exists under high-intensity drying conditions. This is a consequence of the continuously-increasing thickness (thermal resistance) of the dry zone.

Average drying rates are presented in Fig. III.21. This figure demonstrates that, for a given temperature difference, the drying rate increases significantly with mechanical pressure (Bi). At low mechanical pressures, this is probably due mainly to the increase in contact coefficient, while at high pressure (large Bi) it may be due to the increase in thermal conductivity and reduction in web thickness that result from web compression. This latter effect was not accounted for in developing Fig. III.21, which helps to explain the discrepancy between theory and experiment at the highest pressure conditions. Also, the data in Fig. III.21 show that drying rate increases linearly with thermal driving force, in agreement with the model.

The experimentally observed heat flux and vapor pressure behavior (i.e., rapid rise to a peak followed by continuous decline) discussed earlier is quite compatible with the model predictions [Eq. (9) and (12)]. While the <u>peak</u> heat flux tends to correspond in magnitude to a rapid evaporation phenomenon, the heat flux quickly drops down to a range compatible with the heat conduction model of

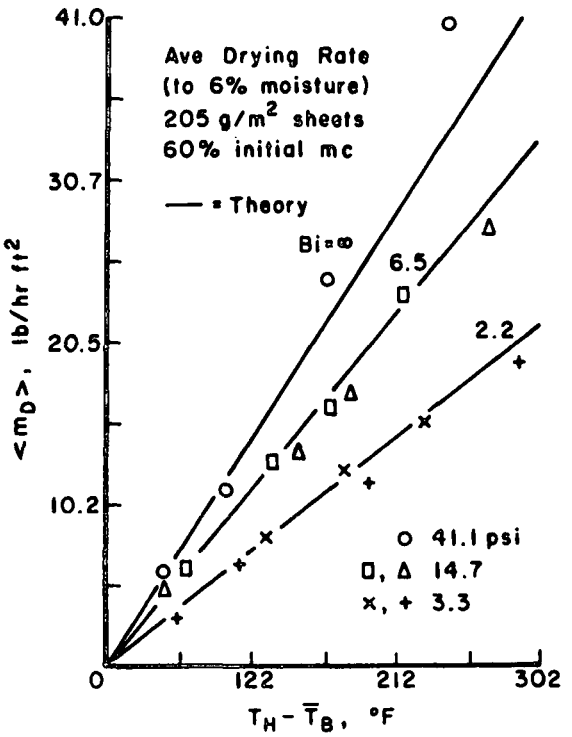

Figure III.21. Average drying rates in high-intensity regime. Ambient pressures: o, Δ, + (vac.), and x (atm.).

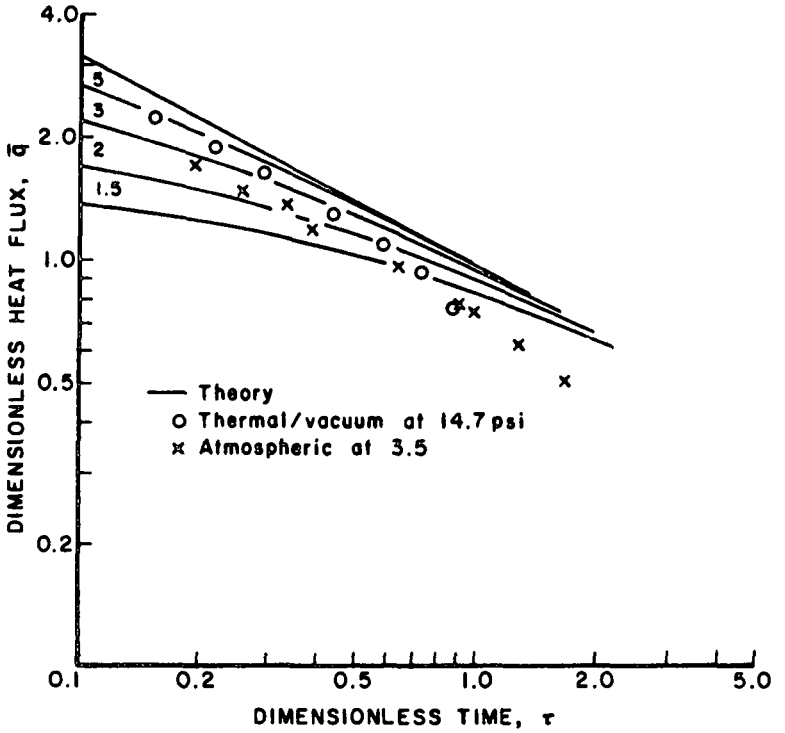

Figure III.22. Instantaneous heat flux (dimensionless) at the hot surface/paper web interface: 205 g/m^2 unbleached softwood kraft at 570 CSF and 60% initial m.c.; surface temperatures: + (400°F), X (431°F).

the dry zone. A comparison of the time dependence of some experimental heat flux data with the model predictions is given in Fig. III.22. The magnitudes and shapes of the experimental results are fairly reasonable with respect to the model for much of the drying period but deviate increasingly toward the end. This may be due to hygroscopic effects or perhaps to a time variation of the heat transfer coefficient. While the model in its present form (particularly, with its assumption of constant heat transfer coefficient) does not describe the heat flux for the low applied pressure case exhibiting "liftoff," this is of no practical consequence, since one would not want to operate a dryer in that regime anyway. The shape of the vapor pressure curve in Fig. III.11 is strikingly similar to the theoretical shape (e.g., for Bi = 5) shown in Fig. III.23, giving additional support to the validity of the mathematical model. Furthermore, matching of the magnitudes of the vapor pressure curves between theory and experiment by adjusting the value of the effective vapor permeability indicates that the permeability is of a realistic order of magnitude (10^{-14} m^2). It was found that the permeability decreases with increasing mechanical pressure. This is reasonable, since the sheet is more compressed at higher mechanical pressure. It should be observed, however, that as sheet compression and flow resistance increase due to operation at higher applied pressures, the vapor pressure (and temperature) difference across the web will become large enough to cause effects not allowed for in the two-zone model. These include liquid flow (shown to be important in impulse drying) and heat transfer through the wet zone. The latter effect would produce evaporation near the open surface and a reduced rate of evaporation at the hot-surface side of the wet zone. The net result could be an enhancement of the effective thermal conductance of the web ($\bar{U}$), leading to higher drying rates than predicted by the two-zone model.

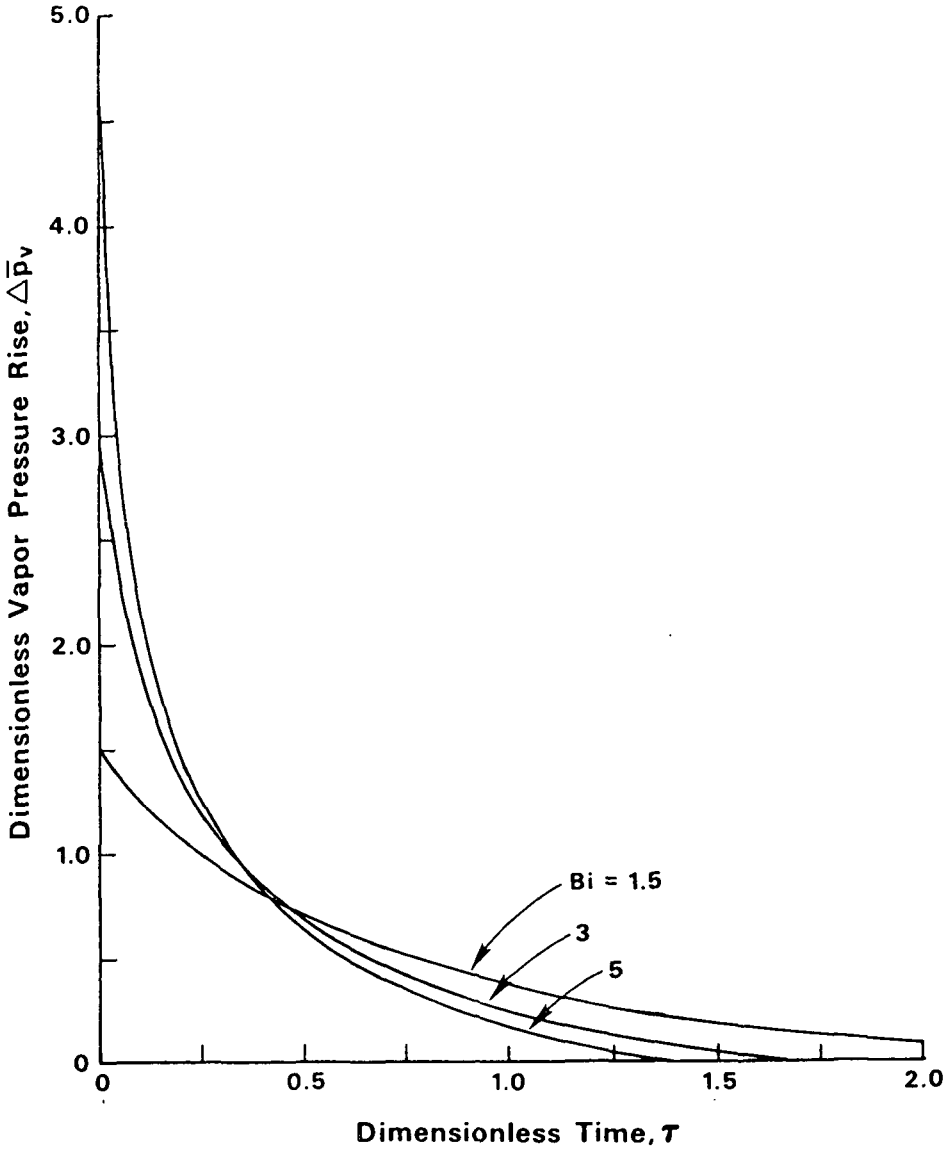

Figure III.23. Vapor pressure response predicted by two-zone model [Eq. (12)].

A final aspect of the two-zone model worth mentioning is that it predicts a value for the average overall heat transfer coefficient ($\bar{U}$) introduced in connection with the heat transfer studies discussed earlier. The result is:

$$\bar{U} = \frac{2\ k_D}{\delta_{T_f}} \left(\frac{Bi}{2 + Bi}\right) \tag{13}$$

Insertion of reasonable values into Eq. (13) does yield close agreement with experimental values. For high mechanical pressure, Bi becomes large and the expression approaches:

$$\bar{U} = 2\ k_D/\delta_f \tag{14}$$

If one represents k_D with a "parallel conductor model"

$$k_D = (1 - \varepsilon)\ k_f \tag{15}$$

where ε is the dry sheet porosity and k_f is the thermal conductivity of the solid fiber material (cellulose), and introduces the basis weight relation

$$BW = (1 - \varepsilon)\ \rho_f\ \delta_{T_f} \tag{16}$$

where ρ_f is the solid fiber density (≈ 1.5 g/cm^3), the overall heat transfer coefficient becomes

$$\bar{U} = 2\ k_f\ \rho_f\ (1 - \varepsilon)^2/BW \tag{17}$$

If the compression relation between porosity and applied pressure were used, one could then quantify the increase of $\bar{U}$ with mechanical pressure. The limiting value ($\varepsilon \longrightarrow o$) from Eq. (17) is indicated in Fig. III.2, discussed earlier. In reality, however, as such a limit is approached through increasing the applied pressure, the flow resistance of the sheet would greatly increase, inducing a large vapor pressure (and temperature) gradient through the web and possibly producing sheet saturation/pressing effects, all of which violate the simplifying assumptions of the two-zone model. A more general model, capable of handling these and several other important effects, is reviewed next.

Extended Zonal Model (Pounder Model)

Recognition of the success and of the limitations of the two-zone model, coupled with the desire to represent the very high-intensity drying regimes (the high-pressure portion of elevated temperature/pressure regime and impulse drying), has led former Institute doctoral student J. Pounder to develop

a greatly extended zonal model.[14] The fundamental extensions contained in this new model are:

1. Incorporation of a quasi-statics sheet compression model, which represents the fiber concentration as being a function of effective structural pressure,* moisture ratio, temperature and refining level (CSF). The model is general enough to allow for both liquid-saturated and unsaturated web conditions.
2. Allowance for liquid flow (and, thus, liquid-phase sheet dewatering) whenever the local degree of saturation of the pore volume is large enough to ensure the presence of interfiber liquid water. The liquid flow is driven by a vapor pressure gradient in the unsaturated web case.
3. Inclusion of an initial heatup/transition period. During the early stages of this period, the web temperature at the hot surface rises to the saturation temperature corresponding to the local liquid pressure, marking the beginning of the development of distinct zones within the sheet. The subsequent evolution to a multizone, piecewise linear temperature distribution configuration is called the transition regime. It should be mentioned that the "expense" associated with inclusion of heatup and transition effects is the need to solve partial differential equations for the corresponding temperature distributions.
4. Allowance for finite flow resistance effects. These include both the buildup of a hydraulic pressure and liquid

*The effective structural pressure is the applied mechanical pressure reduced by the average fluid gage pressure.

flow under saturated sheet conditions during heatup and the vapor pressure (and temperature) gradient development associated with vapor flow through the sheet. The latter effect can yield the occurrence of liquid dewatering, as well as heat transfer through the wet region, which results in development of a second dry zone in the outer part of the sheet.

The extensions just described result in the possibility of a zonal structure more complex than that of the two-zone model. Figure III.24 indicates the required general configuration of the extended zonal model. As suggested in the figure, after transition is complete the drying process is represented by up to four coupled, quasi-steady zone models. The zonal and interface equations, similar to (but more involved than) the ones employed in the two-zone model, predict the time variation of the interface positions and temperatures, and the liquid and vapor contributions to the overall water removal rate. Zone 3 is the only one which permits liquid flow. Whenever the outward liquid flow rate in zone 3 is sufficiently large, zone 4 is prevented from developing. Only in that case can simultaneous liquid and vapor-phase dewatering be present.

In addition to the primary extensions which have been discussed, some other important features have been included in the new model. These include allowance for time varying applied mechanical pressure, use of a variable contact coefficient at the hot surface/web interface that is dependent on mechanical pressure and liquid saturation, inclusion of hygroscopic effects in the effective latent heat, and computation of vapor and liquid permeabilities from empirical correlations involving refining level (CSF), effective structural pressure and liquid saturation level.

As shown in the thesis,[14] the extended zonal model appears capable of yielding predictions in good qualitative agreement with observed macroscopic features of the very high-intensity drying processes, making it a useful tool for investigating and understanding high-intensity drying. However, significant efforts to optimize certain constants in the model in order to produce better quantitative predictions have not yet been made. Furthermore, it should be recognized that additional model extensions might prove to be necessary if highly detailed and accurate predictions are required, or to adequately explain intricate features of the process (e.g., the interaction between the water removal processes and sheet structure/property development). Undoubtedly, the present extended zonal model is a useful starting point for future model developments.

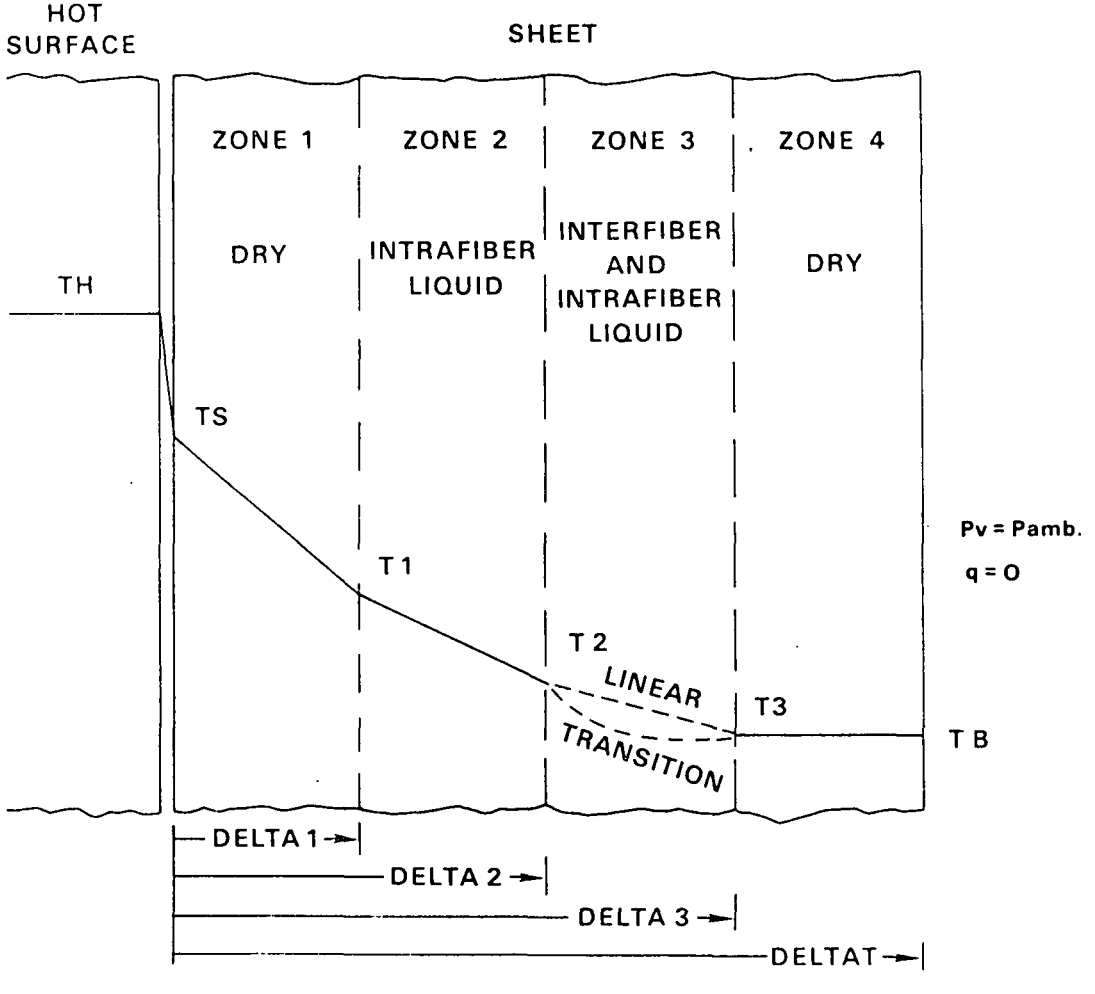

Figure III.24. Configuration of extended zonal model of high-intensity drying.

Continuous Models

The zonal models which have been discussed have the twin virtues of emphasizing a simple physical picture involving only those phenomena considered to be of primary importance to the mechanics of high-intensity drying, and of resulting in relatively easy-to-solve equations requiring modest amounts of computer time. However, since such models depict the web as comprising a small number of unique zones (each with uniform moisture and properties) separated by sharp interfaces at which all evaporation or condensation effects occur, certain physical effects of potential importance are disallowed. These include capillary pressure contributions to the liquid flow driving force, influence of moisture ratio on vapor pressure (due to hygroscopic effects), existence of distributed condensation or evaporation and departure from slug flow of liquid due to nonlinear temperature variations in the heatup and transition periods, and the tendency of nonuniform temperature and fluid pressure to produce nonuniform web compression (especially in impulse drying). The first two of these effects would cause the sharp interfaces between zones to become "fuzzy" transition regions, while the latter two would produce zonal nonuniformities that would suggest the need for "sub-zones" in each major zone of the sheet. Thus, the net result of including any or all of these effects in the mathematical description of high-intensity drying would seem to cause a "continuous" model to be required. Of course, the solution of the partial differential equations of a continuous model by a finite difference method would be equivalent to predicting the time-evolution of conditions within a multiplicity of spatial zones. This would bear some resemblance to the approach used in the previous zonal models.

Some preliminary continuous models of high-intensity drying, with particular emphasis on thermal/vacuum drying, have been developed (e.g., Ahrens and

Journeaux.[15] In all cases, the web has been approximated as a rigid porous material (i.e., compressibility effects have been neglected), making these models of limited value for application to the very intensive processes (e.g., impulse drying). The most complete of these continuous models is a nonlinear model that comprises a continuity equation (governing the transient distribution of liquid saturation in the web), an energy equation (governing the transient temperature distribution), and Darcy's law equations for the liquid and vapor velocities. The model requires the following information: vapor and liquid permeabilities and capillary pressure as functions of saturation level for the given overall porosity, reduced vapor pressure (due to hygroscopic effects) as a function of temperature and moisture content, and several common thermodynamic and transport properties of the web constituents.

The nonlinear model, and some simpler linearized models which can be obtained from it, have yielded qualitatively reasonable predictions, but they appear to offer no real advantage over the zonal models for application to the low-to-moderate pressure regime. The extension of the nonlinear continuous model to the very high intensity region, however, through the inclusion of a suitable web compression model, allowance for a variable contact coefficient at the hot surface, and a review of the appropriateness of the boundary conditions for the open surface, might very well prove worthwhile for the analysis of impulse drying. A transformation to "basis weight coordinates," as introduced by Nelson (1964) and employed in the modeling of conventional drying by Lee and Hinds (1981) and in a wet pressing model by Ceckler and Thompson (1982), would probably be required in such a model.

Supporting Experiments

The discussion of mathematical models which have been, or could be, developed to describe the various high-intensity drying processes has emphasized

that, as the level of detail increases, more and more kinds of properties and parameters appear in the model equations. In most cases, these quantities (e.g., vapor and liquid permeabilities, web compressibility parameters, capillary pressure, etc.) are highly dependent on other web properties or conditions. Unfortunately, data on most of the model parameters are extremely limited (and, in some cases, virtually nonexistent), especially within the ranges of web conditions encountered in high-intensity drying. While there may be some value in (and need for) simply treating the unknown parameters as "adjustible coefficients" whose values are selected so as to maximize the agreement between model predictions and selected experimental observations, it would be useful to have available an independently measured base of data on these parameters. Of course, experimental determinations of the properties of heated, highly-compressed, and partially saturated webs can be expected to present many challenges. The modest completed efforts and plans to deal with the lack of property data relevant to high-intensity drying are as follows.

The vapor permeability plays an important role in all of the high-intensity drying models, since it directly affects the vapor pressure (and temperature) gradient across the wet zone(s) of the sheet. For this reason, it has been the primary focus of property measurement experiments in support of the modeling efforts. A preliminary investigation and use of a steady state heat transfer technique for vapor permeability measurement has been performed (Heindel and Ahrens, 1985). The procedure is based on the measurement of heat transfer rate through a confined thin bed of paper fibers of known porosity and saturation under air-free conditions. The total heat transfer rate is considered to be the sum of a latent heat contribution associated with bulk vapor flow (proportional to vapor permeability) and a conduction contribution that

can be estimated using a parallel-conductor model for the bed thermal conductivity. Thus, using heat transfer and temperature difference data, it is possible to calculate the vapor permeability. The technique is limited to the high-saturation regime because steady state operation requires that a liquid flux of equal magnitude, but opposite direction, to the vapor flux must be present; at low saturation, liquid flow effectively ceases, causing a dry zone to develop at the heated surface of the web. The data which have been obtained so far are very limited but are compatible with the permeability values inferred (with help of the two-zone model) from the vapor pressure response at the hot surface during drying experiments.

Data on liquid permeability for saturated, highly-compressed webs at room temperature are fairly plentiful due to their relevance to wet pressing. Because of possible differences in fiber network configuration or fiber shape at temperature levels to be expected in impulse drying, data from high temperature, permeability experiments would be desirable. Data from such experiments are apparently unavailable at present. For partially saturated webs, liquid permeability values are almost nonexistent for any temperature level. One recently proposed method for the concurrent determination of capillary pressure and liquid permeability in partially saturated webs was implemented by Wanamaker (1984), in a student project in support of the high-intensity drying work. His experimental apparatus was limited to room temperature, high porosity conditions; however, extensions to more meaningful operating conditions may be possible but would be difficult. The basic technique involves measurement of the instantaneous rate of liquid outflow from the web and the total change in equilibrium moisture content resulting from a step change in applied capillary pressure. The permeability is "extracted" from the data with help of a mathematical model. A

series of experiments at different initial saturations is performed to determine the saturation dependence of permeability and capillary pressure.

For impulse drying modeling, data on the web compression characteristics at high temperature are essential. It may be possible to infer this information from the results of detailed impulse drying experiments being performed by Institute doctoral student S. Burton. The success of such an approach would be hampered by strong spatial and temporal variations of temperature, moisture and fiber concentration during impulse drying. A preferred alternative would be to conduct isothermal compression experiments on webs of different moisture ratios, along the lines proposed by Burton (1983).

CONCLUDING REMARKS ON PROCESS DESCRIPTION

Summary Description

The experimental and analytical work discussed in this section has been successful in providing considerable physical understanding and a related mathematical description of the low-to-moderate applied pressure regimes of high-intensity drying, encompassing both atmospheric and thermally-induced vacuum ambient pressures. The description which emerges from this work is briefly as follows. Upon initial contact of the moist sheet with the hot surface, a brief period of rapid evaporation of surface water occurs. This is followed quickly by the initiation at the hot surface of dryout and the growth of a dry layer of ever-increasing thickness for the duration of the drying process. The corresponding increasing thermal resistance yields a continuously decreasing drying rate. The early rapid generation of vapor produces sufficient vapor pressure at the hot surface to drive a bulk flow of vapor into and (after a rapid sheet heatup to the local saturation temperature due to vapor condensation) through the

sheet. In this regime (low-to-moderate applied pressure), web compression levels are typically insufficient to produce a large flow resistance. Combined with the typical vapor fluxes due to evaporation, this results in internal web temperatures only slightly exceeding the ambient boiling point throughout the moist region of the sheet. Unfortunately, at very low mechanical pressure and moderately high surface temperature sufficient vapor pressure can develop to cause "liftoff," making this an undesirable operating combination. Above these low pressure levels, the applied pressure dependency of the drying time-scale is the result of the increases in contact coefficient and dry web thermal conductivity and density with pressure. The important thermal driving force is the difference between the hot surface temperature and the boiling point.

For the very high intensity regimes (especially impulse drying), the process description resulting from completed experimental and analytical work is less complete because the process itself becomes far more complex and more difficult to study experimentally. For example, the relatively short time scale imposed on the impulse drying process by the given applied pressure pulse causes the heatup period to become an appreciable portion of the total process duration. Similarly, the time required for evaporation of "surface water" at the hot surface appears to be a significant part of the process duration. Other complexities and process features indicated by the available information include a rapidly varying state of web compression, due not only to the time varying applied pressure, but also to the large time variation of average web temperature and moisture content. The large quantity of liquid phase dewatering (relative to the total water removal) and the rapid temperature rise at the cool side of the web are indications of a strong vapor pressure/flow driving force for liquid outflow. It is not yet possible, however, to quantify the amount of liquid dewatering due to "wet pressing" effects (perhaps thermally augmented) as compared

to the amount due to the vapor driving force. The model recently completed by Pounder and the experimental investigations in the very high-intensity regimes nearing completion by Devlin and Burton offer the strong likelihood that a considerably more complete process description will soon be available.

Recommendations

Future research is recommended in order to fully maximize the benefits to be achieved from a comprehensive process description, preferably embodied in the form of a mathematical model. The efforts should be focused on the impulse drying process, in view of its great potential importance to the industry, and because it is currently the least understood. The work should continue and extend work in progress by Burton. During "conventional" impulse drying experiments and also during special experiments involving a simpler "square wave" applied pressure pulse, longer nip residence times and preheated webs (singly and in combination), measurement of internal temperature and fiber density distributions should be made. Other measurements should include heat flux and vapor pressure at the hot surface and the amount of liquid dewatering. Supporting work on measurement of compression characteristics and liquid and vapor permeabilities should be pursued. Finally, application and extension of the multizone model and development of a more complete continuous model should be initiated. The adequacy of quasi-static compression relations in the models should be examined.

CONCLUSIONS AND DISCUSSION

EVALUATION OF PROCESS DESCRIPTION

The high-intensity drying processes that are being studied in this project represent a major departure from the most prevalent paper drying process currently in use - hot surface (multicylinder) drying at moderate surface temperature and low contact pressure. The differences are exhibited both at the performance level (drying rate, energy use, and paper properties) and with respect to the important physical mechanisms of heat transfer, water removal and property development. Of course, the performance and process description results presented in Sections II and III clearly confirm that the broad category of high-intensity drying is, itself, not a single process. Rather, it can be viewed as a family of processes or regimes, each having individual features of potential value, but all having a major characteristic in common - the development of a distinctive driving force (internal vapor pressure in excess of the ambient pressure) for rapid energy transport and water removal. This driving force, in turn, has been shown in the present report to be the result of drying at surface temperatures significantly above the ambient boiling point* and at higher than conventional applied pressures. It is these intensive drying conditions that can lead to potentially favorable effects on property development and energy use.

The experimental efforts to define the high intensity drying processes have benefited from the measurement of certain physical quantities (heat flux

*In the case of thermal/vacuum drying, any surface temperature above the ambient vapor condensing temperature is actually sufficient, provided air-free conditions prevail.

and vapor pressure at the hot surface, and fiber concentration distribution*) not heretofore measured in paper drying research, as well as from the use of more prevalent techniques (internal thermocouples, chemical tracers, weight loss). The experiments in the low-to-moderate mechanical pressure portion of the elevated temperature/pressure regime and those involving thermal/vacuum drying were sufficient to define these processes as being similar and adequately described by a simple physical/mathematical model. The experiments at very-high-intensity drying conditions (primarily impulse drying) have indicated several important process features, allowing an initial physical/mathematical model to be developed. However, the considerable complexity of the process at these conditions, indicated by the available data, suggests that further experimentation and analysis will be required to achieve a complete description. Specific recommendations for future work in this area are given at the end of Section III.

EVALUATION OF HIGH-INTENSITY DRYING PROCESSES

Criteria

The three regimes of high-intensity drying which were considered in the exploratory performance studies reported in Section II have shown varying degrees of potential performance benefit. They also present various implementation challenges. As a group, these processes certainly hold the promise of major breakthroughs in water removal, making it reasonable to recommend that further research and development efforts on high-intensity drying be vigorously pursued. The priority or degree of emphasis of future work in each of the three regimes should be based on a ranking that involves the following criteria:

*This measurement has only been made during impulse drying experiments included in the doctoral research of S. Burton.

(1) potential for equipment size/cost reduction (per unit water removal rate), (2) potential energy cost reduction, (3) probable capacity to favorably influence paper properties, (4) apparent extent of applicability, and (5) ease of implementation.

Conclusions

With respect to these criteria the three regimes show the following characteristics. Elevated temperature/pressure drying could be most easily implemented by increases in felt tension and modest increases in steam pressure. However, it is likely that substantial improvements in drying rate via this strategy would demand major redesign of the dryer section. Even then, the practicality of major applied pressure increases is doubtful. If successful, the process would have wide applicability, but the dryer size reduction would be partially offset by high intrinsic structural costs. Modest energy efficiency improvements and very little influence on paper properties would accrue from implementation. Overall, this low-to-moderate pressure portion of the regime represents an extension of current technology that does not appear to warrant or require much additional research. Above the pressure limits imposed by practical felt tensions (with dryer redesign), it is difficult to conceive of ways to implement the elevated temperature/pressure regime except by use of configurations equivalent to thermal/vacuum or impulse dryers.

Thermal/vacuum drying appears to be the most difficult to implement commercially, despite the fact that various configurations have been proposed.[9,10] It does offer the possibility of drying equipment only about 10% the size of today's dryer section, and should be widely applicable. It does offer significant energy cost reduction opportunities, too, but these may be difficult to capture in practice. The paper properties effects appear to be modest. Overall,

the process does appear to warrant some additional consideration, particularly at the engineering implementation and mill-wide impact levels.

The impulse drying process shows far greater equipment size reduction and paper properties impact potentials than the other processes. It also demonstrates a large reduction in energy use, but the quality of the energy needed will be higher. The extent of applicability to various grades needs to be determined. The process appears to be reasonably well-suited for implementation using long residence time press nip technology coupled with externally heated dryer cylinders. Of course, the novelty of the system and the intense operating conditions will present significant engineering challenges. Overall, this process appears to offer the most potential benefits of the greatest magnitude and is recommended for the highest priority in future research.

LONG RANGE PLAN

Most of the work to date in this project, described in this report, has been directed toward investigating the technical feasibility and exploring the performance of high-intensity drying processes, and establishing a level of understanding of their mechanisms. The primary objective of future work in this project should be to extend the current understanding of high-intensity water removal principles to include the comprehensive data base required for their effective and efficient commercial application. Drying performance and paper properties data for a representative range of paper grades and fiber furnishes are needed for engineering studies, overall economic assessment, and to enable matching the various high-intensity concepts with proper applications. Technical questions relating to the design of water removal systems using these high-intensity processes must be answered. In addition, an overall technology assessment

of the potential of advanced water removal systems is needed. The nature of the data and assessments needed to allow commercialization to proceed and the tasks required to produce this information have been reviewed. Based on these considerations, a long-range plan for the project has been formulated.

A diagram exhibiting the key elements of the project, and their interrelationships, is given in Fig. IV.1. For completeness, both past and future areas of effort are included. A brief description of the objectives of these project elements is as follows.

1. Exploratory and Feasibility Studies (Complete):

   Provide early information (via bench-scale experiments) on the technical feasibility of improving the water removal process by application of high-intensity concepts such as impulse drying and thermal/vacuum drying. Quantify the potential benefits of these concepts. This is the work discussed in Section II.

2. Investigation of Water Removal Mechanisms (Partially Complete):

   Develop an understanding (via bench-scale experiments and mathematical modeling) of the processes governing water removal from the paper web and property development under high-intensity operating conditions typical of impulse drying, thermal/vacuum drying, etc., to provide a basis for guiding the development and design of advanced water removal systems. Work in this area is discussed in Section III; additional work is recommended.

3. Technical Performance Data:

   Develop a base of technical data (still by means of tests at the bench scale) on drying performance, energy use, paper properties, etc., for a

representative range of paper grades, fiber furnishes and operating conditions sufficient for identification and assessment of advanced water removal system opportunities. Work in this area is well underway and results will be reported shortly.

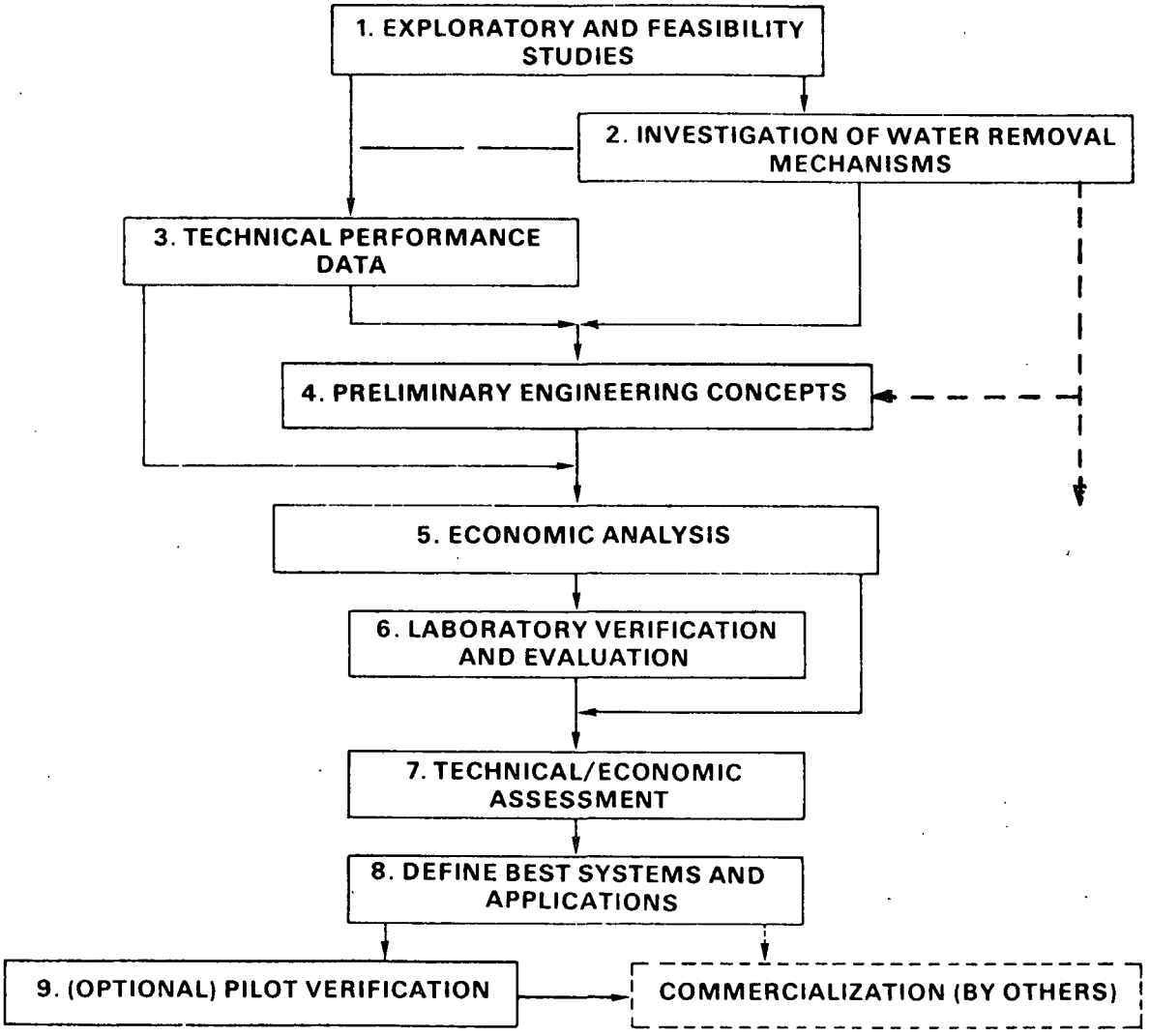

Figure IV.1. Long range project elements.

4. Preliminary Engineering Concepts:

Utilize the technical data gathered in Task 3 to establish preliminary system configurations (i.e., hardware requirements, size estimates, heat

source options, etc.) appropriate for the various paper grades. Work in this area has been initiated.

5. Economic Analysis:

Develop capital and operating cost estimates for the various system concepts which are applicable to each paper or board grade and select those applications worthy of future work. This analysis should include the mill-wide impact of higher drying rates, smaller equipment, and use of different energy forms and rates.

6. Laboratory Verification and Evaluation:

For the most promising systems and grade applications, develop laboratory scale systems (moving web) to verify their general validity, confirm the magnitude of benefits to be expected, and identify operating constraints and resolve problems not discernible at the bench scale.

7. Technical/Economic Assessment:

Use the technical data from the laboratory verification work to improve upon the definition of design alternatives for water removal systems suitable for important paper and board grades and evaluate the mill-wide technical and economic impacts of these systems.

8. Define Best Systems and Applications:

Develop and document the technical and economic data bases characterizing those water removal systems and applications having high payoff potential for the industry.

9. Pilot Verification (Optional):

Design, construct, and operate pilot-scale version(s) of the best system(s), capable of high-speed, continuous web operation, to provide a

more complete and accurate evaluation of the technical and economic impact of improved water removal technology, thereby stimulating the timely development of commercial equipment.

Funding has been received from the U.S. Department of Energy to expedite the accomplishment of the work proposed in this long-range plan.

LITERATURE CITED

1. Hersh, H. N. Energy and material flows in the production of pulp and paper. Argonne National Laboratory, ANL/CNSV-16(1981).

2. Grant, T. J.; Slinn, R. J. Patterns of fuel and energy consumption in the U.S. pulp and paper industry: 1972-1981. American Paper Institute (1982).

3. Chiogioji, M. H. Industrial energy conservation. Marcel Dekker, New York (1979).

4. McConnell, R. R. A review of the state-of-the-art in paper drying. The Institute of Paper Chemistry, Project 3394, Report One (Feb., 1980).

5. Smook, G. Factors which affect steam economy. In: Drying of Paper and Paperboard, G. Gavelin (ed.), Lockwood Publishing Co., New York, 1972, p. 169-177.

6. Pulp and paper manufacture: Papermaking and paperboard making. Second Edition, Volume III, McGraw-Hill Book Co., New York (1970).

7. Han, S. T. Drying of paper. Tappi 53(6):1034-46(June, 1970).

8. Spraker, W. A. Heat and mass transfer from cylinder to paper and within paper. In: Drying of Paper and Paperboard, G. Gavelin (ed.), Lockwood Publishing Co., New York, 1972:22-30.

9. Lehtinen, J. A. 1980. A new vacuum-drying method for paper, board, and other permeable mats. Drying '80: Proceedings of the Second International Symposium, A. S. Mujumdar (ed.), 2:347-54, Hemisphere, Washington.

10. Lehtinen, J. 1982. Some theoretical aspects regarding the basic process and energy economics of the Convac Drying Process for paper and board. Proceedings of the Third International Drying Symposium, Birmingham, England, Sept. 13-16, 1982, John C. Ashworth (ed.), Drying Research Ltd., Wolverhampton, England, Vol. 2, p. 382-94.

11. Devlin, C. P. 1984a. An investigation of the drying mechanism of paper at high temperatures and mechanical pressures. Progress Reports, A-400 Project, The Institute of Paper Chemistry, Appleton, WI (April 27, 1984).

12. Devlin, C. P. 1984b. An investigation of the drying mechanism of paper at high temperatures and mechanical pressures. Progress Report and Supplement, A-400 Project, The Institute of Paper Chemistry, Appleton, WI (May 15, 1984).

13. Myers, G. 1971. Analytical methods in conduction heat transfer, McGraw-Hill, New York (1971).

14. Pounder, J. 1985. A mathematical model of high intensity paper drying, Ph.D. Thesis, The Institute of Paper Chemistry, Appleton, WI.

15. Ahrens, F.; Journeaux, I. 1984. An experimental and analytical investigation of a thermally induced vacuum drying process for permeable mats. In: Drying '84, A. Mujumdar (ed.), p. 281-91, Hemisphere, Washington.

THE INSTITUTE OF PAPER CHEMISTRY

Frederick Ahrens /sb

*Frederick Ahrens

Clyde H. Sprague /sb

Clyde H. Sprague
Acting Group Leader
Papermaking Processes Group

APPROVED BY

Clyde H. Sprague /sb

Clyde H. Sprague
Director
Engineering Division

*Formerly, Research Associate, Papermaking Processes Group, The Institute of Paper Chemistry. Now with the Department of Mechanical and Aerospace Engineering, University of Missouri, Columbia.